

Microscopic identification of plant immune responses in phloem tissue of higher plants relating to bacterial infection

by
Stefanie Vera Buxa

A dissertation submitted in partial fulfilment
of the requirements for the degree of
Doctor rerum naturalium (Dr. rer. nat.)

at the
JUSTUS-LIEBIG-
 UNIVERSITÄT
GIESSEN

Institute for Phytopathology and Applied Zoology,
Department of Phytopathology
Prof. Dr. Karl-Heinz Kogel

Giessen, 2014

Current dean: Prof. Dr. Holger Zorn

Thesis Advisory Committee:

- First reviewer: Prof. Dr. Karl-Heinz Kogel
- Second reviewer: Prof. Dr. Aart van Bel
- Third reviewer: Prof. Dr. Volker Wissemann
- Fourth reviewer: Dr. Rita Musetti (University of Udine)

Day of doctoral examination: 17.09.2014

The work presented in this dissertation was performed at the Institute for Phytopathology and Applied Zoology under the direction of Prof. Dr. Karl-Heinz Kogel between January 2011 and March 2014 at the Justus-Liebig-University Giessen.

Widmung

Diese Doktorarbeit widme ich meinen Eltern,
Edith Buxa-Wiederer und **Wolfgang Wiederer**,
und meiner Schwester,
Melanie Karin Buxa.

This dissertation could not have been finished without the help and support from many professors, research staff, graduate students, colleagues and my family. It is my great pleasure to acknowledge people who had given me guidance, help and encouragement:

I would like to express my special appreciation and thanks to my supervisor **Professor Dr. Karl-Heinz Kogel**. He has been a tremendous mentor for me. I would like to thank him for encouraging my research and for allowing me to grow as a research scientist. I am not sure many graduate students are given the opportunity to develop their own individuality and self-sufficiency by being allowed to work with such independence. He taught me how to question thoughts and express ideas. His patience and support helped me overcome many crisis situations and finish this dissertation.

My gratitude is to my advisor, **Dr. Alexandra C.U. Furch**. I have been fortunate to have an advisor who gave me the freedom to explore on my own and at the same time the guidance to recover when my steps faltered.

This dissertation would not have been possible without **Professor Dr. Aart J.E. van Bel**. He is the reason why I became a researcher and whose passion for research and theory in plant science had lasting effect. I am deeply grateful to him for the long discussions that helped me sort out the technical details of my work. I am also thankful to him for encouraging the use of consistent notation in my writings and for carefully reading and commenting on countless revisions of many manuscripts.

I would also like to thank my advisory committee members, **Professor Volker Wissemann** and **Dr. Rita Musetti** for serving as my committee members. They generously gave their time to offer me valuable comments toward improving my work.

It is my pleasure to acknowledge all my current and previous colleagues in the Department of Phytopathology and the Institute of Botany for their enormous support and providing a good atmosphere in the lab. I will always be grateful to them for helping me to develop the scientific approach and attitude. I am most grateful to **Dr. Katrin Ehlers** for lending me her expertise and intuition to my scientific, technical and personal approach.

My thanks also go out to the support I received from the co-authors and collaboration partner at the Justus-Liebig University, the Boyce Thompson Institute, and the University of Udine, in particular **Dr. Rita Musetti**. Completing this work would have been all the more difficult without her support and friendship. And I hope to keep up our collaboration in the future.

I take this opportunity to express my gratitude to the lab assistants, gardener and secretary who have been instrumental in the successful completion of this project. All of them have been there to support me, when I collected data for my Ph.D. thesis and cheered me on when I was upset. Special thanks to **Susanne Habermehl** and **Dietmar Haffer** for their affectionate advice, support and friendship.

Thanks to my **friends** and to **colleagues** and **roommates**, who become friends, for encouraging, entertaining, cajoling, supporting me through the dark times, celebrating with me through the good, who have been brilliant and understanding when I needed them to be, and celebrated each accomplishment. I take this opportunity to thank them.

Most importantly, none of this would have been possible without the love and patience of my family. Words cannot express how grateful I am to my parents and my sister for all of the sacrifices that you've made on my behalf. I deeply thank my parents, **Edith Buxa-Wiederer** and **Wolfgang Wiederer** for their unconditional trust, timely encouragement, and endless patience. It was their love that raised me up again when I got weary. Foremost, without my sister **Melanie Karin Buxa** by my side through the most difficult times of this journey, accomplishment wouldn't have been half sweet. Without you, I would not be the person I am today. Following your example was the best decision I've ever made.

Microscopic identification of plant immune responses in phloem tissue of higher plants relating to bacterial infection

Plants, like animals, sense microbial invaders by using receptor-based recognition of surface molecules and released effector proteins. Perception of bacterial components, among others, triggers signals that reach the phloem to promote systemical signaling, ultrastructural modification and sieve-element occlusion. Rapid and efficient sieve-element occlusion may form a physical barrier to restrict pathogens and to accumulate signal molecules and reversibility ensures a systemic spread of signals. Reorganization of host cell (sub)structures may serve nutrient supply and systemic spread of the phytoplasmas or rather represents a defense reaction of the plant to prevent pathogen movement and nutrition flow.

In this work, microscopical observations of the phloem of higher plants were performed in order to record immune responses to various bacterial stimuli.

The effect of artificial infection on general immune responses of the phloem due to bacterial infection was examined using purified synthetic surface molecules. Flagellin-triggered sieve-element occlusion was observed in *Arabidopsis thaliana* plants using CLSM. Absence of phloem sealing in flagellin-insensitive mutants indicated sieve-element occlusion as part of the receptor-based immunity cascade. Sieve-element occlusion observed in intact *Vicia faba* plants by dispersion of forisomes after flagellin treatment revealed Ca^{2+} to be involved in sieve-element occlusion. Nonappearance of forisome reaction in *V. faba* sieve-element protoplasts after flagellin treatment indicated the receptor not to be located in the sieve element-companion cell complex, pointing out the sites of flagellin perception and response to be spatially separated. The apparent exclusive presence of flagellin receptors in cortex cells still questioning the mode and composition of signal transfer to the sieve elements.

The effect of natural infection on phloem responses was studied exploring the phytoplasma-phloem relationships at cellular level. CLSM analysis of *V. faba* infected with 'Candidatus Phytoplasma vitis' brought about Ca^{2+} influx into sieve tubes leading to sieve-plate occlusion by callose deposition and/or protein plugging, presumptive dramatic effects on phytoplasma spread and photoassimilate distribution. EFM and TEM studies on *Solanum lycopersicon* infected with 'Candidatus Phytoplasma solani' showed a drastic reorganization of sieve-element membrane structures in infected tissues. Next to typical macroscopical symptoms, structural modifications in the sieve-element plasma membrane - endoplasmic reticulum - cytoskeleton network appeared. However, the exact nature of these modifications remains speculative.

In summary, the results of the present work lead to the conclusion that complex receptor-mediated sieve-element occlusion and reorganization due to bacterial infection is part of the plant's defense strategy against invasion and spread of harmful pathogens. Thus, we assume phloem based immunity belongs, next to other strategies, to the evolutionary concept of the plant immune response that completes a highly effective defense system to resist to potential infestation by microbial pathogens.

Key words: phloem, plant immune response, flagellin, phytoplasma, microscopy

Mikroskopische Untersuchungen zur pflanzlichen Immunantwort im Phloem höherer Gefäßpflanzen in Antwort auf bakterielle Infektion

In höheren Pflanzen, wie auch in Tieren, werden mikrobielle Eindringlinge über Rezeptor-abhängigen Erkennung von Oberflächen- und freigegebenen Effektormolekülen erkannt. Induzierte Immunabwehr führt, neben direkten Abwehrreaktionen, zur Freisetzung von intra- und extrazellulären Signalstoffen. Diese Signale erreichen das vaskuläre System und können dort im Phloem über den Massenstrom weitergeleitet werden. Neben der systemischen Wirkung durch Weiterleitung, Amplifizierung und Modifikation von Signalstoffen, können diese Signalmoleküle auch lokal in die Physiologie und Anatomie des Phloems eingreifen. Schneller und effektiver Verschluss der Siebelemente könnte eine physikalische Barriere gegen Krankheitserreger darstellen und eine Anreicherung von Signalmolekülen in verschlossenen Siebelementen ermöglichen. Die Reversibilität des Verschlusses würde eine systemische Ausbreitung von Signalmolekülen gewährleisten. Reorganisation von Wirtszelle (Ultra-)Strukturen können der Nährstoffzufuhr und systemischen Ausbreitung von Bakterien im Phloem dienen zugleich jedoch eine Abwehrreaktion der Pflanze darstellen, um die Bewegung und Ernährung der Erreger zu unterbinden.

In der vorliegenden Arbeit wurden mikroskopische Untersuchungen des Phloems in höheren Pflanzen angestellt, um die Immunantwort des Siebelement-Geleitzell-Komplexes auf verschiedene bakterielle Reize zu untersuchen.

Der Einfluss von artifiziellen Infektionen auf die generelle Immunantwort des Phloems wurde mit Hilfe synthetisch aufgereinigter Oberflächenmoleküle untersucht. Flagellin-induzierter Siebelementverschluss konnte in *A. thaliana* Pflanzen mit Hilfe der CLSM beobachtet werden. Das Ausbleiben des Verschlusses in Flagellin-unempfindlichen *A. thaliana* Mutanten wies auf eine Beteiligung des Siebelementverschlusses an der Rezeptor-vermittelten Immunität hin. Die Dispersion von Forisomen in intakten *V. faba* Pflanzen nach Flagellin Applikation lässt weiterhin Rückschlüsse auf eine Beteiligung von Ca^{2+} an dem Flagellin-vermittelten Siebelementverschluss vermuten. Fehlende Forisomreaktion in isolierten Siebelementzellen hingegen deuteten darauf hin, dass eine Flagellin Perzeption nicht direkt an den Zellen des Phloems ausgelöst werden. Die scheinbare Beschränkung der Flagellin-Rezeptoren auf Zellen des Cortex werfen bis zu diesem Zeitpunkt noch Zweifel an der Art und Weise der Signalübertragung zu den Siebelementen auf.

Der Einfluss einer natürlichen Infektion auf Morphologie und Physiologie des Phloems wurden mit Hilfe der Phytoplasma-Wirts-Interaktion untersucht. CLSM Beobachtungen von *Candidatus* Phytoplasma vitis infizierten *V. faba* Pflanzen zeigten eine Ca^{2+} -vermittelten Verstopfung des Siebelemente durch Callose- und Proteinablagerungen. Dieser Verschluss der Siebelemente hat neben der Einschränkung der Phytoplasmabewegung einen enormen Einfluss auf die Nährstoffverteilung im Phloem. EFM und TEM Untersuchungen zu *Candidatus* Phytoplasma solani infizierten *S. lycopersicon* Pflanzen zeigten weiterhin eine dramatische Umorganisation von Strukturen des Phloem. Neben den makroskopisch sichtbaren Veränderungen des Pflanzenkorpus, wiesen die Zellen des Phloems eine Reorganisation sowohl des Plasmamembran, des endoplasmatischen Retikulums als auch des Zytoskelettes auf. Durch die Komplexität der Infektion bleibt jedoch der zugrundeliegende Auslöser spekulativ.

Zusammengefasst lassen die Ergebnisse der vorliegenden Arbeit den Schluss zu, dass ein Rezeptor-vermittelten Siebelementverschluss und -reorganisation nach bakterieller Infektion Teil der Pflanze Verteidigungsstrategie gegen die Invasion und Ausbreitung von Erregern ist. Daher nehmen wir an, dass die Beteiligung des Phloem an der pflanzlichen Immunabwehr, neben anderen Strategien, zu einem evolutionären Konzept der pflanzlichen Immunantwort gehört, welche eine sehr effektive Abwehrsystem vervollständigt, um einen möglichen Befall durch mikrobielle Krankheitserreger standzuhalten.

Schlagwörter: Phloem, pflanzliche Immunantwort, Flagellin, Phytoplasmen, Mikroskopie

Table of content

Acknowledgment	I
Abstract	1
Microscopic identification of plant immune responses in phloem tissue of higher plants relating to bacterial infection	1
Mikroskopische Untersuchungen zur pflanzlichen Immunantwort im Phloem höheren Gefäßpflanzen in Antwort auf bakterielle Infektion	2
Table of content.....	4
1. Introduction	8
1.1. Phloem.....	8
1.1.1. Anatomy and function	8
1.1.2. Phloem-based defense mechanism and signaling.....	10
1.2. Phloem-restricted pathogenic bacteria: Phytoplasmas	15
1.2.1. Phytoplasma-related disease symptoms: tactical calculus or defense response? ..	17
1.2.2. Sieve-element immunity in phytoplasma infection	21
1.2.3. Impact of phytoplasma infection on phloem morphology and transport.....	21
1.2.4. Concentrated efforts of plant immunity in phytoplasma-host interaction.....	23
1.3.1. Goal part “Flagellin”	14
1.3.2. Goal part “Phytoplasma”	25
2. Material and Methods	26
2. Deep tissue imaging of phloem-complex	26
2.1. Plant lines and growth conditions	27
2.2. Plant treatment	27
2.2.1. Microbe-associated molecular pattern inoculation.....	27
2.2.2. Phytoplasma infection	28
2.3. <i>In vivo</i> observation.....	29
2.4. Protoplast isolation	30
2.5. Free hand sectioning	31
2.6. Embedding procedures and ultracut sectioning	31
2.6.1. Immunocytochemistry and Transmission Electron Microscopy	31
2.6.2. Conventional Transmission Electron Microscopy	32
2.7. Fluorescent probes and Confocal Laser Scanning Microscopic imaging.....	32
2.7.1. (5)6-carboxyfluorescein diacetate	33
2.7.2. Carboxy-2,7-difluorodihydrofluorescein diacetate.....	33
2.7.3. 4',6-Diamidino-2-phenylindole.....	33
2.7.4. 5-chloromethyl-fluoresceindiacetate/5-chloromethyl-eosin-diacetate.....	33

Table of content

2.7.5. Aniline-Blue	34
2.7.6. 1,2-bis(o-aminophenoxy)ethane-N,N,-N',N'-tetraacetic acid	34
2.8. Fluorescent probes, immunofluorescence staining and Epifluorescence Microscopy imaging ...	34
2.8.1. 4',6-Diamidino-2-phenylindole	34
2.8.2. N-(3- triethylammoniumpropyl) -4- (4- (4- (diethylamino) phenyl) butadienyl) pyridineiumdibromide	35
2.8.3. ER-Tracker Green.....	35
2.8.4. Texas Red conjugated antibody	35
2.9. Immunogold labeling and Transmission Electron Microscopy	36
2.10. Statistical analyzes	36
3. Results	37
3.1. Microscopical examination of artificial contaminated plant samples	37
3.1.1. Spatial and temporal resolution of forisome reaction in intact phloem	37
3.1.1.1. Distribution and reactivity	37
3.1.1.2. Flagellin-triggered forisome reaction.....	41
3.1.2. Observation of mass flow interference.....	43
3.1.3. Signal perception, release and transduction in sieve-element occlusion	44
3.2. <i>In planta</i> observation of natural infection	48
3.2.1. Plant materials and phytoplasma detection by PCR.....	48
3.2.2. Optical phytoplasma detection and mass flow.....	49
3.2.3. Occlusion events and Ca ²⁺ concentration.....	52
3.3. Ultrastructural analysis of plant-pathogen interaction	57
3.3.1. Plant materials and phytoplasma detection by PCR.....	57
3.3.2. Imaging of phytoplasmas by Epifluorescence Microscopy.	58
3.3.3. Sieve-element membrane network visualization by Epifluorescence Microscopy and Transmission Electron Microscopy.....	59
3.3.4. Sieve-element actin and SER network visualization and connections with phytoplasma cells.....	61
4. Discussion	64
4. Observation of phloem immune response to bacterial invasion	64
4.1. Distant flagellin-triggered signal induces Ca ²⁺ -mediated phasic sieve-element occlusion	65
4.1.1. Flagellin-triggered Ca ²⁺ influx leading to forisome reaction.....	68
4.1.2. Flagellin-induced biphasic sieve-element occlusion.....	71
4.1.3. Remote flagellin perception and signal transduction trigger phloem immune response.....	72
4.2. Phytoplasma infection leads to Ca ²⁺ -mediate alteration of phloem morphology and transport ...	75
4.2.1. Phytoplasmas trigger Ca ²⁺ influx leading to sieve-element occlusion.....	78
4.2.2. Phytoplasma infection is associated with re-organization of plasma membrane-ER network and actin structure in sieve elements	80

Table of content

5. List of references	86
6. List of Figures and Tables	104
7. Appendix.....	106
Supplemental Image 1: Autofluorescence and reflection in CLSM imaging.....	106
Supplemental Image 2: Autofluorescence and reflection in CLSM imaging.....	106
Supplemental Image 3: Autofluorescence and reflection in CLSM imaging.....	107
Supplemental Image 4: Autofluorescence and reflection in EFM imaging	107
Supplemental Table 1: Phytoplasma detection in <i>Vicia faba</i> plants	108
Supplemental Table 2: Phytoplasma detection in <i>Solanum lycopersicon</i> plants.....	108
List of own publications	II
Affirmation	III
Curriculum Vitae	IV

1.1. Phloem

475 million years ago plants conquered the land (Wellman *et al.* 2003). However, this important step was first possible with many adaptations of plant structure and reproduction. In the course of evolution, plants developed a cuticula to protect themselves against evaporation, they stabilized their body by strengthening tissue and formed a water independent-reproduction. Furthermore, the organization of the plant changed significantly: plants developed a tripartite body composed of root, shoot and leaves.

The shoot forms the connection between the photosynthetically active leaves and the anchoring and water intake serving roots. Through this division and the ever-increasing distances between the different structures, plants developed specialized vascular tissue to spread nutrients and water throughout their different parts. While the structure and the function of xylem transport system are simple and limited, the phloem system represents a complex vascular tissue.

1.1.1. Anatomy and function

The phloem of vascular plants is composed of highly differentiated, longitudinally-connected sieve tubes (Behnke and Sjolund 1990). To ensure symplastically transport, phloem cell complex undergoes complex differentiation processes during ontogenesis (Esau 1969; van Bel and Hess 2003).

Originated from unequal division of common parental cells, the two parental cells develop different function and morphology (Esau 1969). While the companion cells (CC) are characterized by a dense, physiologically highly active cytoplasm, an enlarged nucleus and increased organelle frequency, the cell of the sieve element (SE) exhibits selective degenerative autolysis, a process which is referred to a partial programmed cell death (van Bel 2003). During this process the nucleus is degraded, the vacuolar membrane breaks down and ribosomes, Golgi apparatus and mitochondria are greatly reduced in number. The mature sieve elements retain only, next to the plasma membrane and a thin marginal cytoplasm area, the endoplasmic reticulum, the cytoskeleton and phloem-specific proteins and plastids (Knoblauch and van Bel 1998; Hafke *et al.* 2013).

Due to the high hydrostatic pressure inside the sieve tubes, the sieve-element cell walls are strongly thickened (Esau and Cheadle 1958). In order to prevent cell isolation, sieve-element cell walls are partial perforated by modified and enlarged pores. To connect the sieve element and the companion cells, highly branched pore-plasmodesma units (PPUs; van Bel 1996), lined with endoplasmic reticulum, enable sufficient transport of substances

Introduction

such as assimilates, proteins (Yoo *et al.* 2002; Mitton 2009; Lattanzio *et al.* 2013) and RNA (Oparka and Santa Cruz 2000; Lucas *et al.* 2001) to provide nutrient and signal to the sieve elements, that lacks important metabolic functions necessary for cell maintenance (van Bel and Knoblauch 2000). At the longitudinal ends, circumscribed groups of sieve pores (van Bel 2003) afford an impermeable pipe that enable a systemic mass flow of water and solutes by a pressure gradient from source to sink (Münch 1930).

The function of the phloem is to ensure symplastic long-distance transport of nutrients from source to sink tissues. The phloem system can be subdivided into three different phloem regions (van Bel 1996). The collective phloem is responsible for loading, the released phloem for unloading. The two phloem types are connected by the transport phloem, representing the largest phloem network (van Bel 2003).

Synthesized in mesophyll cells of photosynthetic-active tissue, sucrose moves down a concentration gradient towards the sieve element through plasmodesmata (Turgeon and Ayre 2005; Schulz *et al.* 2005; Rennie and Turgeon 2009). As the sucrose symplastically reaches the phloem parenchyma-bundle sheath intersection, the sugar loading can species-dependent occur apoplastic or symplastic (van Bel 1993; Rennie and Turgeon 2009; Slewinski and Braun 2010). Moreover, heterogeneous phloem loading and transport allows plants to rapidly adapt to environmental changes, such as biotic and abiotic stresses (Shalitin and Wolf 2000; Shalitin *et al.* 2002; Slewinski *et al.* 2013). In addition to sucrose, polyols (mainly sorbitol and mannitol) as well as oligosaccharides (of the raffinose family) can be loaded into the phloem (Rennie and Turgeon 2009). All types of carbohydrate serve as organic nutrients for energy metabolism. In addition, these molecules can act as a signal involved in growth and development (Koch 2004; Müller *et al.* 2011).

Next to the transport of water and nutrients, this transmission of phloem-mobile signals from source to sinks is an essential part of phloem function. Multiple components of systemic signaling can regulate plant development. Systemic spread of signal molecules like proteins (Le Hir and Bellini 2013), phytohormones (Golan *et al.* 2013), diverse RNA species, such as microRNA (Kehr 2013) and mRNA (Hannapel *et al.* 2013), as well as RNA-binding proteins (Pallas and Gomez 2013) and electrical signal (Fromm *et al.* 2013) differ the mode of action on their target cells.

Next to the role in plant development and reproduction, long-distance transport of signal molecules is known to be essential for plant defense reaction in response to abiotic and biotic stresses.

1.1.2. Phloem-based defense mechanism and signaling

Even though plants lack circularly immune cell system as well as circulating immune receptors, plants are able to generate systemic immune responses. In this context, the phloem seems to play a critical role. Phloem-based defense signaling requires local generation, long-distance translocation, and perception of an inducing signal in remote tissues. Environmental interactions like pathogen infection or abiotic stresses stimulates phloem-mobile defense signaling that in turn induces systemic gene regulation, supposed to be integral parts of induced systemic resistance response of plants (van Bel and Gaupels 2004).

As first line of defense, the plants developed preformed physiological barriers, such as waxy cuticle and strong cell walls, as well as constitutive antimicrobial molecules, such as saponins on the cell surface (Bednarek and Osbourn 2009) and defensins (de Beer and Vivier 2011), to restrict pathogen invasion and growth.

By overcoming this first passive line, intimate plant-microbe interaction occurs, involving several plant and pathogen genes. Perception of pathogen invasion provides basal defense responses in plants (Jones and Dangl 2006). This pattern-triggered immunity (PTI) serves as the first active level of basal disease resistance, sufficient for most harmful pests.

As second active line, immune response is activated in the presence of virulence effector proteins (Boller and He 2009). Release of effector proteins by pathogen invaders into the host cells serves to bypass or overcome PTI by suppressing plant cell death and immunity (Abramovitch *et al.* 2006; Zhang *et al.* 2007b; Block *et al.* 2008; Gohre *et al.* 2008) resulting in effector-triggered susceptibility (ETS). In turn plants sense effector in reliant on cytoplasmic resistance (R) proteins leading to effector-triggered immunity (ETI) to actively defend against host-adapted immune suppression (Nürnbergger *et al.* 2004; Glazebrook 2005; Jones and Dangl 2006).

The co-evolution of violence and defense moreover culminates in pathogenic effector capability to interfere with ETI (Rosebrock *et al.* 2007) resulting again in ETS. This

Introduction

evolutionary arm race (Bent and MacKey 2007) is explained by zick-zack model (Jones and Dangl 2006).

However immune response related to ETI arise faster and stronger than the reactions of the PTI, suggesting that PTI is a weak variant of ETI (Tao *et al.* 2003; Jones and Dangl 2006; Tsuda *et al.* 2009; Tsuda and Katagiri 2010), both seem to share similar network and activate a largely overlapping set of genes (Navarro *et al.* 2004; Zipfel *et al.* 2006 Tsuda *et al.* 2009).

Next to local immune responses such as cell wall reinforcement at the side of infection (Mauch *et al.* 1988), hypersensitive response (HR)-based cell death (Greenberg and Yao 2004; Naito *et al.* 2008; Coll *et al.* 2010), local production of antimicrobial metabolites (Bednarek and Osbourn 2009) and enzymes (Mauch *et al.* 1988) as well as transcriptional reorganization (Ding and Voinnet 2007; Zhang *et al.* 2007), systemic immune responses are known to be initiated during plant-pathogen interaction (Ryals *et al.* 1996; Durrant and Dong 2004; Mishina and Zeier 2007; Dempsey and Klessig 2012).

Upon pathogen attack (van Loon 1985), systemic expression of antimicrobial pathogenesis-related (PR) genes and oxidative burst are induced to develop enhanced systemic acquired resistance (SAR) in remote plant organs (Alvarez *et al.* 1998; Durrant and Dong 2004; Grant and Lamb 2006; Zhang and Zhou 2010). The long-lasting memory effect of SAR (Kuc 1987) and broad-spectrum disease resistance (van Loon and van Strien 1999) are associated with cell survival rather than cell death. SAR is accompanied by the local and systemic accumulation of salicylic acid (Malamy *et al.* 1990; Métraux *et al.* 1990) as well as the production of other mobile signals such as methyl salicylic acid (MeSA), azelaic acid (AzA), jasmonic acid (JA), glycerol-3-phosphate (G3P), defective in induced resistance 1 (DIR1) and abietane diterpenoid dehydroabietinal (DA). The long distant transport of these mobile signal molecules is required for inducing SAR in distinct leaf tissues. Most likely, phloem mass flow provides the transmission of SAR-mediate signal molecules (Durrant and Dong 2004; Park *et al.* 2007; Attaran *et al.* 2009; Jung *et al.* 2009; Mitton *et al.* 2009; Chanda *et al.* 2011; Chaturvedi *et al.* 2012).

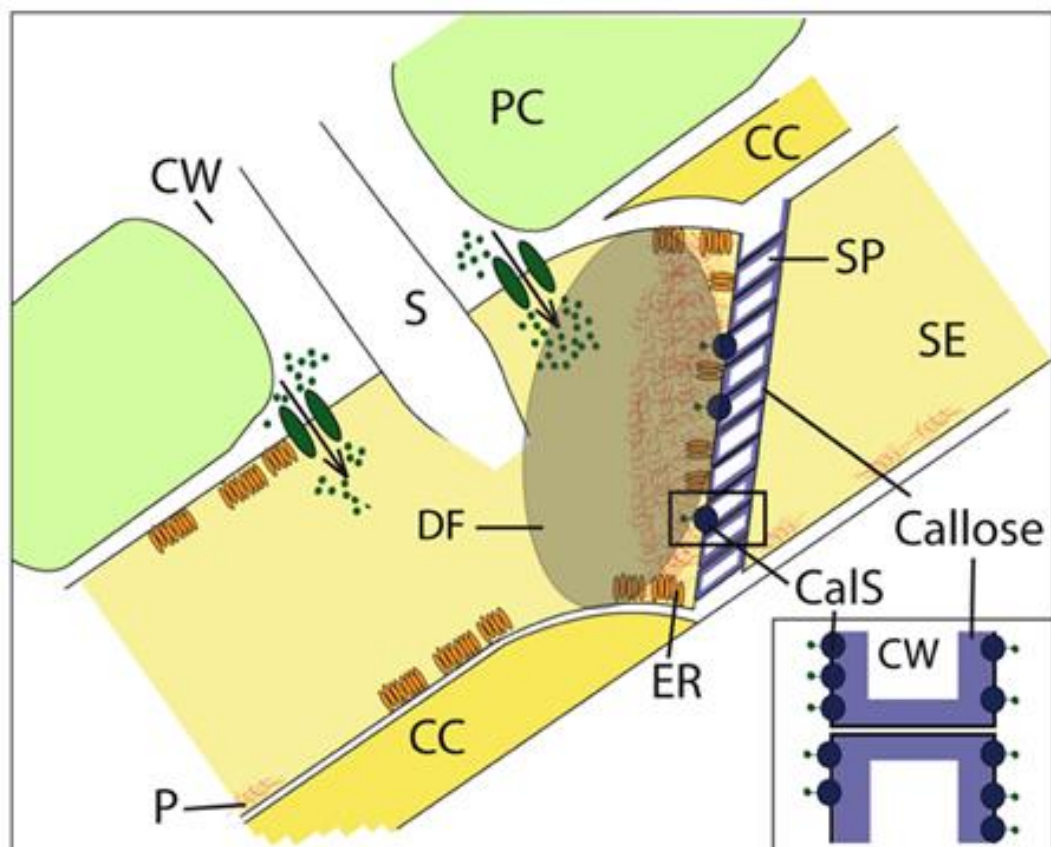
In addition to signal transmission, phloem cells are known to be involved in resistance response to pathogen and insects. Accumulation of defense-related compounds with toxic properties, such as sterols (Behmer *et al.* 2013) and alkaloids (Lee *et al.* 2007), as well as viscous and sticky compounds, like phloem proteins (Gaupels and Ghirardo 2013) interferes with biological pests.

Introduction

Furthermore, direct phloem-based defense mechanisms like sieve tube sealing occur not only in abiotic interactions (Knoblauch *et al.* 2001; Furch *et al.* 2007; 2009; Thorpe *et al.* 2010) but similarly in biotic relationship, provided by aphid styletpenetration (Jekat *et al.* 2013), by fungal attacks (Gaupels *et al.* 2008) or by phytoplasmas (Musetti *et al.* 2010) and other fastidious prokaryotes (Koh *et al.* 2012). Thus, sieve-element occlusion seems to have an effective part in defense response.

In response to stimuli, sieve-element occlusion is initiated by Ca^{2+} influx into the sieve tubes (Hong *et al.* 2001; Knoblauch *et al.* 2003), based on gating of Ca^{2+} -permeable channels (Furch *et al.* 2009; Hafke *et al.* 2009). Reopening of sieve element is achieved by the degradation of callose and rearrangement of phloem proteins, most probably due to the activity of Ca^{2+} -ATPases allowing Ca^{2+} efflux (Kudla *et al.* 2010; Huda *et al.* 2013).

Sieve-element occlusion *via* callose deposition (Furch *et al.* 2007; 2009) and protein plugging (Ernst *et al.* 2012; Knoblauch *et al.* 2012) and most probably incorporating with components, such as sieve element plastids (Ernst *et al.* 2012), leads to impaired mass flow (Knoblauch and van Bel 1998) by sealing the sieve pores.



Introduction

Figure 1: Phloem defense response. In response to injury, Ca^{2+} channels are activated leading to rapid Ca^{2+} influx from the apoplast and most probably from the endoplasmic reticulum. Previously parietal orientated phloem proteins as well as the giant protein body are relocated to the sieve pores. Furthermore, *de novo* synthesized callose seals the sieve pores. Both, callose deposition and phloem protein agglutination lead to Ca^{2+} dependent sieve-element occlusion. CaS: callose synthase, CC: companion cell, CW: cell wall, DF: dispersed forisome, ER: endoplasmic reticulum, P: protein, PC: parenchyma cell, S: stylet; SE: sieve element, SP: sieve plate. Green dots are indicating Ca^{2+} ions; insert shows higher magnification of callose synthase. Illustration Will *et al.* 2013

Phloem proteins are usually parietal orientated or arranged as giant protein bodies to prevent dragging by mass flow and potential clogging of sieve pores (Ernst *et al.* 2012).

In response to Ca^{2+} influx (Fig. 1 green ovals) phloem proteins agglutinate (Fig. 1 DF and red filaments) and function as one of the key players in rapid sieve tube sealing (Furch *et al.* 2007; 2009; Rüping *et al.* 2010; Ernst *et al.* 2011; 2012). In addition to phloem proteins callose is the second key player to accomplish long-lasting sealing of sieve plates (Fig. 1 purple formation). In intact phloem tissue, callose deposition is involved in functioning and development of the sieve elements and mass flow regulation (Barratt *et al.* 2011; Xie *et al.* 2011). Upon Ca^{2+} influx into the sieve element *de novo* synthesis of callose lead to sieve-pore sealing (Furch *et al.* 2007; 2009).

1.3.1. Goal part “Flagellin”:

Contrasting to the progress made in signal transduction and accumulation of defense-related compounds, very little is known about classification of phloem-based immune responses. It is important to understand the mechanisms and reactions of sieve-element cells concerning immune reaction to bacterial infection. Exploring this particular field of pathogen-host interaction will help to understand the complexity of innate and adaptive plant immunity. Prospectively, this knowledge can lead to the development of innovative approaches for crop protection by developing new strategies and specific targets for resistance induction.

Though, the role of phloem as route of systemic signaling in plant immunity is adequately reported (van Bel and Gaupels 2004), the roles of immunity-based modification of phloem function and morphology are insufficiently understood. In particular, information about the participation of phloem cells in pathogen perception and signal initiation as well as the involvement of sieve-element occlusion, as first line of defense, are lacking so far.

Based on this deficiency, the aim of this part of the work was to identify phloem defense mechanism imposed by plant pathogens that are involved in resistance response of plants. Mass flow interruption as well as investigations on the receptor-mediated response of calcium-based phloem reaction was investigated using intact and dissected tissue in Light Microscopy (LM) and Confocal Laser Scanning Microscopy (CLSM). In particular we addressed following questions: (1) Does application of bacterial elicitor induces Ca^{2+} influxes into sieve-elements? And does this (2) induces calcium dependent forisome reaction and (3) sieve-element occlusion? And, (4) does the perception of bacterial elicitor occurs at the sieve-element cells?

1.2. Phloem-restricted pathogenic bacteria: Phytoplasmas

Phytoplasmas are plant-pathogenic prokaryotes belonging to the class *Mollicutes*, a group of wall-less micro-organisms phylogenetically related to the low G+C Gram-positive bacteria (Weisburg *et al.* 1989). Given the high diversity of biological, phytopathological and molecular properties, the monophyletic group of 'Candidatus Phytoplasma', formerly known as mycoplasma-like organisms, is divided in several sub-taxa (IRPCM 2004) although they share a high 16S rRNA gene sequence similarity.

Phytoplasmas have a minimal gene set, variable among phytoplasma strains between 530-1350 kb (Fraser *et al.* 1995; Oshima *et al.* 2004), and lack many genes otherwise considered to be essential for cell metabolism (Marcone *et al.* 1999.) Thus the survival of phytoplasma is probably due to the absorption of host cell substances (Galletto *et al.* 2007).

Because of the absence of a rigid cell wall (Seemüller 1990), phytoplasmas are highly pleomorphic. Thus the size varies between 200 nm to 800 nm in diameter (Kirkpatrick 1992; Lee *et al.* 2000). The bacterial body is surrounded by a double plasma membrane (Verdin *et al.* 2003), predominantly consisting of immunodominant proteins (Berg *et al.* 1999), which represent the majority of total cellular proteins (Kakizawa *et al.* 2004). Based on non-homologous protein sequences in various phytoplasma strains the immunodominant proteins can be classified into 3 types (Bertaccini and Duduk 2009): (1) immunodominant membrane protein (Imp), (2) immunodominant membrane protein A (IdpA) and (3) antigenic membrane protein (Amp).

The occurrence of phytoplasmas in the host plants is restricted to the sieve elements. In nature phytoplasmas are transmitted to healthy plants by sieve-tube sap feeding insects in a persistent manner (Hogenhout *et al.* 2008). The vector-borne transmission of phytoplasma relies on phloem-sucking insects (Weintraub and Beanland 2006), such as *Cicadellidea* (leafhoppers), *Fulgoridea* (cicada), *Psyllidae* (psyllids) and *Aphidoidea* (plant lice). Once a vector fed from sieve elements of infected plants, phytoplasmas enter the vector through the insect stylet (Fig. 2 A). Inside the vectors the phytoplasmas move through the midgut and are thereby absorbed into the hemolymph (Christensen *et al.* 2005). This leads to a systemically infection of the vector (Fig. 2 B). After replication inside the vector the phytoplasmas invade the salivary glands (Christensen *et al.* 2005). Inside the saliva, the phytoplasmas are transmitted to other plants by vectors feeding from the

Introduction

phloem (Fig. 2 C). Inside the sieve elements the phytoplasmas moved systemically through the plant and lead to phytoplasma-related symptoms (Fig. 2 D).

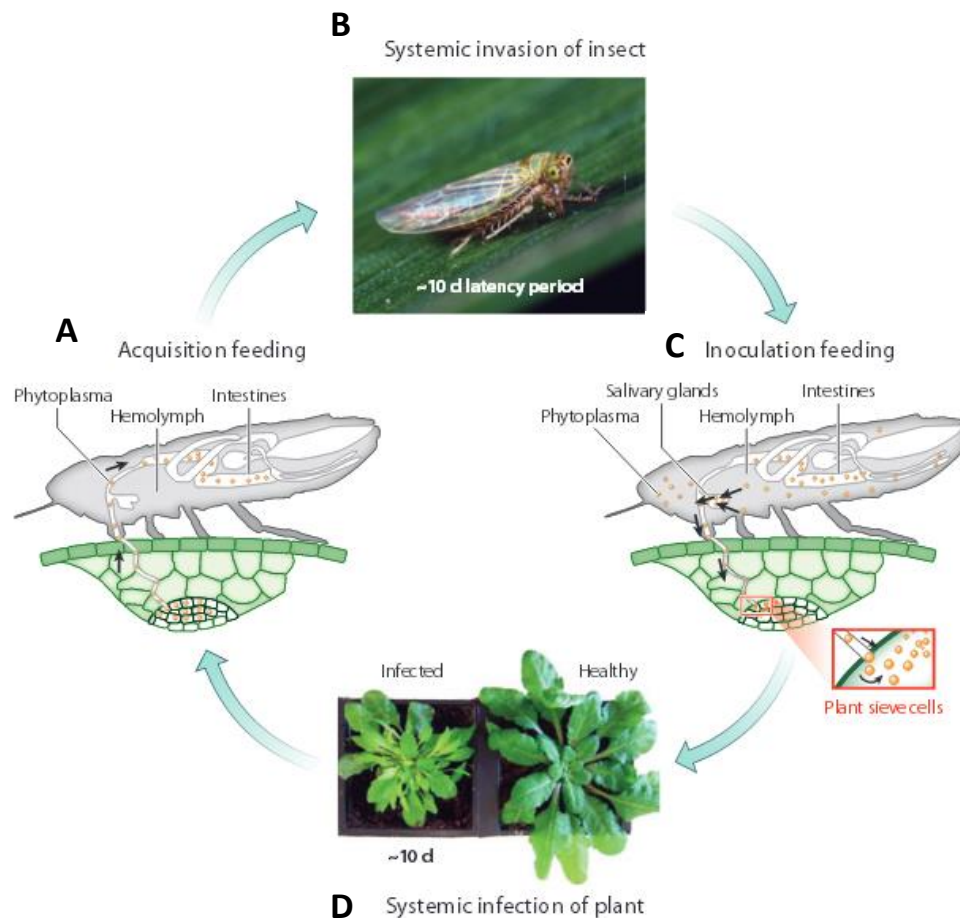


Figure 2: Vector-borne phytoplasma transmission. A) Diverse members of the Hemiptera order serve as vectors for phloem-restricted phytoplasma pathogens. By feeding from infected host phloem, the phytoplasmas enter the intestine. B) Inside the vector, the phytoplasmas multiply and systemically infect the vector by invading the hemolymph. C) After migration of the phytoplasmas into the salivary glands, infected vector transmit the phytoplasmas inside the host plant *via* phloem sucking. D) Inside the host phytoplasmas spread systemically and lead to typical disease symptoms. Illustration Sugio *et al.* 2011

Since the first plant diseases symptoms were related to phloem colonizing bacteria (Doi *et al.* 1967) several hundred of diseases affecting economically important crops, such as ornamentals, vegetables, fruit trees and grapevine, before thought to be associate to viral agents, were related to phytoplasma infection (Lee *et al.* 2000).

Despite their economic importance, progress on deciphering the plant-phytoplasma interactions has been slow as compared to other plant bacterial pathogens. To date, the physiological relationship between phytoplasmas and their hosts has remained largely unexplored (Hogenhout *et al.* 2008) since methods for *in vitro* culture of phytoplasmas are

not yet available, except of one that awaits further confirmation of feasibility (Contaldo *et al.* 2012). The current lack of technique keeps the door shut to transform or genetically modify phytoplasmas, or simply to isolate individual strains from mixtures present in nature (Seemüller *et al.* 2013).

1.2.1. Phytoplasma-related disease symptoms: tactical calculus or defense response?

Depending on phytoplasma strain, plant species, season and plant development stage (O'Mara *et al.* 1993), symptoms, such as incomplete lignification of canes (Milkus *et al.* 2004), short internodes and increased cell proliferation of auxiliary shoots (Lee *et al.* 1997), increase in size of the internodes looking like witches broom (Lee *et al.* 2000), flower abortion by phyllody (Dafalla and Cousin 1988) and virescence (Lee *et al.* 2000), curling and discoloration of leaves (Munyaneza *et al.* 2011) with intervein yellowing or reddening (Wahid and Ghani 2007) as well as vein swelling (Loebenstein *et al.* 2009) and stunting (Bertaccini 2007), lead to typical phenotype of phytoplasma infected plants.

Symptoms are known to be related to reduced photosynthesis rate (Bertamini and Nedunchezian 2001; Bertamini *et al.* 2002 a; b; 2004; Endeshaw *et al.* 2012) by accumulation of starch and disorganization of thylakoids (Musetti 2006) as well as stoma closure (Matteoni and Sinclair 1983; Vitali *et al.* 2013), misbalance of hormones (Leon *et al.* 1996; Tai *et al.* 2013) and altered gene regulation (Pracros *et al.* 2006). Furthermore, redistribution of carbohydrate such as anomalous accumulation of carbohydrates in source leaves, reduction in sink leaves and the roots (Lepka *et al.* 1999) and disrupted mass flow (Kartte and Seemüller 1991) are known to be associated to typical phytoplasma symptoms. Many of these symptoms are believed to be induced by pathogen-host specific interaction since the resulting symptoms are, with few exceptions (Himeno *et al.* 2014), beneficial for phytoplasma viability and spread by insect vectors (Sugio *et al.* 2011).

Phytoplasma genes, which are important in the relationship with host plants and/or insect vectors, seem to primarily encode small proteins (effectors) that target host cells (Hogenhout *et al.* 2008; Sugio *et al.* 2011). Effector proteins, both membrane-associated and cytoplasm released proteins, can interact directly with vector and host to influence developmental processes (Hogenhout *et al.* 2008).

Introduction

Unlike plant pathogens that colonize apoplastic area, intracellular phytoplasmas do not need protein secretion systems like type III secretion system present in other bacteria such as *Pseudomonas* spp. (Block *et al.* 2008) to release proteins from the bacterial body (Hogenhout *et al.* 2008). Instead, phytoplasma proteins are more likely secreted by the Sec secretion system. Genes coding SecA, SecY and SecE proteins, all essential components of the Sec translocation system, were found in diverse phytoplasma strains and known to be functional (Kakizawa *et al.* 2004; Bai *et al.* 2006; Lee *et al.* 2006). Sec translocation system among others includes transmembrane protein forming pore and the peripheral Adenosinetriphosphatase (ATPase), latter providing the motor of the export machinery. The ATP-dependent translocation of proteins secreted by the Sec pathway can be described in three stages: (1) Targeting of characteristic signal sequence at the N-terminal of the unfolded secretion protein. (2) Transmembrane crossing through a channel in the cytoplasmic membrane and (3) release of the protein into the ambient area (Economou 1999). Once inside the host cytoplasm, additional periplasmic factors trigger required protein fold into their correct conformation (Rizzitello *et al.* 2001). The proteolytic progressing of the secreted proteins by plant host factor (Matsubayashi 2011) enables the resulting small peptides to function as signaling molecules to interfere with host developmental processes (Sugawara *et al.* 2013).

Because of the presence and the cleavage of the N-terminal signal sequence, an antigen membrane protein (AMP) is suggested to be transported by the Sec secretion system (Kakizawa *et al.* 2004). As above mentioned, the immunodominant membrane protein, one of the most abundant proteins in phytoplasmas, was identified in several phytoplasma strains (Kakizawa *et al.* 2006). After released by the phytoplasmas it remains at the bacterial surface, exposed to the environment, and interacts with vector cytoskeleton (Suzuki *et al.* 2006; Galetto *et al.* 2011) or plant-host actin filaments (Boonrod *et al.* 2012) indicating the interaction to be involved in phytoplasma transmissibility. The failure to interact with non-hosts or -vectors indicates phytoplasma species-specificity (Barbara *et al.* 2001; Suzuki *et al.* 2010).

Based on the presence of N-terminal signal peptides several secreted proteins are known to target host structures. Such, the secreted phytoplasma effector AY-WB protein 11 (SAP11) was found to have a nuclear localization signal in the host (Bai *et al.* 2009). Once inside the host, SAP11 mediates phenotype modification of the plant body that makes the host more attractive to the vector and violate plant immune response to the advantage of

Introduction

the insect vector (Sugio *et al.* 2011) and growth of bacterial pathogen (Lu *et al.* 2014). While SAP11 targets host structures beyond the phloem, the effector protein SAP54 leads to alteration of flower development resulting in leaves like flowers (MacLean *et al.* 2011) and tenu-su inducer (TENGU), inducing witches` broom effect (Hoshi *et al.* 2009), are proposed to target directly the phloem or neighboring cells (MacLean *et al.* 2014). Unloading of effector proteins is assumed to be achieved by plasmodesmatal transport (Hogenhout and Loria 2008). While it is reported that most effector proteins are less than 40 kDa (Bai *et al.* 2009) the size exclusion limit in the sink tissue is about 50 kDa (Imlau *et al.* 1999), permitting effective protein transport.

The morphological deformation effect and down regulation of immune responses implies the secreted proteins to act as virulence factors (Hoshi *et al.* 2009; MacLean *et al.* 2011; Sugio *et al.* 2011) inside and beyond the phloem cells.

Recent study focused on the impact of secreted and membrane-associated proteins on alteration of plant morphology and defense response lacks the information about the origin of the occurring symptoms. While the structural effect of the effector can be driven by the phytoplasma (compatible interaction) to manipulate the plant metabolism as beneficial for the pathogen growth and distribution (Sugio *et al.* 2011; Lu *et al.* 2014), host plant may activate resistance genes, able to detect the presence of phytoplasma virulence factors to initiate an immune response (incompatible interaction), leading also to the morphological alteration (Zhong and Shen 2004).

Usually pathogen effectors target host molecules that are involved in plant immunity to suppress immune reaction and in turn allow colonization of hosts (Guo *et al.* 2009). In presence of compatible resistance genes, plant initiate effector-triggered immunity (ETI) to defend against pathogen invasion (Jones and Dangl 2006; Nürnberger *et al.* 2004). In phytoplasma-host interaction it is unknown whether effector proteins activate ETI or further interfere with ETI during effector-triggered susceptibility (ETS) by acquiring additional effectors (Jones and Dangl 2006). Even though pathogenesis-related (PR) proteins are increased in diseased and symptomatic tissues (Zhong and Shen 2004), the high amount of phytoplasmas, the severe host symptoms and the suppression of salicylic acid-mediated defense responses during infection tend to favor insufficient plant immunity or ETS. Moreover, effectors may be non-visible for plant immunity and thus serve as

Introduction

signaling molecule to actively manipulate host immunity and so causing disease symptoms.

Indeed, phytoplasmas lack cell wall and genes coding for flagellin, thus no surface microbe-associated molecular pattern (MAMPs), like flg22, a 22-amino acid sequence of flagellin, are present in the host-pathogen interaction (Lee *et al.* 2000; Bertaccini and Duduk 2009). Nonetheless, phytoplasmas produce intracellular proteins, such as coldshock protein (CSPs; Tran-Nguyen *et al.* 2008; Wang *et al.* 2010; Andersen *et al.* 2013) and elongation factor (EF-Tus; Schneider *et al.* 1997; Berg and Seemüller 1999; Kouï *et al.* 2003) that can act as MAMPs in pattern-triggered immunity (PTI) in host-phytoplasma interaction. During PTI microRNAs (miRNA), among others, target auxin receptor mRNAs and thus negatively regulate auxin signaling (Navarro *et al.* 2006; Hoshi *et al.* 2009; Robert-Seilaniantz *et al.* 2011) by post-transcriptional gene silencing to restrict pathogen growth. Both, phytoplasma infection (Ehya *et al.* 2013; Zhao *et al.* 2013; Gai *et al.* 2014) as well as expression of effector proteins (Lu *et al.* 2014) in transgenic plants leads to host-pathogen-specific increased transcription of phytoplasma-responsive miRNAs, such as miRNA399 and miR393, the latter known to be also induced by flg22 (Navarro *et al.* 2006). Thus secreted proteins as well as released MAMPs induce phytoplasma triggered PTI to participate in basal resistance against bacterial pathogens.

Experiments focusing on regulation of diverse miRNA after phytoplasma infection, like down-regulation of miR166h-3p targeting III HD-Zip protein 6 involved in shoot meristem and vascular development or up-regulation of miR529b targeting chlorophyll synthase gene, lead to the conclusion that due to up- and down-regulation of miRNA, disorder symptoms can be caused by regulation of specific targets (Gai *et al.* 2014). Furthermore, studies on the impact of auxin signaling on regulation on plant developmental processes showed hormone balances to be involved in modification of plant architecture by cell proliferation and development (Nacry *et al.* 2005; Jain *et al.* 2007; Pérez-Torres *et al.* 2008). This indicates the phytoplasma-induced miRNAs-based auxin modification as possible effects on symptoms, as in the past, alteration in auxin signaling due to phytoplasma infection has been supposed to be the driven force in phytoplasma-related symptoms (Musetti 2010). Recent studies on miRNA overexpression in transgenic plant now confirming the assumption that typical phytoplasma-related symptoms, such as high degree of branching and the formation of small leaves, appear due to plant immune reaction in response to phytoplasma infection (Shikata *et al.* 2012; Ehya *et al.* 2013).

These results underline the role of the plant immune response not only in defense signaling against phytoplasma but likewise in architectural modification of host structure due to alteration of hormones, metabolism and development balances.

1.2.2. Sieve-element immunity in phytoplasma infection

It has long been assumed that the cells of the sieve elements are not directly involved in initiation of immune response to pathogenic infection, since there are a few drawbacks.

While PRR-mediate immune responses occur in the extracellular space (Bent and Mackey 2007), phytoplasma presence is restricted to the intracellular space of sieve-element cells. Thus phytoplasmas have the ability to hide from host recognition and immune defense reaction inside the phloem cells. Yet, they fail to remain undetected. One possible reason is the release of effector proteins into the cytoplasm, which can be recognized intracellularly (Bent and Mackey 2007) unlikely the sieve-element cells do not contain significant organelles like a nucleus, chloroplasts or the Golgi-apparatus (Knoblauch and van Bel 1998) indispensable for most plant immune responses. Again, they fail to remain undetected or succeed to be recognized.

Probably, recognition occurs not directly in the sieve elements but most likely in the neighboring cells since effector proteins are produced in the phloem, but accumulate in nuclei of cells beyond the phloem (Bai *et al.* 2009). Released effector proteins or MAMPs induce signaling in adjacent cells, which in turn access the phloem cells to initiate immune responses affecting plant development (Hoshi *et al.* 2009).

1.2.3. Impact of phytoplasma infection on phloem morphology and transport

Not only increased attractiveness in favor of the vector is triggered by phytoplasma-induced macroscopical symptoms, but also microscopically anatomical aberration inside the phloem occurs in infected plants. Since phytoplasmas are not evenly distributed over the sieve tubes (Faoro 2005), despite the systemic spread *via* the phloem, phloem impairment and the subsequent development of the disease symptoms cannot be simply explained by the presence of phytoplasmas plugging the sieve elements, but also by the impact of phytoplasma-specific effector-based alteration of plant cells morphology and function (Hogenhout *et al.* 2008). Regardless whether the effector proteins are released and unloaded or remain bound to/in the bacterial body, both mechanism induce signals by targeting host molecules in infected area and *via* transport through phloem spread systemically.

Introduction

Several studies demonstrated that phytoplasma infection induces important cytological and physiological modifications in the phloem of host plants, in several cases severely affecting phloem transport (Braun and Sinclair 1978; Kartte and Seemüller 1991; Lepka *et al.* 1999; Maust *et al.* 2003). Impaired function due to mass flow blockage and phloem cytological modification such as sieve-element necrosis (Braun and Sinclair 1978), phenolic incorporation (Musetti *et al.* 2000), abnormal callose deposition at the sieve plates (Christensen *et al.* 2005), phloem lignification (Gatineau *et al.* 2002) as well as disordering and thickening of sieve-element walls (Musetti *et al.* 2000) and collapse of sieve elements and companion cells (Kartte and Seemüller 1991), lead to alteration of host structure and result in symptoms such as reduction of productivity, general decline, reduced plant vigor (Kartte and Seemüller 1991).

It has been speculated that mechanisms involved in phloem impairment could differ between pathosystems and vary with the plant susceptibility to infection (Kartte and Seemüller 1991; Musetti and Favali 1999). Due to sieve-tube blockage, accumulation of carbohydrate in source leaves and reduction in sink leaves and in roots (Lepka *et al.* 1999) occurs. Sieve-element occlusion would be among the key events leading to formation of physical barriers preventing movement of phytoplasmas *in planta* (Musetti *et al.* 2010) or either represents the first beneficial proceedings of phytoplasma to accumulate nutrition (Chen 2014).

Expression of genes, responsible for callose deposition in sieve tubes is finely tuned. This is exemplified by the role of Glucan Synthase-Like 7 activity in normal sieve-element maturation as well as in the response to wounding (Barratt *et al.* 2011; Xie *et al.* 2011) showing that callose production is a balance act for plants. An analogous trade-off event must occur in infected plants: massive callose deposition restricts host colonization by phytoplasmas, but at the same time impedes photoassimilate transport. A high degree of sieve-tube occlusion, required to permanent immure of phytoplasmas is accompanied by an appreciable up-regulation of callose synthase, as reported in phytoplasma-infected apple plants and grapevines (Musetti *et al.* 2010; Santi *et al.* 2013).

It is known that sieve plates are plugged by proteins in response to mechanical injuries prior to callose deposition (Furch *et al.* 2007; 2010). Structural proteins in sieve tubes have been observed for a long time (Cronshaw and Sabnis 1990). Some of these proteins, later named sieve element occlusion (SEO) proteins (Pelissier *et al.* 2008), are involved in

Introduction

sieve-tube plugging. In Fabaceae, SEOs are aggregated in giant protein bodies called forisomes (Knoblauch *et al.* 2001). In response to different stresses, such as wounding, burning and cooling, forisomes undergo a conformational change from a condensed to a dispersed state, which plugs the sieve plates and prevents loss of photoassimilates (Knoblauch *et al.* 2001; Furch *et al.* 2007; Thorpe *et al.* 2010). Genes encoding SEO protein components do not only occur in Fabaceae (Pelissier *et al.* 2008), but also appear to be widespread among dicotyledonous plants (Rüping *et al.* 2010). Preliminary gene expression analyzes for SEO protein components revealed a tendential up-regulation in phytoplasma-infected apple trees as compared to healthy ones (Musetti *et al.* 2011) indicating potential involvement in phloem occlusion in response to phytoplasma colonization.

Callose synthesis as well as phloem-protein aggregation are Ca^{2+} -dependent phenomena (Köhle *et al.* 1985; Knoblauch *et al.* 2001) triggered by Ca^{2+} influx into the sieve elements (Furch *et al.* 2007; 2009; 2010). Occlusion events (Musetti *et al.* 2008) thus suggest that phytoplasma infection induces gating of Ca^{2+} channels and consequent influx of Ca^{2+} into sieve elements (Rudzińska-Langwald and Kamińska 2003; Musetti *et al.* 2008).

1.2.4. Concentrated efforts of plant immunity in phytoplasma-host interaction

Although plant immunity reaction seems to be insufficient most of the infection time, leading to typical symptoms, a spontaneous remission of symptoms, called recovery, occurs in previously infected plants in nature (Caudwell 1961). A complete or partial, temporary or permanent recovery of symptomatic plants takes place in different species and regions (Osler *et al.* 2003).

Based on environmental factors (Braccini and Nasca 2008) and plant variants (Bellomo *et al.* 2007) infection with arbuscular mycorrhizal fungi (Lingua *et al.* 2002), plant growth promoting rhizobacteria (D'Amelio *et al.* 2007), endophytic fungi (Musetti *et al.* 2007) and bacteria (Lherminier *et al.* 2003) are supposed to provoke recovery. Next to natural induction, artificial trigger such as abiotic stress, like mechanical injury (Osler *et al.* 1993; Borgo and Angelini 2002; Zorloni *et al.* 2002; Romanazzi and Murolo 2008), or non-specific resistance inducer, like Indole-3-Acetic Acid (Curković Perica 2008) or Acibenzolar-S-Methy (Romanazzi *et al.* 2009) can lead to decreased symptom severity in infected plants.

The absence of symptoms is associated with the disappearance of phytoplasmas in the crown probably due to restricted motility and agglutinations and degeneration of

Introduction

phytoplasma cells in the aerial parts, which are still present and alive in the roots (Carraro *et al.* 2004). Induction of biochemical defense responses in the phloem, like accumulation of H₂O₂ in sieve elements (Musetti *et al.* 2005) and increased Ca²⁺ concentration (Musetti *et al.* 2008) as well as complete sieve tube-sealing by accumulation of proteins and callose (Musetti *et al.* 2010; Santi *et al.* 2013) are the basis of recovery (Osler *et al.* 1999; Musetti *et al.* 2004; 2007) and lead to host-induced antagonizing phytoplasma virulence (Musetti *et al.* 2005).

1.3.2. Goal part “Phytoplasma”:

Knowledge about physiological plant-phytoplasma interactions is essential to understand the progression of phytoplasma disease symptoms and the molecular and ultrastructural impact on phloem cells. Profound knowledge in the respective field of phytoplasma-host interaction will help to understand phytoplasma virulence mechanism(s). In consequence, this can lead to the development of innovative control strategies aimed to prevent losses in crop yields related to phytoplasma diseases. Next to phytoplasma-resistant varieties and recovery induction, innovative technologies, such as RNAi (Zhang *et al.* unpublished), antimicrobial peptides (Du *et al.* 2005) and plantibody (Le Gall *et al.* 1998) specifically expressed in grafted phloem cells (Zhao *et al.* 2004; Maghuly *et al.* 2008) targeting Sec-dependent secretion system can lead to an effective control of phloem pathogen motility and related host symptoms.

Even if the macroscopic consequences of phytoplasma activity in the host plants are amply described (Bertaccini 2007), phytoplasma pathogenic effects on the sieve-element ultrastructure are poorly investigated. In particular, fundamental phytopathogenic traits such as mass flow interruption, adhesion capability to sieve-element membrane, as well as the relationship with the sieve-element endoplasmic reticulum and actin are lacking so far. As unequivocal *in vivo* evidence for phytoplasma-mediated sieve-tube occlusion is lacking thus far, one aim of this work was to design and optimize a method to perform *in vivo* observation of the phloem in phytoplasma-infected intact plants. Deposition of callose and phloem-protein conformation (forisomes), as well as phloem mass-flow, were examined and compared between healthy and phytoplasma-infected plants by using Confocal Laser Scanning Microscopy (CLSM). In particular, we evaluated if phytoplasmas induce Ca^{2+} influx leading to occlusion by callose deposition and/or protein plugging and inherent impairment of mass flow. Since phytoplasmas presumably may exert their action on plants by binding to sieve-element components (Christensen *et al.* 2005) second part of this work focused on the following questions: (1) Do phytoplasmas attach to the sieve-element plasma membrane and (2) what are the structural characteristics of such a link? (3) Do phytoplasmas interact with sieve-element actin or (4) sieve-element endoplasmic reticulum? To address these questions, the sieve-element plasma membrane–endoplasmic reticulum–actin network continuum was examined in relation to phytoplasma localization in healthy and phytoplasma-infected tissue by combined use of embedded tissue for Epifluorescence (EFM) and Transmission Electron Microscope (TEM).

2. Deep tissue imaging of phloem-complex

Through its protected position inside the plant corpus, the phloem is a difficult candidate for microscopical investigations (Truernit *et al.* 2014).

The most appropriate solution is the so-called “*in vivo* observation” method, developed by Knoblauch and van Bel (1998). This non-destructive technique allows the examination and imaging of *in planta* processes. Furthermore, *in vitro* methods like sieve-element protoplast isolation and precise sectioning of fresh plant material can reflect proximate natural conditions. Conducting analysis using embedded tissue and semi/ultrathin sectioning furthermore gains knowledge into ultrastructural characterization of vascular tissue.

In this work, an integrated approach using combination of *in vivo* and *in vitro* experiments was set up using Light (LM), Confocal Laser Scanning (CLSM), Epifluorescence (EFM) and Transmission Electron Microscopy (TEM) in order to obtain a concept of the processes occurring in the phloem that occur during a pathogen infection.

2.1. Plant lines and growth conditions

Vicia faba ('cv Witkiem major' and 'cv Aguadulce supersimonia') and *Solanum lycopersicum* plants ('cv Micro-Tom') plants were cultivated in pots in a greenhouse under standard conditions (21° C, 60-70% relative humidity, and a 14/10 h light/dark period). For growth in soil, *Arabidopsis thaliana* Col-0 and *fls2-24* (*Arabidopsis* Biological Resource Center) seeds were germinated and grown in growth chambers (21° C, 60-70% relative humidity, and a 16/8 h light/dark period). Supplementary lamp light (model SONT Agro 400 W; Philips Eindhoven, The Netherlands) led to an irradiance level of 200–250 $\mu\text{mol}^{-2} \text{s}^{-2}$ at the plant apex. Plants were used in the vegetative phase just before flowering. For experiments, mature leaves with a size of approximately 8x6 cm (*V. faba*), 6x3 cm (*S. lycopersicum*) and 4x1.5 cm (*A. thaliana*) were used.

2.2. Plant treatment

2.2.1. Microbe-associated molecular pattern inoculation

For experiments with artificial stimulus, plants were elicited with flagellin (flg22) synthetic peptides (GenScript, USA) solved in apoplasmic buffer (see 2.3.). *A. thaliana* leaves were pressure infiltrated 2 cm from the leaf tip, 0.5 cm right and left of the midrib between the veins (Fig. 3).



Figure 3: Technical procedure of pressure infiltration. A) Stabilization of the upper side of the leaf. B) Infiltration of the liquid with gentle pressure on the syringe. C) Infiltration zones left the main vein in the center of the leaf (red circle).

One finger on the upper side of the leaf stabilized the leaf while placing a syringe (without a needle) on the lower surface of the leaf (Fig.3 A). The solution was infiltrated with a gentle pressure on the plunger (Fig. 3 B), filling the intercellular space (Fig. 3 C). As a control, plants were infiltrated with apoplasmic buffer. For *in vivo* experiments *V. faba*

Material and Methods

plants were treated by flooding the observation window with flg22 or buffer as a control. Protoplast reaction was induced *via* replacing the bath medium by a solution containing additional flg22. As a control, bath medium (see 2.4.) was exchanged by fresh medium.

2.2.2. Phytoplasma infection

For *in planta* experiments *V. faba* plants were infected with the phytoplasma associated to Flavescence Dorée (FD) of grapevines, '*Candidatus* Phytoplasma vitis' ('*Ca. P. vitis*') strain C (16SrV-C; Lee *et al.* 2004). FD-infective leafhoppers (*Euscelidius variegatus*) were caged to inoculate 15-day-old broadbean seedlings in a controlled environment insectarium (22° C, 16 h photoperiod) for a week. Test plants were sprayed with an insecticide solution after the inoculation period and kept in a greenhouse for further growth. Control plants were not exposed to leafhoppers. Phytoplasma presence was assessed by real-time (RT)-PCR analyzes. Total DNA was extracted from 1 g frozen leaf midribs according to Doyle and Doyle (1990). Primers were designed on the 16S rRNA gene of '*Ca. P. vitis*' (accession N° AY197645, M. Martini, unpublished data) and were 16S(RT)F1 (5'-TTCGGCAATGGAAACT-3') and 16S(RT)R1 (5'-GTTAGCCGGGGCTTATTAAT-3'). RT-PCR analyzes were performed in a DNA Engine Opticon[®]2 System using 40 ng of DNA, 10X PCR Buffer, dNTPs 2.5 mM, MgCl₂ 25 mM, primers 300 nM each, 0.15 µl of AmpliTaq Gold DNA Polymerase 5 U/µl (Applied Biosystems, USA) and 10X SYBR[®] Green I in DMSO (Molecular Probes, Invitrogen, USA) in a total volume of 25 µl. Thermocycling was performed using the following conditions: 11 min at 95 °C, 40 cycles of 15 sec at 94 °C, 15 sec at 57° C, 20 sec at 72° C, 8 min at 72° C. The melting curve was performed with a ramp from 65 to 95° C at 0.2° C/sec.

Next to *V. faba*, *S. lycopersicum* plants were infected with the stolbur phytoplasma '*Candidatus* Phytoplasma solani' ('*Ca. P. solani*' subgroup 16 SrXII-A, Quaglino *et al.* 2013), by grafting. Shoot tips from naturally infected *S. lycopersicum* plants grown in the field were used as scions and grafted onto healthy *S. lycopersicum* plants grown from seeds in a greenhouse. Control plants were growing without grafting. Phytoplasma presence was assessed in randomly collected leaf samples by real time RT-PCR analyzes. Total RNA was extracted from 1 g of frozen leaf midribs using RNeasy Plant Mini Kit (Qiagen GmbH, Germany). RNAs were reverse-transcribed using a QuantiTect Reverse Transcription Kit (Qiagen GmbH, Germany) with random hexamers, following the manufacturer's instructions. Real time RT-PCR analyzes were performed using the primers 16S stol F2/R3 based on the 16S rRNA gene of '*Ca. P. solani*' (accession n° AF248959, Santi *et al.* 2013). Real time RT-PCR reactions were set up with 2X Sso Fast™

Material and Methods

Eva Green[®] Supermix (Bio-Rad Laboratories Co., USA), primers at 400 nM each, and 10 ng of cDNA in a total volume of 10 μ l. The reactions were performed in a CFX96 Real Time PCR Detection System (Bio-Rad Laboratories Co., USA) using the following conditions: 95° C for 2 min, 40 cycles of 95° C for 15 sec and 60° C for 1 min. The melting curve was performed with a ramp from 60 to 95° C.

2.3. In vivo observation

For *in vivo* observation of sieve tubes, cortical cell layers were removed from the lower side of the main vein of a fully expanded leaf, still attached to an intact plant, to create an observation window (Fig. 4; Knoblauch and van Bel 1998).

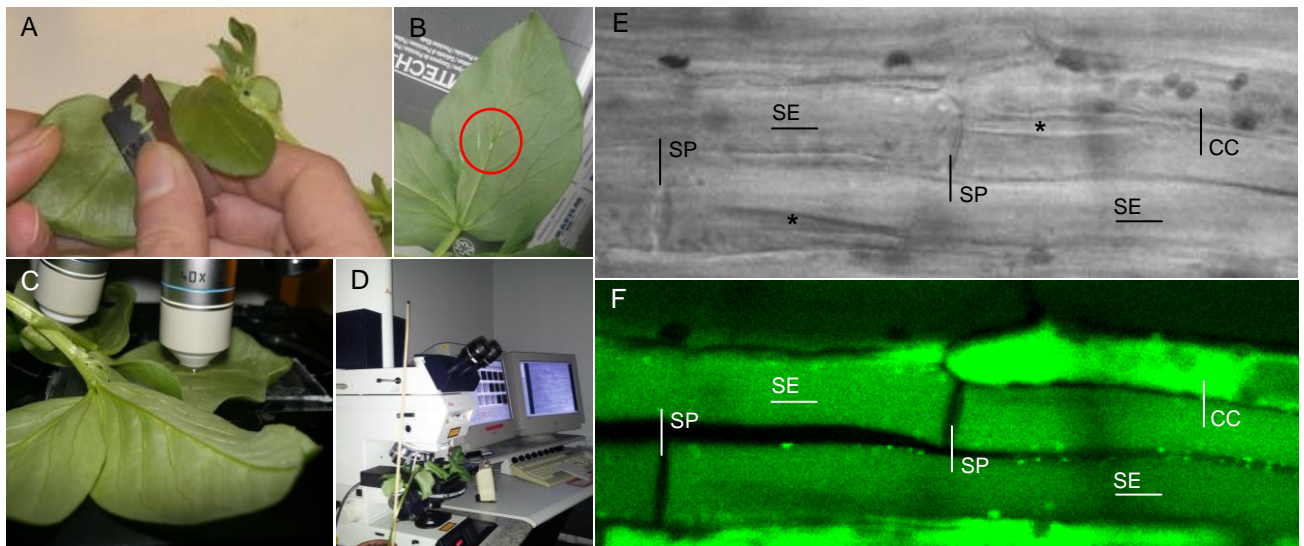


Figure 4: Technical procedure of *in vivo* observation method. A) Cut off the cells of the midrib down to the phloem using a razor blade. B) Cover the resulting wound (red circle) with apoplasmic buffer. C) Stick the leaf to a glass slide. D) Attach the experimental device including the intact plant to the microscope. Observe the phloem in transmission (E) or fluorescence mode (F).

Access to the phloem was created by removing the cortical layer of the main vein by longitudinal slicing with a fresh razor blade (Fig. 4 A). After the exact number of cell layer was removed (one less, unclear image; one more, phloem injury) the open wound was protected with apoplasmic physiological buffer containing 1 mM $\text{CaCl}_2 \cdot 2\text{H}_2\text{O}$, 2 mM KCl, 50 mM mannitol, 2.5 mM $\text{MES} \cdot \text{H}_2\text{O}$, 1mM $\text{MgCl}_2 \cdot 6\text{H}_2\text{O}$, pH 5.7 (Fig. 4 B). The leaf was adhered to a glass slide (Fig. 4 C) and attached to a microscope (Fig. 4 D). After the intactness of the phloem tissue was checked microscopically, transmission light (Fig. 4 E)

Material and Methods

as well as a set of vital fluorescent probes (Fig. 4 F) was used to observe phloem anatomy and reaction.

2.4. Protoplast isolation

For analyzes at single cell-level, protoplast of *V. faba* plants were isolated as described in Hafke *et al.* 2007 with the following modifications (Fig. 5). For coarse mechanical isolation of stem phloem strands, tangential tissue sheets were sliced of the split internode and separated by threadbarring the internodes (Fig. 5 A; Knoblauch *et al.* 2003).

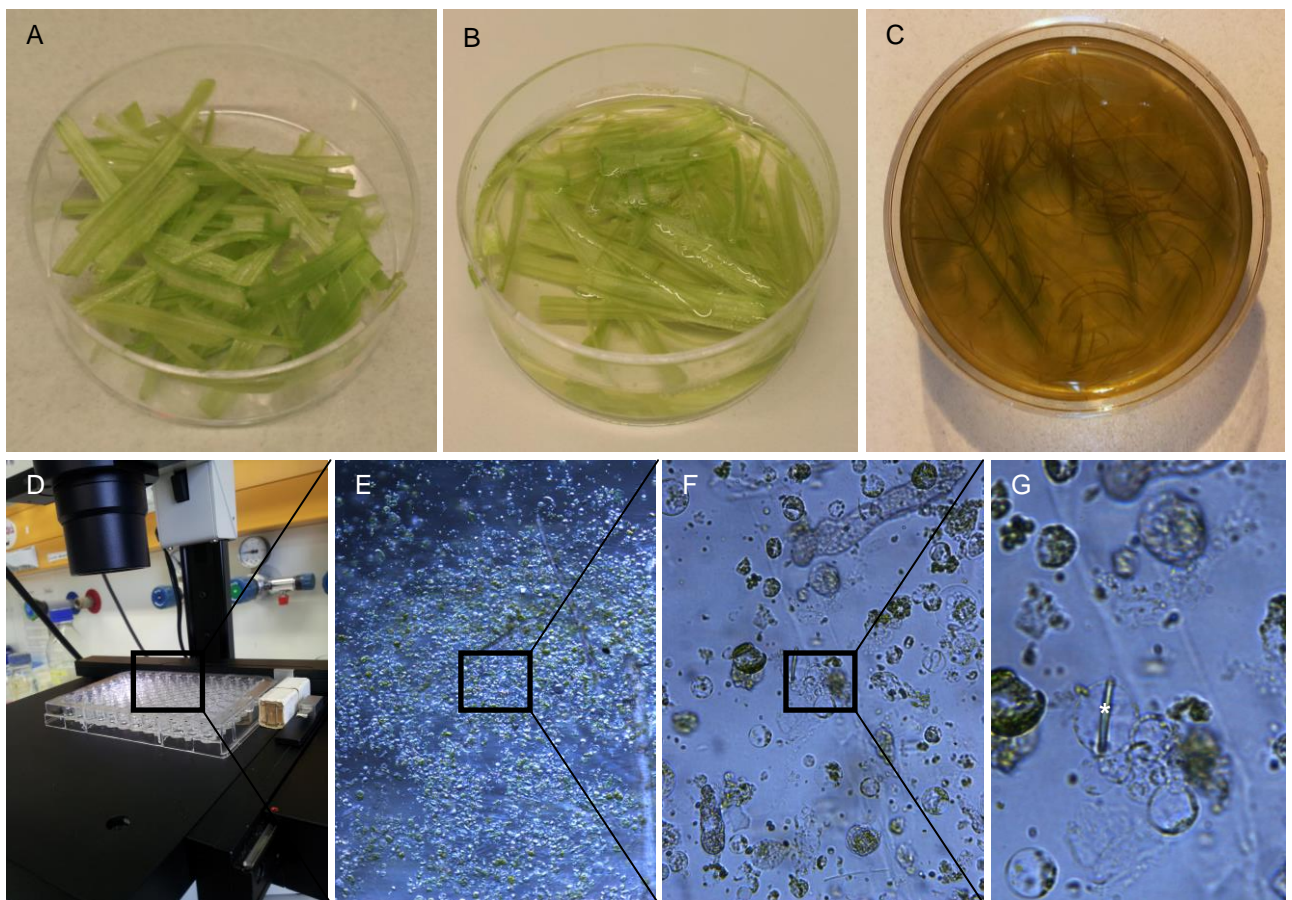


Figure 5: Technical procedure of protoplast isolation. A) Longitudinal cuts of *V. faba* stem were transferred into enzyme mixture (B) containing cellulose and pectolyase. C) Overnight enzyme treatment digested the plant cell wall, releasing the protoplast into the solution. Only big 'woody' parts of the stem remain in the petri dish. D) Immersed in bath medium the protoplasts were located at the bottom of the well plate. E-F) Using increasing magnification sieve-element protoplasts (G) were identified by the presence of forisomes (white asterisk).

The tissue was placed into a standard bath medium containing 600 mM mannitol, 1 mM DL-dithiotreitol (DTT), and 25 mM MES/NaOH, pH 5.7 (Fig. 5 B). After 15 min of incubation the tissue was transferred into an enzyme mixture containing 400 mM mannitol,

Material and Methods

100 mM KCl, 5 mM MgCl₂, 1 mM DTT, 0.2% (w/v) polyvinylpyrrolidone-25, 0.5% (w/v) bovine serum albumin, 0.5% (w/v) cellulase 'Onuzuka' RS (Yakult Honsha Co., Japan), 0.03% (w/v) pectolyase Y-23 (Seishin Pharmaceuticals, Tokyo), and 25 mM MES/NaOH, pH 5.7 (compare with Hafke *et al.* 2007) and placed gently moving on a Lab Shaker (IKA, Germany) at 40 rpm overnight (Fig. 5 C). After incubation, remaining tissue was removed and protoplasts solution was transferred to microcentrifuge tube (Eppendorf, Germany) and centrifuged 1 min at less than 1000 rpm. The remaining supernatant was discarded and centrifugation was repeated. The lasting pellet was solved in fresh bath medium and transferred into a 96 well-plate (Fig. 5D). Sieve-element protoplasts were identified by the presence of huge protein polymers (Fig. 5 G; forisomes). The mechanism of forisome reaction was observed under inverted microscopy using transmission and fluorescence light.

2.5. Free hand sectioning

To observe the transport of fluorochromes in the mass flow of the sieve tubes in *A. thaliana*, free hand sections of fresh unfixed leaves were made. Keeping the detached leaf between the thumb and forefinger of one hand and the razor blade in the other hand result in precise and thin cross sections. Incurred sections were placed on a slide, mounted with apoplasmic medium. Covered with a coverslip, the samples were observed in light and fluorescence microscope mode.

2.6. Embedding procedures and ultracut sectioning

2.6.1 Immunocytochemistry and Transmission Electron Microscopy

For fluorescence and immuno-electron microscopy randomly chosen leaf midrib segments, sampled, respectively from infected and healthy *S. lycopersicum* plants, were excised and cut into small portions (6-7 mm in length) and fixed in 0.2% glutaraldehyde, rinsed in 0.1 M phosphate buffer (PB), pH 7.4 and dehydrated in graded ethanol series (25-, 50-, 75%, 30 minutes each step) at 4° C. After one hour of the final 100% ethanol step, the samples were infiltrated in hard grade London Resin White (LRW, Electron Microscopy Sciences, USA) - 100% ethanol mixture in the proportion 1:2 for 30 minutes, followed by LRW:ethanol 2:1 for 30 minutes, and 100% LRW (two immersion periods: the first for 1 hour, followed by overnight infiltration) at RT. The samples were embedded in Eppendorf tubes using fresh LRW containing benzoyl peroxide 2% (w/w) according to manufacturer's

Material and Methods

protocol and polymerized for 24 h at 60° C (Musetti *et al.* 2002). For Light and Fluorescence Microscopy semithin sections (1 to 2 µm) were cut using a diamond knife on a Reichert Leica Ultracut E ultramicrotome (Leica Microsystems, Germany). Several serial semithin sections from each of the two plant groups (healthy and stolbur-diseased) were collected on glass slides. For Transmission Electron Microscope observation, several serial ultrathin sections (60–70 nm) of LR-White-embedded samples from each plant group (healthy or stolbur-diseased) were cut and mounted on carbon/formvar 400 mesh coated nickel grids (Electron Microscopy Sciences, USA).

2.6.2. Conventional Transmission Electron Microscopy

For ultrastructural analysis, randomly chosen leaf midrib segments, comprising 1–2 mm of blade on each side, sampled respectively from infected and healthy *S. lycopersicum* plants, were excised and cut into small portions (6–7 mm in length) and immersed in a solution of 3 % glutaraldehyde in phosphate buffer (PB) 0.1 M, pH 7.2, for 2 h at 4° C, washed for 30 min at 4° C in PB and post-fixed for 2 h with 1 % (w/v) OsO₄ in the above buffer at 4° C (Musetti *et al.* 2011). Fixed samples were dehydrated in ethanol and propylene oxide, embedded in Epon/Araldite epoxy resin (Electron Microscopy Sciences, USA). Serial ultrathin sections (60-70 nm) of at least 100 samples from each plant group (healthy or stolbur-diseased) were cut using the ultramicrotome (Leica Microsystems, Germany) and collected on 200 mesh uncoated copper grids, stained and then directly observed under a PHILIPS CM 10 (FEI, Eindhoven, The Netherlands) Transmission Electron Microscope operating at 100 kV.

2.7. Fluorescent probes and Confocal Laser Scanning Microscopic imaging

In translocation experiments, phloem-mobile dyes were administered to the phloem after having removed the leaf tip. In the other studies, fluorochromes were administered directly on the bare-lying protoplast or phloem tissues at the observation window. All dyes were either solved in apoplasmic or phosphate saline buffer and incubated in the dark. The fluorochromes were imaged by Confocal Laser Scanning Microscopy using a Leica TCS 4D/ TCS SP2, equipped with a HCX APO L 40X /0.80 W U-V-I water immersion objective (Leica Microsystems, Germany). Image capturing, processing and analysis were performed using Leica Confocal Software. To eliminate misinterpretations due to diffuse autofluorescence or reflection, all samples were observed by CLSM at the same excitation wavelengths and settings used for the below-mentioned fluorochromes as controls

(Supplemental Fig. 1-3). Transmission images were captured using the transmission detector in CLSM or by the use of a Leica DM LI inverted contrasting microscope equipped with a DFC300 camera (Leica Microsystems, Germany). Digital image processing was executed using Adobe Photoshop (CS, USA) to optimize brightness, contrast, and coloring.

2.7.1. (5)6-carboxyfluorescein diacetate

The phloem-mobile dye CFDA (Molecular Probes, Invitrogen, USA) was used to investigate phloem flow, according to Hafke *et al.* 2005. In healthy *A. thaliana* Col-0, *fls2-24* and *V. faba* as well as FD-infected *V. faba* plants a droplet of freshly prepared 1 μ M CFDA solution was applied, followed by an incubation period of 2 hours at RT. The phloem tissue was examined at a wavelength of 488 nm.

2.7.2. Carboxy-2,7-difluorodihydrofluorescein diacetate

To visualize reactive oxygen species (ROS) accumulation in sieve-element protoplasts of *V. faba*, H₂DFFDA (Invitrogen Molecular Probes, USA) was applied to the bath medium at a final concentration of 10 μ M. After incubation of 30 min, protoplasts were washed and again immersed in bath medium. Observations were performed at 488 nm wavelength line.

2.7.3. 4',6-Diamidino-2-phenylindole

Local staining by DAPI enabled detection of DNA, including plant and phytoplasma DNA, inside intact sieve elements. A drop of 1 μ g/ml DAPI (Molecular Probes, USA) was applied to the observation window. After incubation for 15-20 min at RT in darkness, DAPI was removed, replaced by the apoplasmic buffer and the tissue was observed at wavelength of 405 nm. In the majority of experiments, DAPI and CFDA were applied in succession (or in the reverse order) and the phloem tissue was observed at wavelength of 405 nm as well as 488 nm.

2.7.4. 5-chloromethyl-fluoresceindiacetate/5-chloromethyl-eosin-diacetate

CMEDA/CMFDA mixtures (Molecular Probes, USA), both membrane-permeant fluorochromes, were used to highlight forisome and protein accumulation in intact sieve tubes (Furch *et al.* 2007). Drops of a freshly prepared 1:1 mixture (v/v) were applied to the observation window and incubated for 1 h at RT. Tissues were observed at wavelength of 488 nm.

2.7.5. Aniline-Blue

In order to visualize callose depositions in sieve elements, a drop of aniline blue, (Merck, Germany) at the non-lethal concentration of 0.005% (Furch *et al.* 2007), was applied to the observation window and incubated for 30 min at RT. Aniline blue fluorescence was detected at wavelength of 405 nm.

2.7.6. 1,2-bis(o-aminophenoxy)ethane-N,N,-N',N'-tetraacetic acid

To reach a qualitative indication of Ca²⁺ concentrations in sieve elements, the membrane-permeant Ca²⁺ marker Oregon Green BAPTA-1 (Invitrogen Molecular Probes, USA) was applied to the observation window at a concentration of 5 µM and incubated for 30 min. After removal of dye by rinsing with apoplasmic buffer for 30 min, observations of phloem tissue were performed at wavelength of 488 nm.

2.8. Fluorescent probes, immunofluorescence staining and Epifluorescence Microscopy imaging

In experiments using LRW embedded tissue, fluorochromes were administered directly on the semithin sections. All dyes were dissolved in phosphate saline buffer and incubated in the dark. Transmission light and fluorescence imaging were captured by automated Leica DM4000 Epifluorescence Microscope equipped with a DFC digital camera and a 40X PL APO N.A. 1.25 oil immersion objective (Leica Microsystems, Germany). Image capturing, processing and analysis were performed using Leica Application Suite Advanced Fluorescence (LAS AF®). Digital image processing was executed using Adobe Photoshop (CS, USA) to optimize brightness, contrast, and coloring. To eliminate misinterpretations due to autofluorescence, unstained samples were observed at the same excitation wavelengths used for the fluorochromes as visual controls (Supplemental Fig. 4).

2.8.1. 4',6-Diamidino-2-phenylindole

To detect phytoplasmas inside sieve elements as well as to localize nuclei in companion and parenchyma cells, sections were incubated in 0.3 µM of the DNA-specific dye DAPI (Invitrogen Molecular Probes, USA) for 2.5 hours (Loi *et al.* 2002). Briefly before examination of the sections, the dyes were removed and slides were washed twice with PB and air-dried. For observation, slides were consecutively exposed to excitation wavelengths within the spectral windows of 340 nm to 380 nm. Fluorescence signal was observed using long-pass filter starting from a wavelength of 425 nm.

2.8.2. N-(3-triethylammoniumpropyl) -4- (4- (4- (diethylamino)phenyl)butadienyl) pyridiniumdibromide

To highlight plant cell and phytoplasma membranes, sections were treated with the membrane marker RH-414 (Invitrogen Molecular Probes, USA) for 2.5 hours at a final concentration of 4.3 μ M (Furch *et al.* 2007). Again slides were washed twice with PB and air-dried. Observations were performed within an excitation wavelength of 470 nm to 490 nm. Fluorescence signal was observed using long-pass filter starting from wavelength of 505 nm.

2.8.3. ER-Tracker Green

To detect sieve-element reticulum, sections were incubated for 2.5 hours in 1 μ M of ER-Tracker Green (Molecular Probes, Invitrogen, USA; Furch *et al.* 2009). Briefly before microscopic examination, ER Tracker Green was removed and slides were washed twice with PB and then air-dried. For microscopic observation, slides were exposed to excitation wavelengths within the spectral windows of 450 nm to 490 nm. Fluorescence signal was observed using long pass filter starting from a wavelength of 515 nm.

2.8.4. Texas Red conjugated antibody

To identify and distinguish actin structures in healthy and stolbur-diseased *S. lycopersicum* leaf tissues, a secondary immunofluorescence technique was adopted (modified after Baskin *et al.* 1992). After blocking the unspecific binding sites in blocking solution (1% bovine serum albumin (BSA), 3% NaCl, 0.3% Triton X 100, 10% Tris HCl pH 9.5, dimethyldicarbonate (DMDC) H₂O) for 30 min, slides were incubated in a commercially available unlabeled primary antibody against actin (clone 10-B3, monoclonal, 1:1000) diluted in 0.01 M PBS, pH 7.4, containing 15 mM sodium azide (Sigma-Aldrich Milan, Italy) for 30 min at RT. Subsequently, slides were incubated for 30 min at RT in a secondary a Texas Red (TR)-conjugated antibody targeted against mouse IgG, diluted 1:100 in 1x PBS (Santa Cruz Biotechnology Inc., Santa Cruz, CA, USA). Between the incubation steps, free antibodies and blocking solution were removed by washing steps in PBS.

To test the specificity of the first antibody, control setups were performed without primary antibody (Supplemental Fig. 4). For observation, slides were excited using a dichroic filter cube, excitation a wavelength of 540 nm to 580 nm and passing starting from 595 nm.

2.9. Immunogold labeling and Transmission Electron Microscopy

For ultrastructural analysis of actin distribution in healthy and stolbur-diseased *S. lycopersicum* plants, experiments using LRW embedded tissue and immunogold labeling of plant actin was performed as follows (modified after White *et al.* 1994). To block unspecific binding sites, grids were placed on droplets of blocking solution made up of normal goat serum (NGS) diluted 1:30 in 1% BSA in PBS, pH 7.6, for 2 h at RT. Then, grids were incubated overnight at 4° C with primary mouse monoclonal antibody against actin (MAB anti-actin, clone C11, Agrisera, Vännäs, Sweden), diluted 1:200 in blocking solution. Control grids were incubated in 1 % BSA/PBS without primary antibody. All grids were then rinsed with PBS, and treated for 1 h at RT with secondary goat antimouse antibody coated with colloidal 5 nm gold particles (GAM 5, Auro Probe EM GAM G5 Amersham, USA), diluted 1:40 in 1% BSA/PBS. Sections were stained in 3 % uranyl acetate and 0.1% lead citrate (Reynolds 1963) and observed under a PHILIPS CM 10 (FEI, Eindhoven, The Netherlands) Transmission Electron Microscope operating at 100 kV.

2.10. Statistical analyzes

Statistical analyzes were carried out using SPSS[®] (IBM[®] SPSS[®] Statistics 20). Required analysis on normally distributed data was performed on Shapiro-Wilk or Kolmogorov–Smirnov test. Depending on variance analysis by Levene's test, the significance level was measured using Welch's t test or Student's t-test. Statistical significance level was set to 5% ($p < 0.05$).

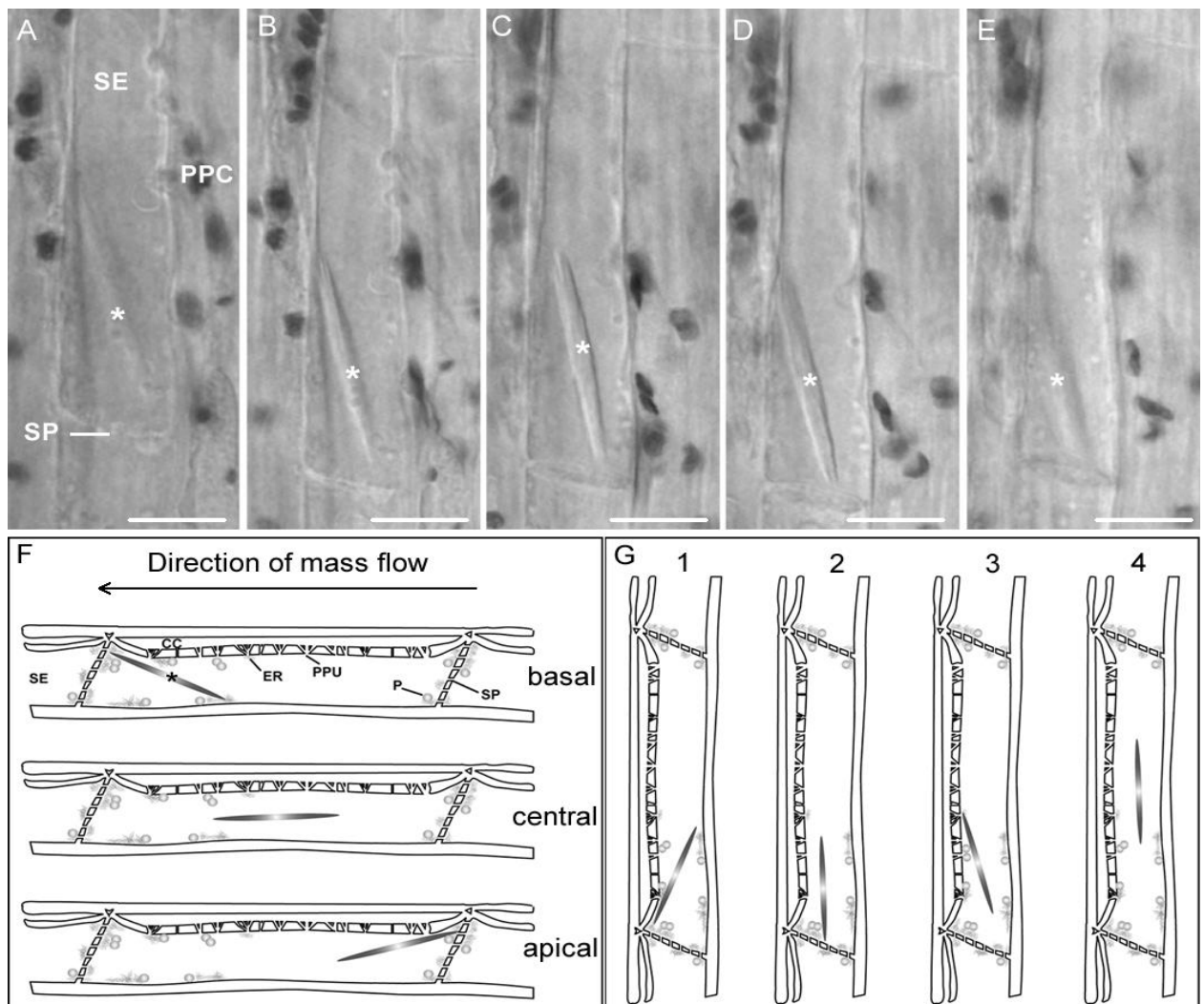
Results

3.1. Microscopical examination of artificial contaminated plant samples

3.1.1. Spatial and temporal resolution of forisome in intact phloem

3.1.1.1. Distribution and reactivity

To observe phloem-based immune reactions triggered by bacterial elicitor, *in vivo* investigation of phloem tissue were made. This technique offers the opportunity to study phloem morphology and function in native plant tissue (Knoblauch and van Bel 1998). To assess knowledge about phloem immune responses, first the initial state of unstimulated phloem tissue was examined (Fig. 6). Based on the Light Microscopy z-stack analysis (Fig. 6 A to E), to ascertain the exact localization, forisomes were classified in 12 different positions within the sieve element of *V. faba* (Fig. 6 F and G). Forisomes were first classified in terms of the location relative to the sieve element and the mass flow (Fig. 6 F). For this purpose the sieve elements were conceptually divided into three parts. Forisomes in the second third of the sieve element were classified as central. Forisomes upstream from the second third of the sieve element referred to as apical, downstream as basal.

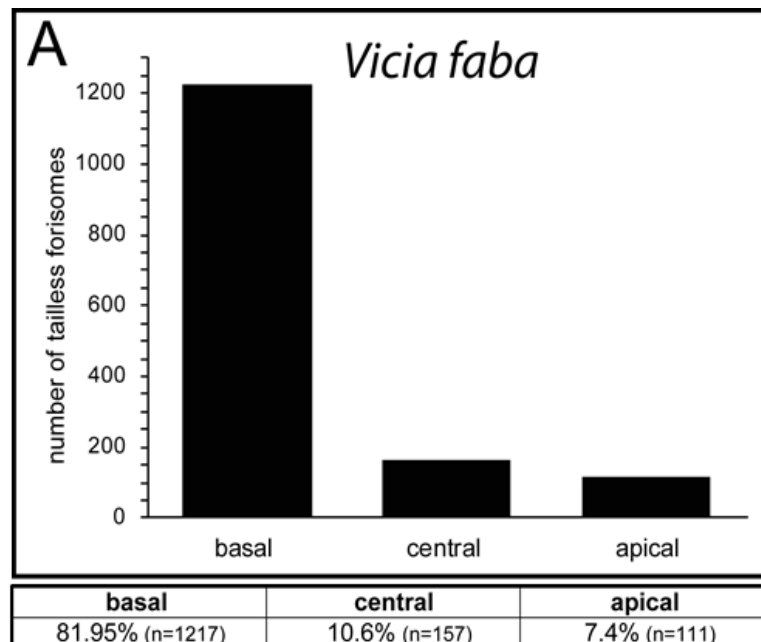


Results

Figure 6: Classification of *V. faba* forisome position based on 3-D analysis. A to E: Set of images taken at different focal planes of phloem tissue z-stack. Transmission images were collected at 4 μm intervals. Image (D) represents the main working plane. F to G: Schematic illustration of various locations and positions of forisomes in sieve elements. F) Depending on the direction of mass flow locations of forisomes can be grouped in basal, central and apical. G) In basal and apical location, forisomes can be located in contact to the sieve plate and the plasma membrane (1), only in contact to the sieve plate (2) or the plasma membrane (3) or without any contact to the sieve element (4). In central location, forisomes can only be located in position (3) and (4). CC: companion cell, ER: endoplasmic reticulum, P: plastids, PPC: phloem parenchyma cell, PPU: pore-plasmodesmata-unit, SE: sieve element, SP: sieve plate. Asterisk indicated forisome. Bars correspond to 10 μm . Illustration Furch *et al.* unpublished

Following these location-specific differentiation, the forisomes were classified due to their contact to the sieve element (Fig. 6 G). Forisomes in contact to both, the sieve plate and the plasma membrane, are sub-divided in position 1. Forisomes only in contact to the sieve plate or the plasma membrane are termed position 2 and position 3, respectively. Forisomes without contact to the sieve element are grouped in position 4.

Regarding the location of forisomes in unstimulated phloem of *V. faba*, forisomes were mainly located at the basal side of the sieve element (Fig. 7 A). Out of 1485 tested forisomes in *V. faba* about 82% were located basal in the direction of the mass flow, 11% central and 7% apical in the sieve element. Out of these basal (Fig. 7 B) and apical (Fig. 7 D) located forisomes, around 80% of the forisomes showed a contact to the sieve element. In turns, more than 40% were in contact to both the sieve plate and the plasma membrane, including nearly 30% facing the companion cell membrane. In central located forisomes (Fig. 7 C) less than 35% of the forisome showed sieve-element contact.



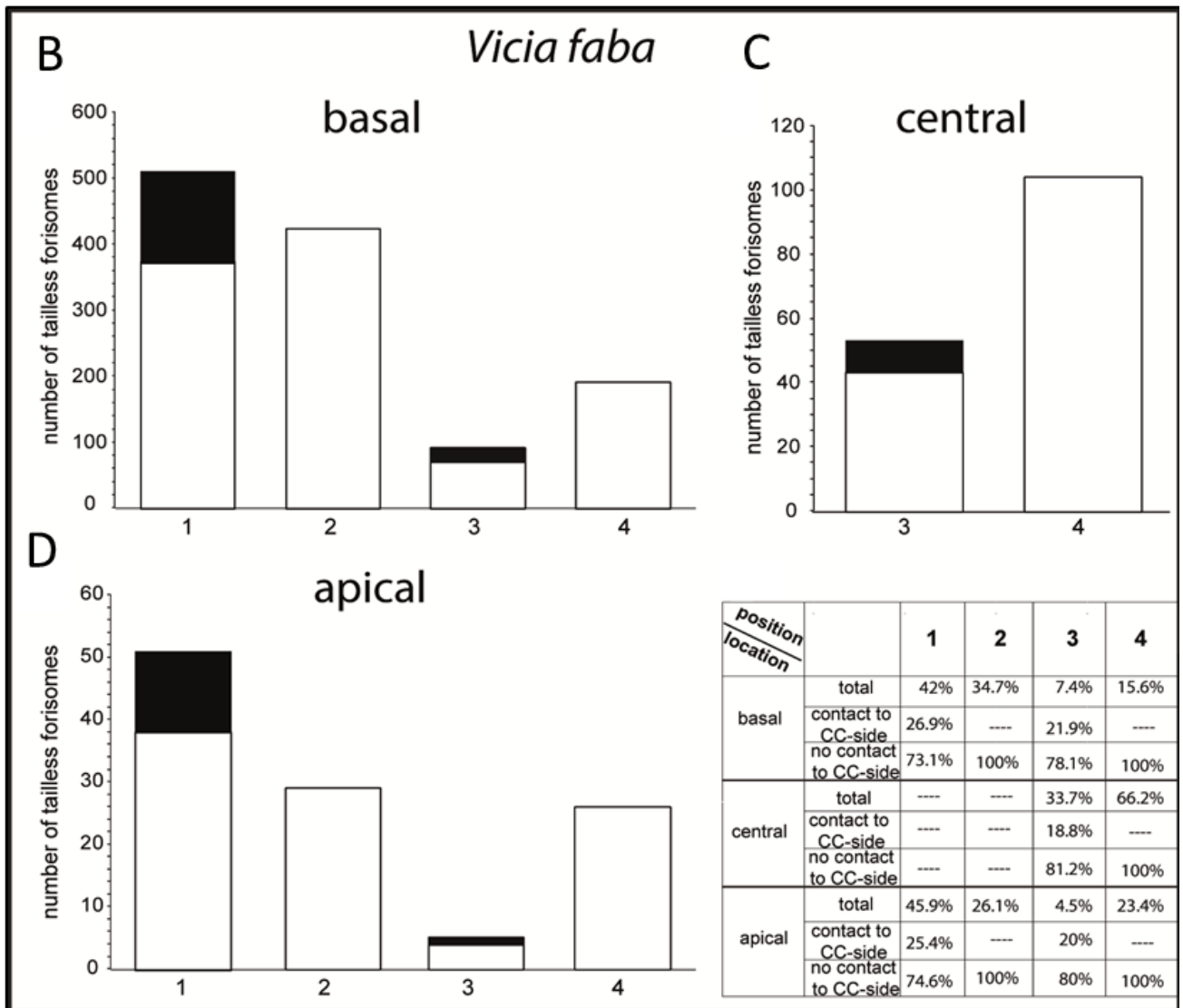


Figure 7: Absolute frequency of forisome relative to location and positions in the sieve element of *V. faba*. A) Forisomes are grouped based on their appearance in the sieve element in basal, central and apical locations. B to D: Forisome position are furthermore sub-divided into forisomes that have contact to the sieve element with both ends (1) only one end (2,3) or do not have contact to the sieve element-membrane (4). Differentiation of the positions was made in basal (B), central (C) and apical (D) located forisomes. Black bars in B,C,D represent forisomes in contact to the companion cell membrane.

The reactivity of the forisomes in intact *V. faba* plants were tested by carefully burning the leaf tip. After application of a distant heat shock, examinations of forisome reactivity at the respective locations were made (Fig. 8). Initiated by the burning of the leaf apex of *V. faba*, forisomes showed typical morphological modification (Furch *et al.* 2007). The dispersion of the forisome occurred in all cases in less than 30 seconds after heat application. While the reaction times (time lapse between stimulus and dispersion) were the lowest for basal forisomes, no significant differences between the locations or the positions as well as no clear correlation between reaction time and recondensation times could be shown (Fig. 8 A,B; Significance was defined as $p < 0.05$; correlation coefficient $R < 0,005$).

Results

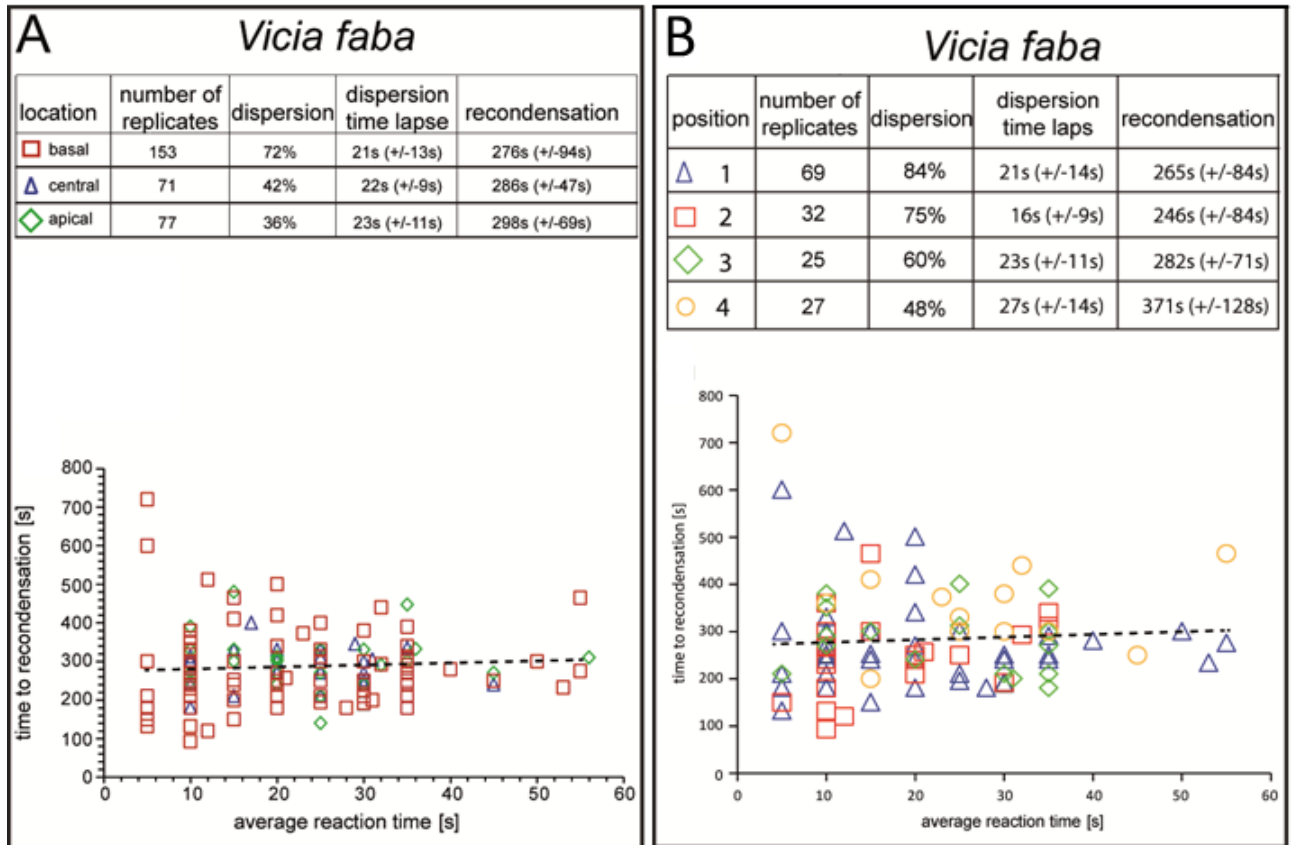


Figure 8: Forisome reaction of *V. faba* in response to heat stimuli. Dispersion and recondensation time in defined locations (A; basal, central, apical) and positions (B; 1, 2, 3, 4) were recorded.

However, immense variances were visible in the reactivity of the forisomes. More than 70% of the basal forisomes showed a stimulus-based reaction, while less than 40% of the central and apical located forisomes showed a reaction (Fig. 8 A). Basal located forisomes in contact to the sieve plate showed with more than 70% due to heat stimulus the highest reactivity (Fig. 8 B). Forisomes without contact to the sieve plate or without any contact only showed 60% and less than 50% reactivity, respectively (Fig. 8 B).

Considering the location of forisome after recondensation in relation to the position prior to dispersion, it is striking that forisomes mainly recondense in a slightly different position (Fig. 9). As reported above, in unstimulated sieve elements forisomes are most likely laying in the basal location in contact to both the sieve plate and the plasma membrane (Fig. 9 A). Already less than 20 seconds after burning the leaf tip, due to dispersion, the forisome is no longer visible in transmission light mode (Fig. 9 B). Only seconds after application of heat stimulus, the forisome reappears due to recondensation (Fig. 9 C). Comparing the angle of the forisome to the sieve plate before dispersion (Fig. 9 A) and

Results

after recondensation (Fig. 9 C), the inclination reduced noticeable. While the forisomes prior to the stimulus were laying at a 20° angle inside the sieve elements (Fig. 9 A), forisomes after recondensation are laying in only 9° angle (Fig. 9C). Time-related movement of the forisome achieved the return of the initial position during the first 5 minutes after heat stimulus (Fig. 9 D).

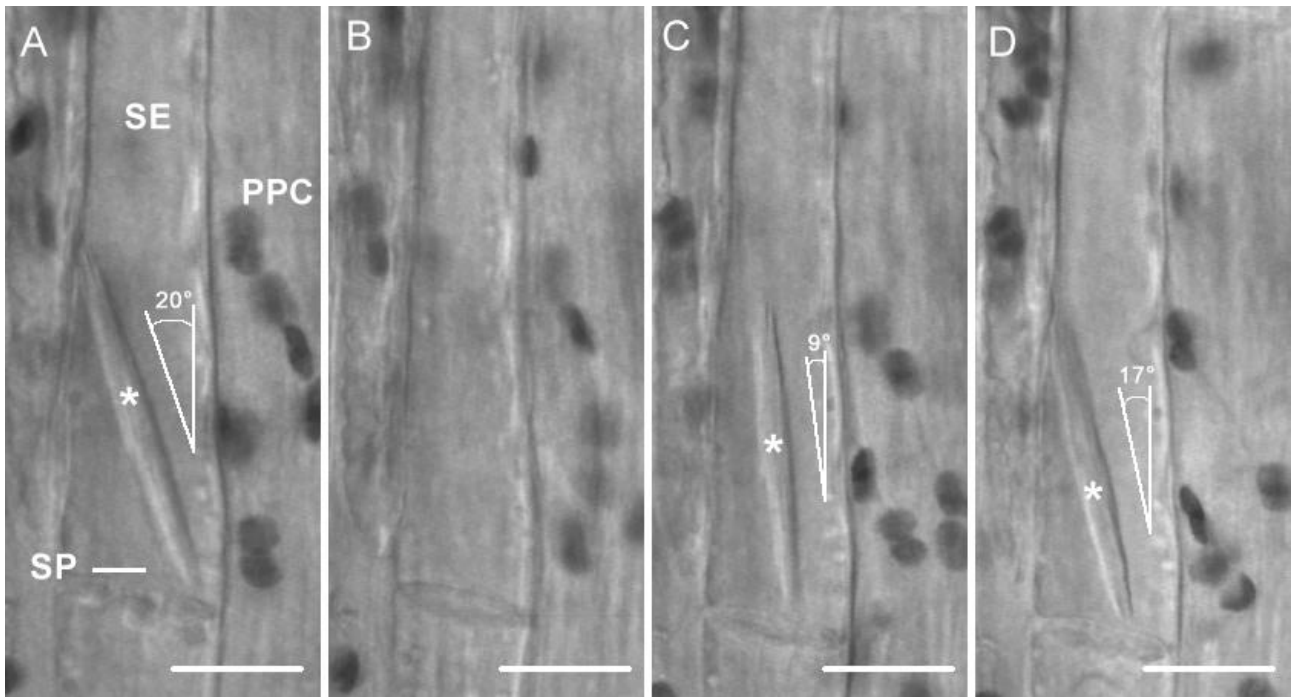


Figure 9: Change of forisome position in *V. faba* due to distant stimulus. Prior to stimulus (A) basal forisome is laying in position 1 inside the sieve element. Shortly after dispersion (B) forisome recondense in position 2 (C) and moves back to position 1 within few minutes. PPC: phloem parenchyma cell, SE: sieve element, SP: sieve plate. In A,C,D asterisk indicated forisome; the angle is indicating the inclination of the forisomes to the sieve plate. Bars correspond to 10 μm.

The results from *in vivo* observation of forisomes in *V. faba* shown above (some of them consistent from the master thesis “Controlling the movement of forisomes in *Vicia faba* and *Phaseolus vulgaris* by S.V. Buxa) correspond to the statement made by Furch *et al.* 2009.

3.1.1.2. Flagellin-triggered forisome reaction

To investigate the phloem-based immune responses triggered by bacterial elicitor, forisome reaction of *V. faba* in *in vivo* experiments was observed after replacing apoplasmic buffer against buffer containing diverse flagellin concentration (Fig. 10).

In unstimulated *V. faba* plants condensed forisomes were located at the downstream side of the sieve element in contact to the sieve plate and the plasma membrane (Fig. 10 A, F,

Results

K, and P). In response to application of 10 μM synthetic flagellin (n=14) to the apoplasmic buffer in the observation window (Fig. 10 B to E) the average forisome dispersion occurred 2 minutes after application (shown for 4 min; Fig. 10 C) indicating a Ca^{2+} -based forisome reaction (Furch *et al.* 2007).

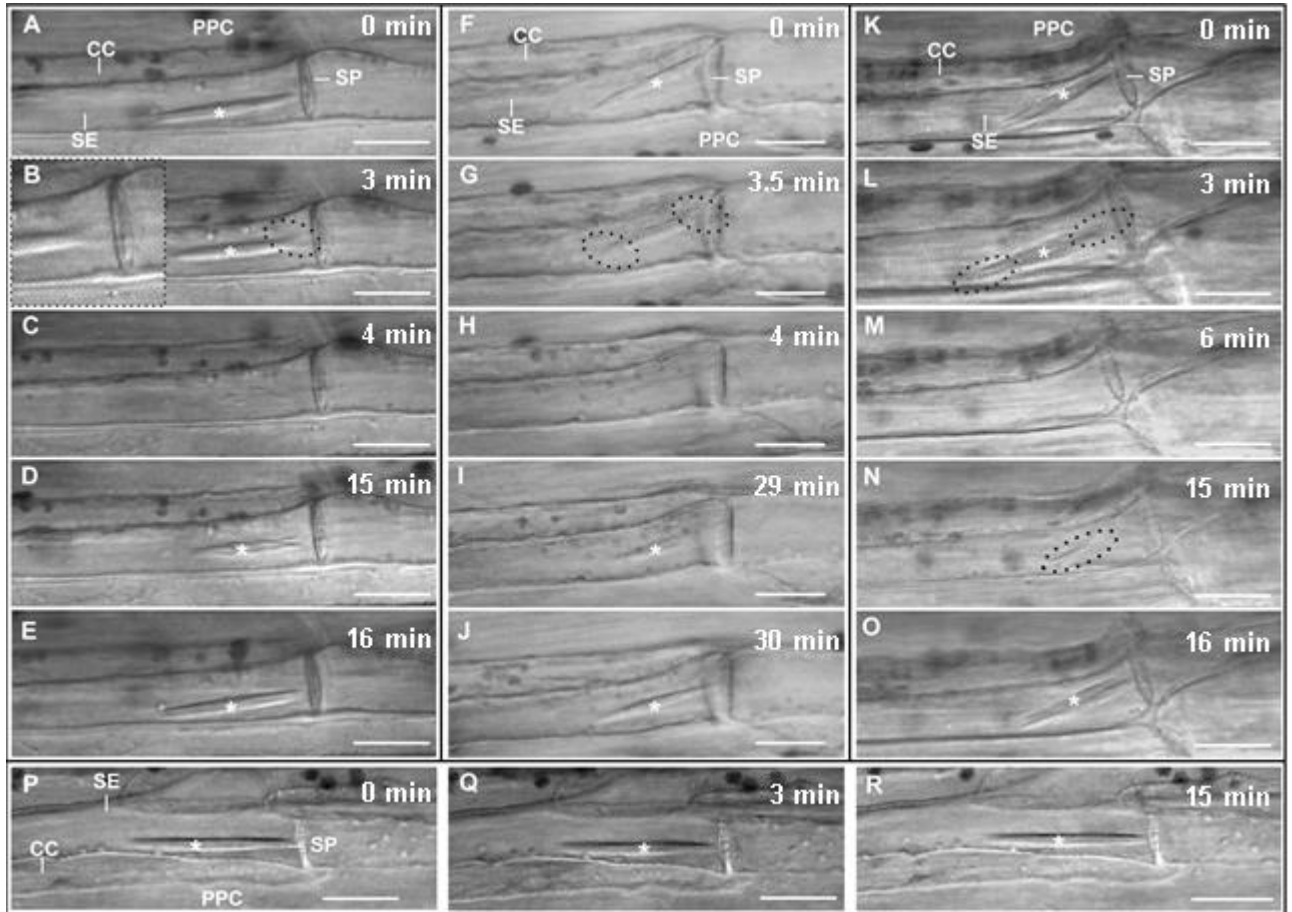


Figure 10: Forisome reaction to application of various flagellin concentrations to intact sieve elements of *V. faba*. Application of 10 μM (A to E), 1 μM (F to J) and 0.1 μM (K to O) purified flagellin lead to slow dispersion of forisomes. 0.01 μM did not induce forisome reaction (P to R). CC: companion cell, PPC: phloem parenchyma cell, SE: sieve element, SP: sieve plate. Asterisk indicated forisome; dotted line indicate dispersion started from the ends of the forisomes. Bars correspond to 10 μm .

In average time between 10 min (shown for 15 min; Fig. 10 D) and 18 minutes (shown for 16 min; Fig. 10 E) the forisome recondense slowly. Descending concentration of flagellin leads to a delayed reaction. Application of 1 μM flagellin (n=24; Fig. 10 G to J) triggers average forisome dispersion time of 4 to 6 minutes (shown for 4 min; Fig. 10 H) and average recondensation time between 15 minutes (shown for 29 min; Fig. 10 I) and 30 minutes (shown for 30 min; Fig. 10 J) after application. Flagellin concentrations of 0.1 μM (n=12; Fig. 10 L to O) infrequent trigger forisome reaction (3 out of 12) while reaction time

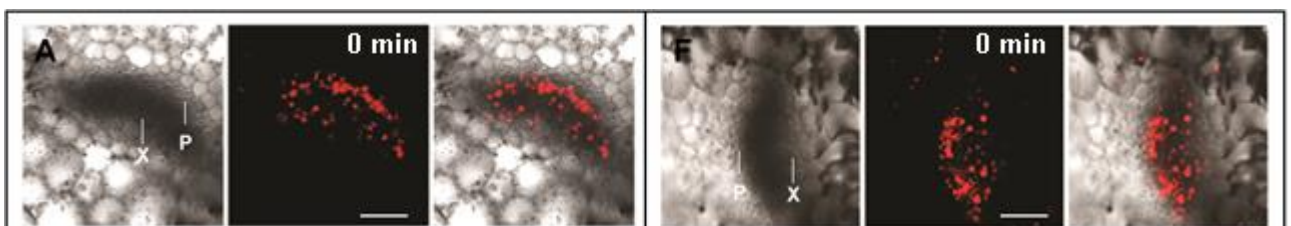
Results

remains stable compared to 1 μM flagellin stimuli. Of particular note is the initial dispersion of all forisomes apparently from the forisome tip (Fig. 10 B, G, and L spotted line). Flagellin concentrations lower than 0.1 μM are not able to trigger forisome reaction ($n=15$; Fig. 10 Q and R).

3.1.2. Observation of mass flow interference

To visualize alterations of sieve-element mass flow due to bacterial elicitor, phloem-mass flow was observed under Confocal Laser Scanning Microscopy (CLSM) using leaf cross-sections and CFDA ((5)6 carboxyfluorescein diacetate) to exposed sieve elements leads to a phloem restricted transport of the fluorescent CF. The membrane-permeant, colorless CFDA enters sieve elements *via* the plasma membrane and, following de-esterification, the membrane-impermeant CF is translocated by mass flow through the sieve tubes (Oparka *et al.* 1994). Most of it is retrieved by companion cells and phloem parenchyma cells along the pathway and sequestered in the vacuoles (Knoblauch and van Bel 1998).

In unstimulated plants the CF signal is visible along the flooded sieve elements of collateral vascular bundle in *A. thaliana* leaf main vein ($n=8$; Fig. 11 A and F). Both, basal cross sections (2 cm from leaf tip; Fig. 11 A), and apical sections (6 cm from leaf tip; Fig. 11 F), showed CF fluorescence. 10 minutes after pressure infiltration of 1 μM flagellin (Fig. 11 B and G) into the leaf, 4 cm from the leaf apex, phloem-mobile fluorescent dye was still visible at cross sections prior to the application side ($n=5$; Fig. 11 B) while no signal was visible at the cross sections behind the infiltration area (Fig. 11 G). However, 90 minutes after flagellin infiltration, fluorescence of CF was visible at both sides of the infiltration area ($n=5$; Fig. 11 C and H). A secondary lack of CF fluorescence 180 minutes after infiltration at cross sections behind the application side ($n=5$; Fig. 11 I) was again recovered 240 minutes after flagellin treatment ($n=6$; Fig. 11 J) indicate a lifting of sieve-tube blockage. In both time points CF signal was visible in cross section in front of the application side (Fig. 11 D and E).



Results

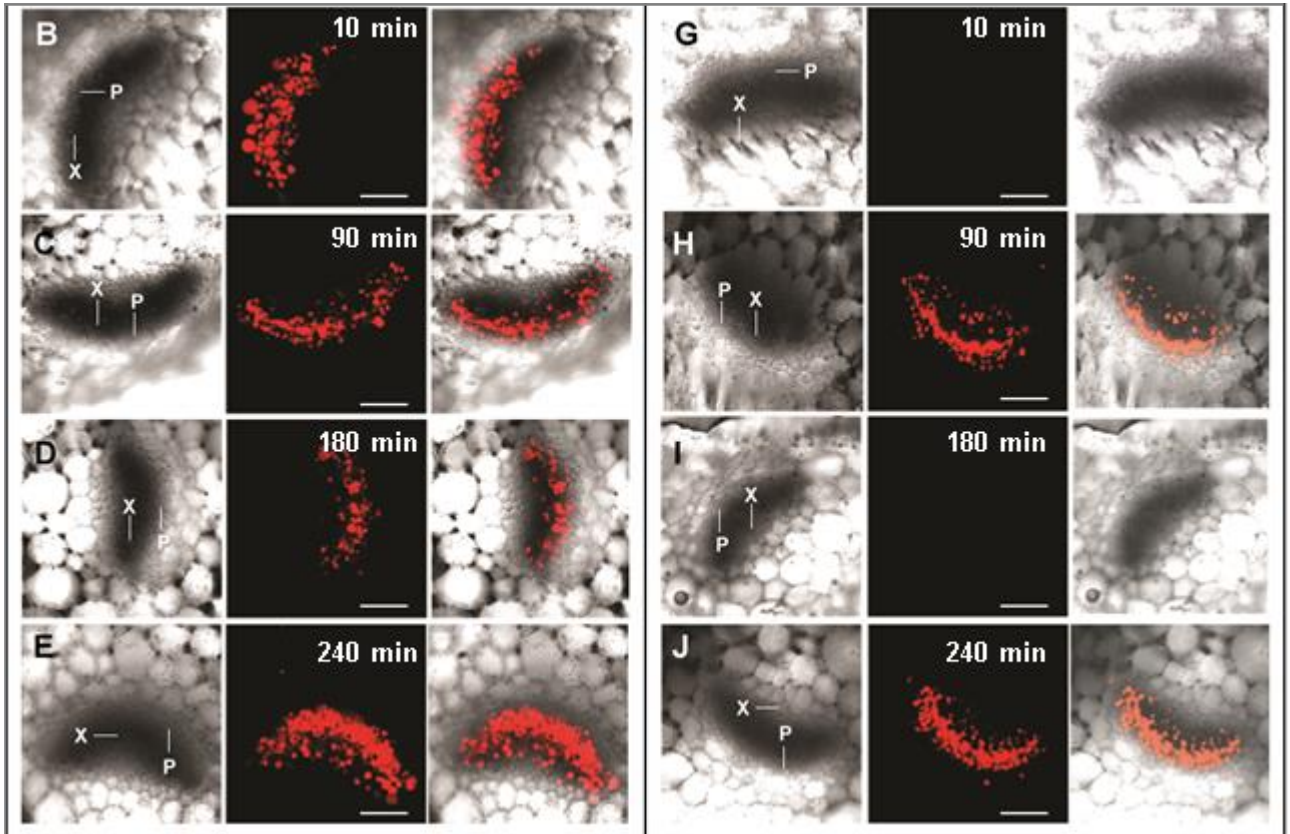


Figure 11: Observation of mass flow in sieve tubes after pressure infiltration of 1 μ M flg22 in the leaves of wild type *A. thaliana* (*Col-0*). The fluorescence of CF in the sieve elements of wild type *A. thaliana* was observed at cross-sections in front of and behind the infiltration area of flg22 at different time points. A to E: Cross sections 2 cm from leaf tip. F to J: Cross sections 6 cm from leaf tip. In untreated plants (A,F), CF fluorescence was detected at both sides of the application site. 10 min and 3 hours after flg22 treatment, no CF fluorescence was observed behind the application site (G,J), however, CF signal was detected in front of the infiltration area (B,D). 1.5h (C,H) and 4 hours (E,J) after treatment CF fluorescence was detected at both cross-sections. P: phloem, X: xylem. Bars correspond to 20 μ m.

3.1.3. Signal perception, release and transduction in sieve-element occlusion

To identify the role of phloem-based defense reactions in accordance to general plant immune responses, CF experiments were used for flagellin-insensitive *fls2* mutants (Fig. 12). These *fls2* mutants lack flagellin-specific receptor fundamental for bacteria recognition (Gómez-Gómez and Boller 2000).

In the *Arabidopsis fls2* KO mutant, continuous CF fluorescence was observed (n=25; Fig. 12) under CLSM. At any monitored time points, after pressure infiltration of 1 μ M flagellin, CF signal was detected in front of (Fig. 12 A) or behind (Fig. 12 B) the infiltration area, indicating undisturbed mass flow through sieve tubes at all times.

Results

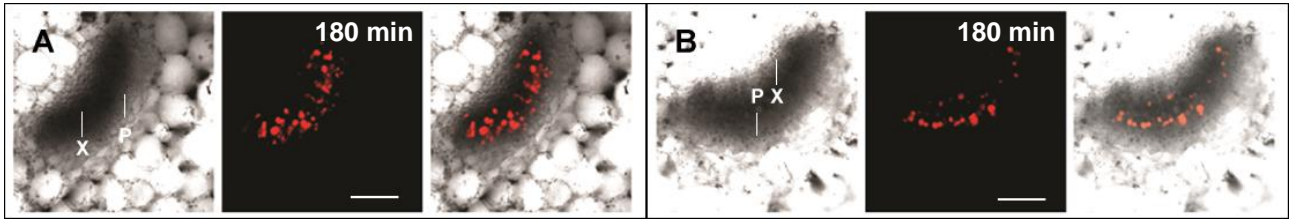
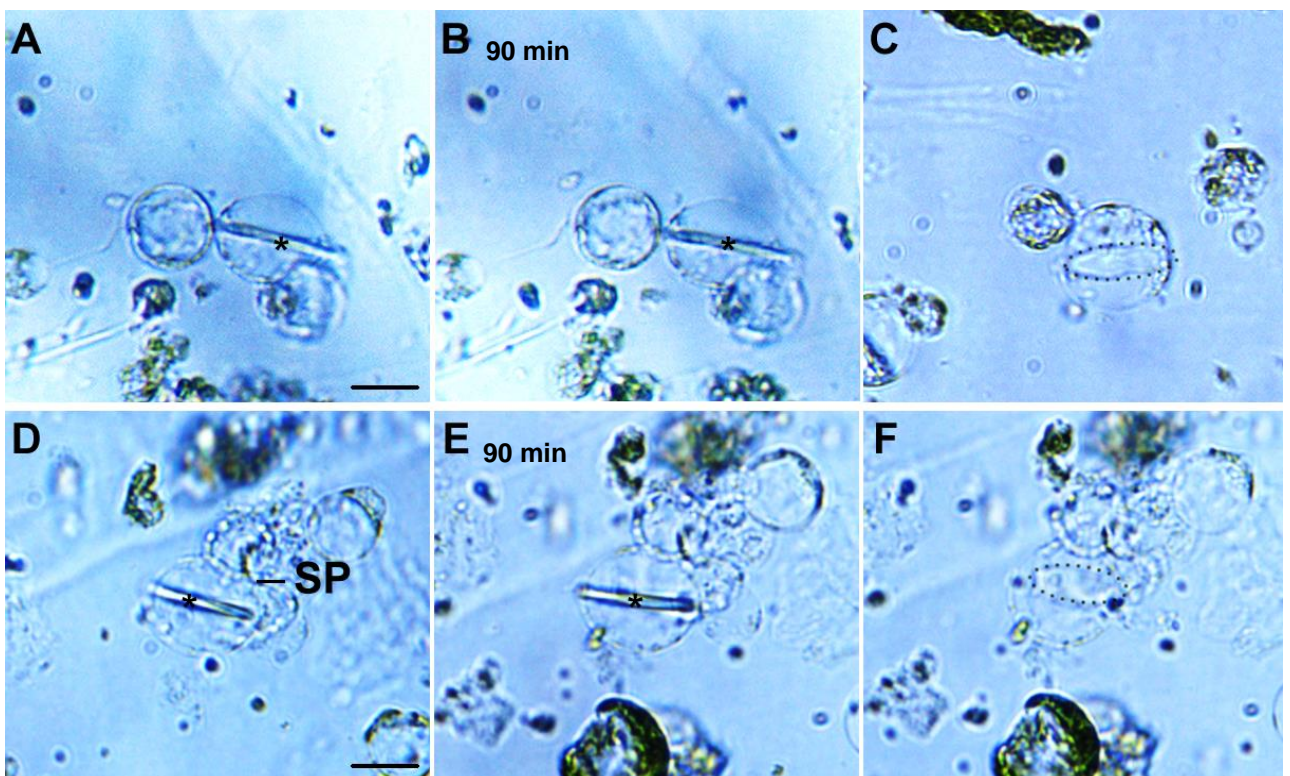


Figure 12: Observation of mass flow in sieve tubes after pressure infiltration of 1 μM flg22 in the leaves of *A. thaliana* (*fls2*). In the *Arabidopsis fls2* KO mutant, the CF fluorescence in the sieve elements was detected in front of and behind the infiltration area of 1 μM flg22. Exemplarily shown for cross section 3 hours after stimuli (A,B). P: phloem, X: xylem. Bars correspond to 20 μm .

To study the role of phloem cells in initiation of plant immune responses, tissue-independent analyzes of functional sieve-element protoplasts were investigated. Isolated plant cells are adequate tool to study physiological properties of cell-autonomous behavior of intact tissue (Davey *et al.* 2005), including observation of receptor-based plant immune responses (Hwang and Sheen 2001; Tena *et al.* 2001). Protoplast represents regular cell performance in perception and reaction to environmental changes as well as biochemical elicitors (Sheen 2001). Protoplasts were isolated according to Hafke *et al.* 2007 and observed under Transmission Light Microscopy (Fig. 13).



Results

Figure 13: *V. faba* sieve-element protoplast reaction in response to application of flagellin and high mannitol concentration. Intact sieve-element protoplasts were identified by the presence of condensed forisomes (A,D). After application of 1 μ M flagellin, lacking forisome reaction was observed over a time-period of 90 min (B,E). Exchange of bath medium containing 600 mM mannitol by hypo-osmotic solution containing only 60 mM mannitol, forisome disperses (C,F). SP: sieve plate. In A,B,D,E asterisk indicated forisome, in C and F dotted line outline dispersed forisomes. Bars correspond to 10 μ m.

Identification of forisomes in *V. faba* sieve-element protoplasts offers the opportunity of tissue-specific observation (Hafke *et al.* 2007). Intact sieve-element protoplasts from *V. faba* plants were characterized by the presence of condensed forisomes (Fig. 13 A and D black asterisk).

Immediately to application of a final concentration of 1 μ M flagellin to the bath medium, containing 600 mM mannitol and 1 mM free Ca^{2+} forisome reaction was observed (Fig. 13 B and E). Even 90 min after flagellin stimulus none of the tested forisomes (n=14) showed a reaction (Fig. 13 B and E) indicating compromised perception of flagellin. Integrity of protoplast was tested by causing a turgor-induced shock (Hafke *et al.* 2007). After application of hypo-osmotic bath medium, containing only 60 mM mannitol, forisomes disperse directly (Fig. 13 C and D dotted line), indicating Ca^{2+} -dependent forisome dispersion (Hafke *et al.* 2007; Hafke and van Bel 2013).

To test the vigor of the protoplast after enzymatic digestion, protoplast reactivity was verified using H_2DFFDA . In plant cells application of colorless H_2DFFDA (carboxy-2,7-difluorodi-hydrofluorescein diacetate) leads to inclusion of fluorescent form when cleavage by intracellular esterases. Due to oxidation by reactive oxygen species, triggered by abiotic and biotic stimuli (for review see Shapiguzov *et al.* 2012), the fluorescent signal increases significantly.

Using CLSM incubation of isolated protoplast did not lead to a remarkable signal in untreated cells (Fig. 14 A to C). Neither sieve-element protoplasts (black asterisk) nor mesophyll protoplast showed an oxygen-dependent signal. Only signals due to autofluorescence (red signal) coming from the chloroplasts showed up.

Results

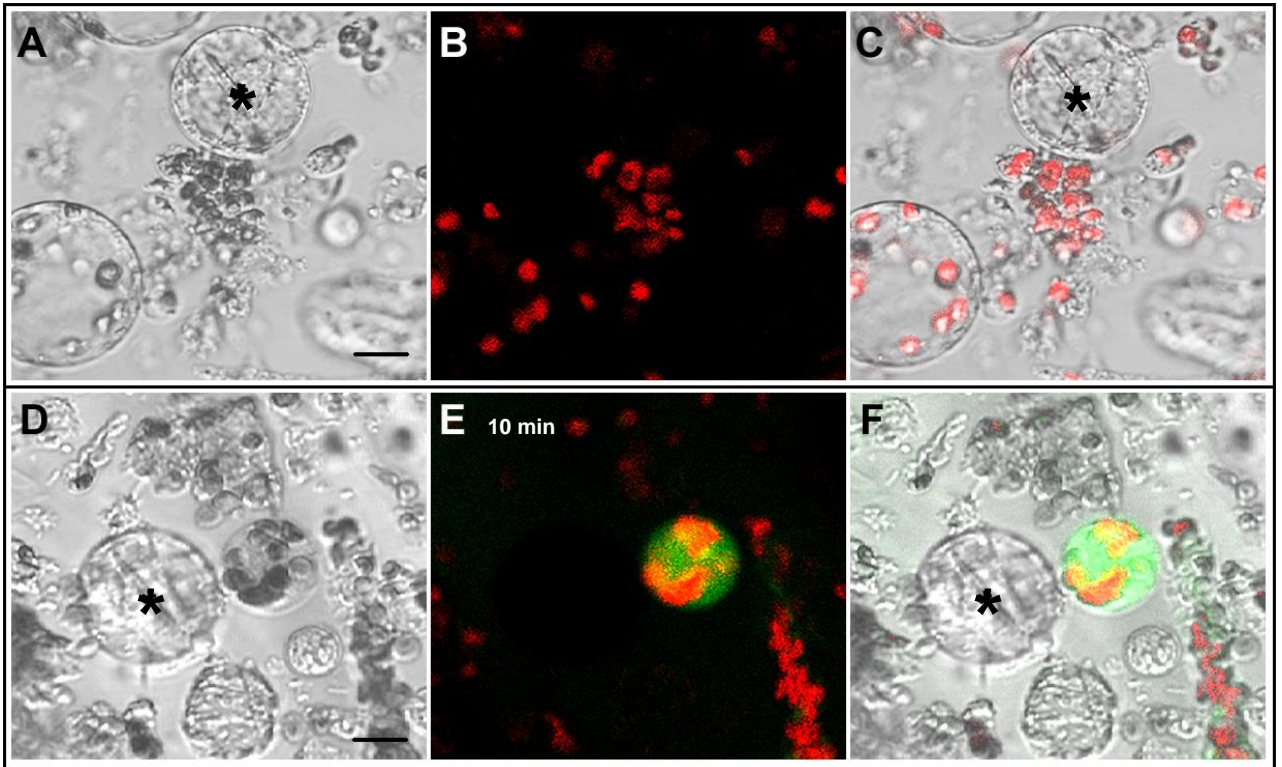


Figure 14: Observation of ROS production in isolated protoplasts. Protoplast solution of *V. faba* plants was incubated with H₂DFFDA and observed under CLSM. Unstimulated protoplasts did not show H₂DFFDA specific signal (A,B,C). 10 minutes after application of 1 μ M flagellin mesophyll protoplast showed a fluorescent signal (D,E,F). Sieve-element protoplasts did not show a signal. In A,C,D,F asterisk indicated forisome. Bars correspond to 10 μ m.

Treatment of the protoplast solution with a final concentration of 1 μ M flagellin induced a fluorescence signal in mesophyll cells (green signal) but not in the sieve-element protoplast (Fig. 14 D to F; n=6).

Results

3.2. *In planta* observation of natural infection

3.2.1. Plant materials and phytoplasma detection by PCR

To identify innate host-pathogen interaction *V. faba* plants were phytoplasma infected *via* insect transmission. Control *V. faba* plants, not exposed to leafhoppers showed regular growth without disease symptoms (Fig. 15 A and B). In infected plants, typical FD symptoms, such as leaf-size reduction, leaf yellowing and curling (Fig. 15 C and D) emerged about one month after inoculation by the insect vectors.



Figure 15: Images of healthy (left half of the panel) and Flavescence Dorée (FD)-infected (right half) *V. faba* plants. Whole plants and leaf details. (A,B) Healthy *V. faba* plants showed regular growth and do not develop disease symptoms. In FD-infected plants (C,D) typical symptoms were visible, such as general decline, beginning leaf decoloration and leaf deformation.

Real-time (RT)-PCR of ‘*Ca. P. vitis*’ 16S rRNA confirmed the presence of phytoplasmas in infected *V. faba* leaf samples before microscopy examination. Starting from 40 ng of total DNA, FD-phytoplasma 16S rRNA was detected in symptomatic samples, while no amplification of the 16S rRNA gene was obtained in healthy ones. DNA isolated from FD-diseased *Catharanthus roseus* and FD-infected *Vitis vinifera* were also amplified as positive parallel controls (Supplemental Table 1).

Observations were performed using four healthy and four diseased six-week-old *V. faba* plants, as soon as symptoms appeared on the infected ones. For Confocal Laser Scanning Microscopy (CLSM) observation, experiments were repeated on at least two different leaves per plant.

Results

3.2.2. Optical phytoplasma detection and mass flow

To assess phytoplasma-induced phloem modification *in vivo* experiments of healthy and phytoplasma-infected *V. faba* were investigated. Healthy sieve elements were characterized by the presence of condensed forisomes (Fig. 16 A, asterisk), while the sieve plates were free of visible occluding substances (Fig. 16 A) under transmission light.

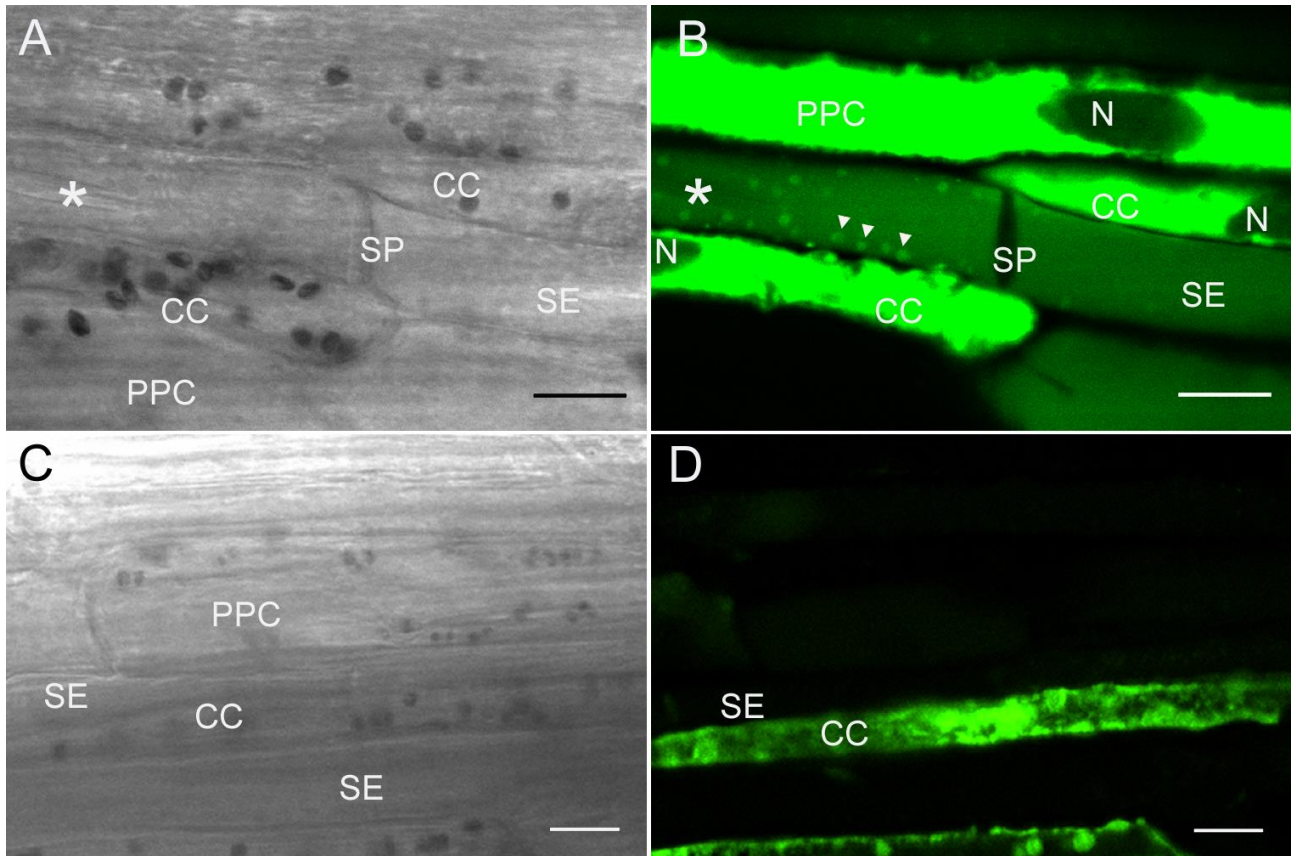


Figure 16: CLSM images of phloem tissue in intact healthy (upper part of the panel) and FD-infected (lower part) *V. faba* plants stained with CFDA. Healthy (A,B) and FD-infected (C,D) phloem under transmission light (A,C) and after distant CFDA application, observed at 488 nm wavelength (B,D). In healthy *V. faba* plants sieve elements were characterized by the presence of forisomes (A) and plastids (B). FD-infected *V. faba* plants did not show remarkable content in transmission light (C). Following sieve-tube translocation of CFDA in healthy plants (B), CFDA was accumulated in the vacuoles of companion and phloem parenchyma cells. With the exception of the vacuoles of companion cell, fluorescence was absent in sieve elements of FD-infected plants (D), indicative of mass-flow inhibition. CC: companion cell, N: nucleus, PPC: phloem parenchyma cell, SE: sieve element, SP: sieve plate. In A and B asterisk indicated forisome, in B arrowheads indicate phloem plastids. Bars correspond to 10 μ m.

After CFDA ((5)6 carboxyfluorescein diacetate) application to visualize the mass flow in intact phloem, phloem-mobile CF was translocated through the sieve tubes of healthy *V. faba* plants and accumulated in the companion cells, which indicates a regular mass flow and a high degree of metabolic activity in companion cells (Fig. 16 B). As reported previously for other cell types (e.g. Goodwin *et al.* 1990), CF accumulated in the vacuoles

Results

of phloem parenchyma cells. In stained sieve elements, several parietal plastids were visible (Fig. 16 B), probably anchored to the plasma membrane (Ehlers *et al.* 2000). Nuclei were recognizable both in companion and phloem parenchyma cells (Fig. 16 B) probably after CFDA movement through plasmodesmata. It was more difficult to focus and discern sieve tubes in FD-diseased plants due to the presence of thicker cell walls and sediments onto the sieve plates (Fig. 16 C). In such plants, only few sieve elements were weakly fluorescent after CFDA application indicating that mass flow was blocked or strongly reduced (Fig. 16 D). Even when mass flow in sieve tubes appeared to be reduced or eliminated, CFDA was observed to accumulate in the vacuoles of companion cells (Fig. 16 D) which may evidence the maintenance of some metabolic ability.

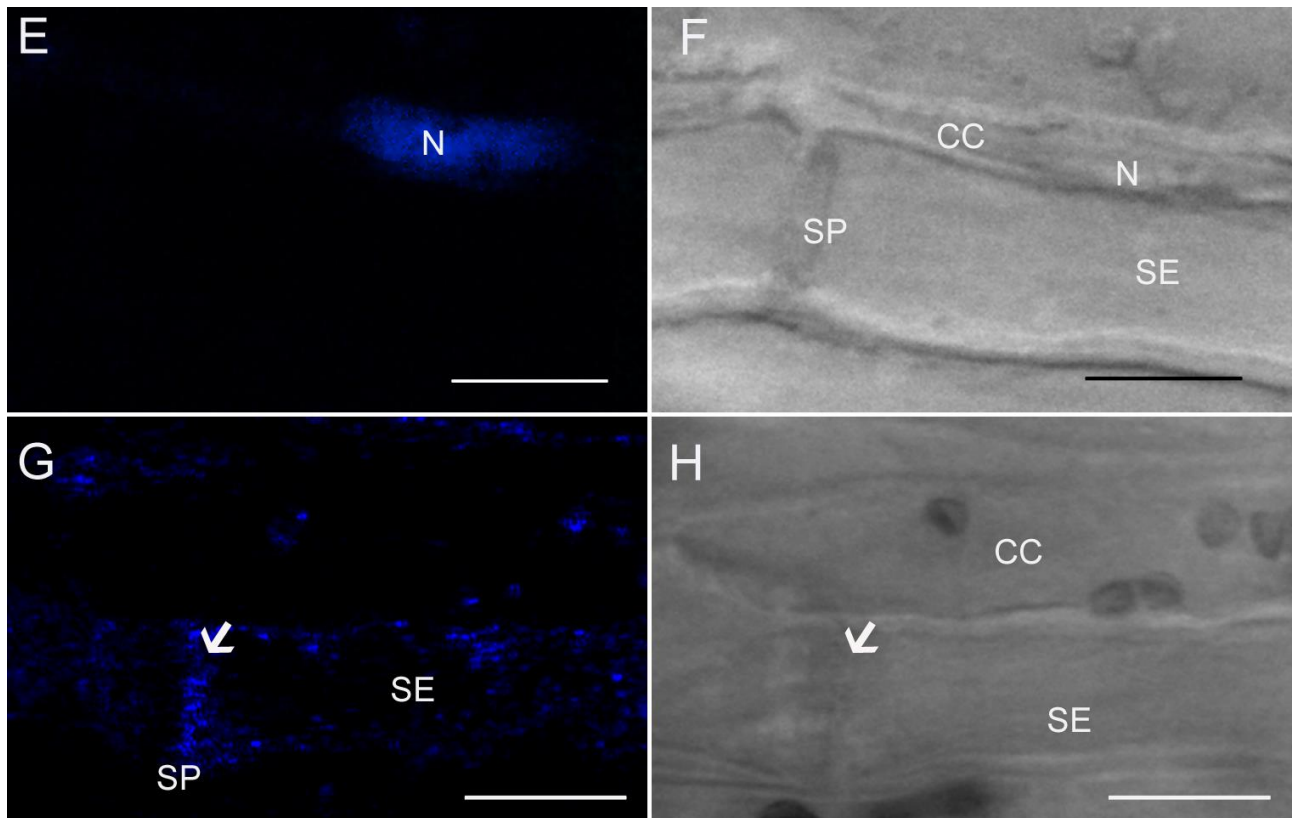


Figure 17: CLSM images of phloem tissue in intact healthy (upper part of the panel) and FD-infected (lower part) *V. faba* plants stained with DAPI. Healthy (E,F) and FD-infected (G,H) phloem after DAPI staining, observed at wavelength of 405 nm (E,G) and under transmission light (F,H). In sieve elements of FD-infected plants, blue fluorescent dots mainly aggregated on both sides of the sieve plate (G). Phloem in healthy plants remained unlabeled apart from the stained nuclei (E). Under transmission light, in healthy plants (F) cell walls and sieve plate thickening seemed inconspicuously. Note the distorted thickened cell walls and sieve plate thickenings visible in FD-infected plants (H). CC: companion cell, N: nucleus, SE: sieve element, SP: sieve plate. In G and H arrows indicate phytolasmal/DAPI fluorescence. Bars correspond to 10 μ m.

Results

After DAPI (4',6-diamidino-2-phenylindole) application to enable phytoplasma detection, no DAPI fluorescence showed up in sieve elements of healthy plants; only the nuclei of companion cells and phloem parenchyma cells were stained (Fig. 17 E). Under transmission light, the sieve elements were well-preserved and unstained in healthy plants (Fig. 17 F). In FD-diseased plants, dotted fluorescent aggregates were accumulated predominantly at the sieve plates (Fig. 17 G, arrows). In FD-diseased sieve elements, cell walls and sediments onto the sieve plates were thicker than in control plants (Fig. 17 H) as described above.

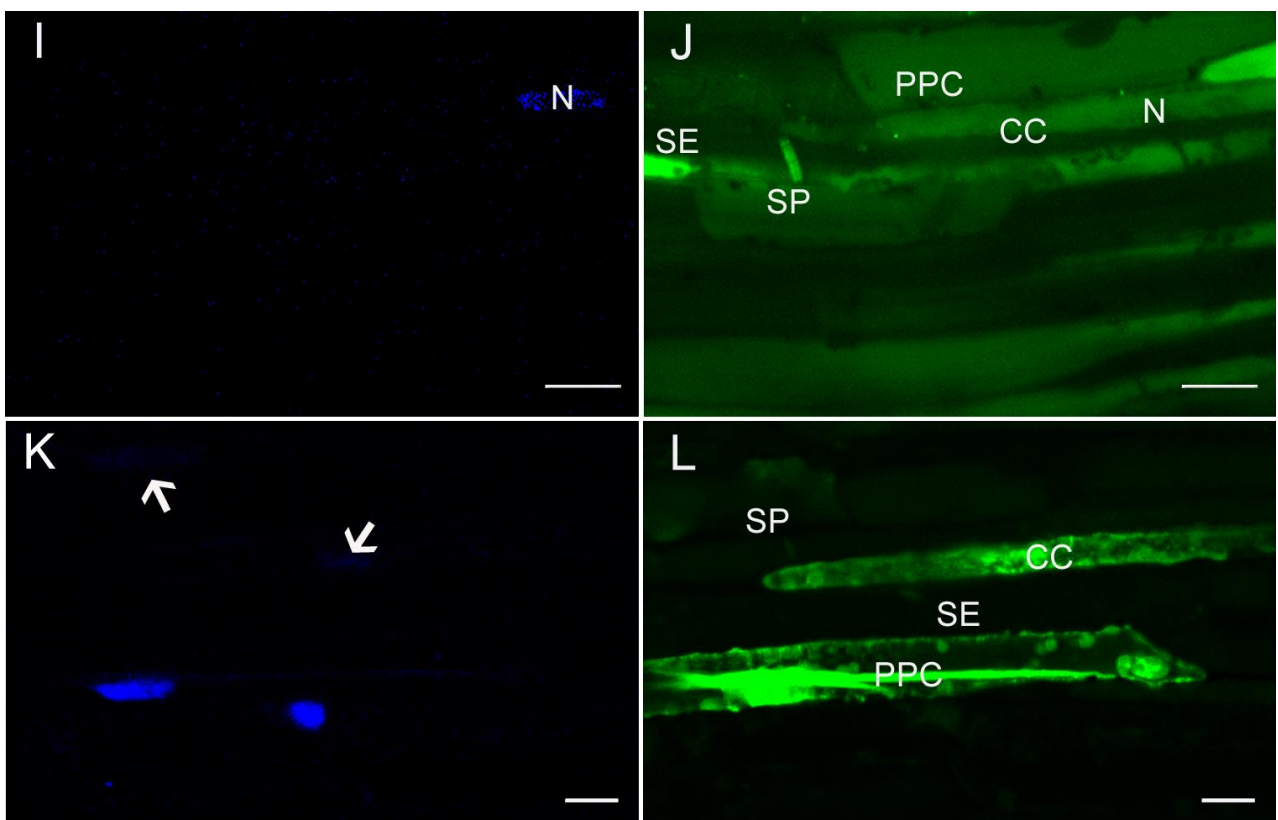


Figure 18: CLSM images of phloem tissue in intact healthy (upper part of the panel) and FD-infected (lower part) *V. faba* plants stained with DAPI and CFDA. Subsequent local DAPI staining and distant CFDA application demonstrated that absence of DAPI staining (I) apart from the stained nuclei, concurred with regular CFDA translocation (J) in the phloem of healthy plants. By contrast, DAPI fluorescence, indicating phytoplasma presence (K), seemed to coincide with impaired sieve-tube translocation in infected plants (L). CC: companion cell, N: nucleus, PPC: phloem parenchyma cell, SE: sieve element, SP: sieve plate. In K arrows indicate phytoplasma/DAPI fluorescence. Bars correspond to 10 μ m.

Successive local DAPI and distant CFDA staining demonstrated that the absence of DAPI staining is related with intense CFDA translocation in the phloem of healthy plants (Fig. 18 I and J). By contrast, DAPI fluorescence (Fig. 18 K) coincides with impaired sieve-tube translocation in infected plants (Fig. 18 L). Both in healthy and in infected plants the

Results

reverse CFDA/DAPI double-staining procedure produced results similar to those for DAPI/CFDA staining (Fig. 19 M to P).

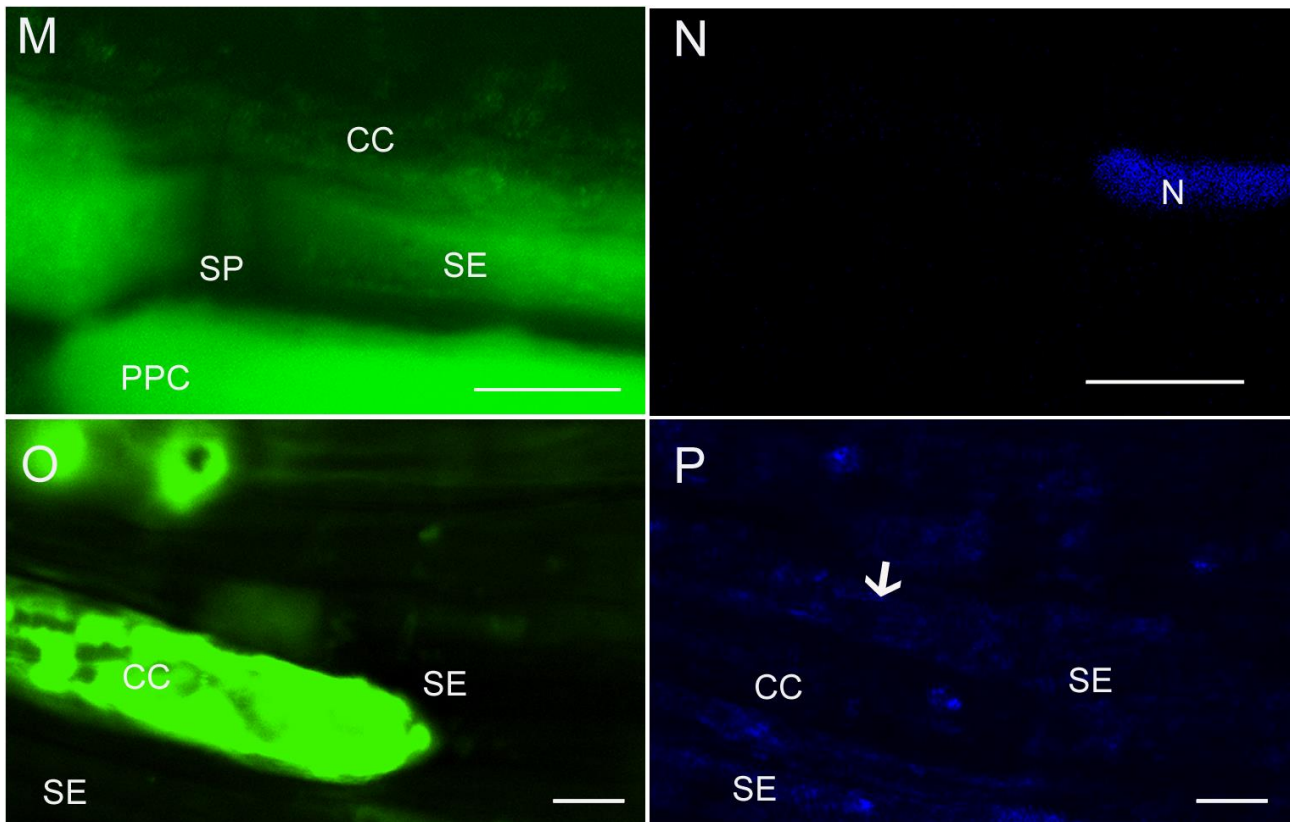


Figure 19: CLSM images of phloem tissue in intact healthy (upper part of the panel) and FD-infected (lower part) *V. faba* plants stained with CFDA and DAPI. The reverse CFDA/DAPI double-staining procedure rendered results similar to those obtained with DAPI/CFDA treatment both in healthy (M, N) and infected plants (O, P). CC: companion cell, N: nucleus, PPC: phloem parenchyma cell, SE: sieve element, SP: sieve plate. In P arrow indicate phytoplasma/DAPI fluorescence. Bars correspond to 10 μm .

3.2.3. Occlusion events and Ca^{2+} concentration

Combined CMEDA/CMFDA (5-chloromethyl-fluoresceindiacetate/5-chloromethyl-eosindiacetate) staining provided unequivocal information on the forisome conformation and protein distribution inside the sieve elements of healthy and FD-diseased plants in CLSM images (Fig. 20). The membrane-permeant, colorless CMEDA/CMFDA diffuse into the sieve elements *via* the plasma membrane and, following the cleavage of the acetate groups are by intracellular esterases, the membrane-impermeant chloromethyl-fluorescein is able to target proteins (Furch *et al.* 2007). In healthy plants, forisomes were always in the condensed, spindle-shaped form (Fig. 20 A and B) and were mostly located near the sieve plates at the downstream end of the sieve elements. In FD-diseased plants, discrete forisomes were not detectable (Fig. 20 C and D), which is indicative of their dispersion

Results

(Knoblauch *et al.* 2001). Unidentified protein structures, dispersed forisomes or clogged P-proteins, occurred in FD-diseased sieve elements (Fig. 20 C).

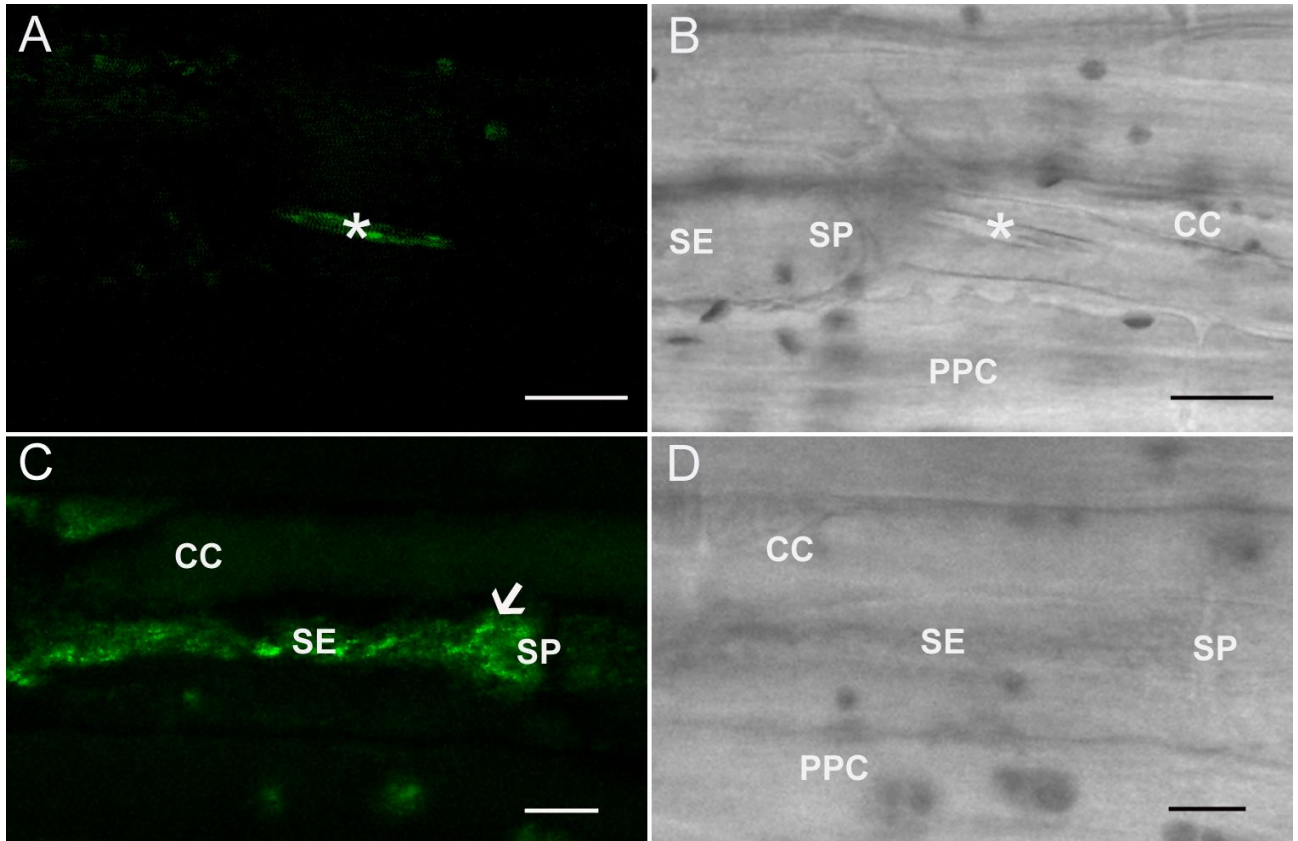


Figure 20: CLSM images of phloem tissue in intact healthy (upper part of the panel) and FD-infected (lower half) *V. faba* plants stained with CMEDA/CMFDA. Phloem tissue, observed at wavelength of 488 nm (A,C) and under transmission light (B,D) after combined CMEDA/CMFDA staining. In healthy sieve elements, forisomes occurred in the condensed conformation (A,B). In FD-infected phloem, forisome bodies were not visible (C,D) and non-identified proteinaceous dispersed material was present along the sieve elements (C). CC: companion cell, SE: sieve-element, PPC: phloem parenchyma cell, SP: sieve plate. In A and B asterisk indicated forisome, in C arrow indicate protein structures. Bars correspond to 10 μ m.

Aniline blue at non-lethal concentrations (Furch *et al.* 2007) was administered to bare-lying phloem tissue to acquire a qualitative *in vivo* estimate of callose deposition in sieve elements (Fig. 21). In healthy plants, callose was not detectable (Fig. 21 E) or occurred in minor amounts at the margins of the sieve plates (Fig. 21 G) and the sieve elements were well preserved containing condensed forisomes (Fig. 21 F and H). By contrast, aniline blue signals were much stronger in FD-diseased *V. faba* plants indicating massive callose depositions at the sieve plates and along the sieve elements, probably at the pore-plasmodesmata-unit (PPU) orifices (Fig. 21 I; Furch *et al.* 2009) to the point of plug formation (Fig. 21 K, arrows).

Results

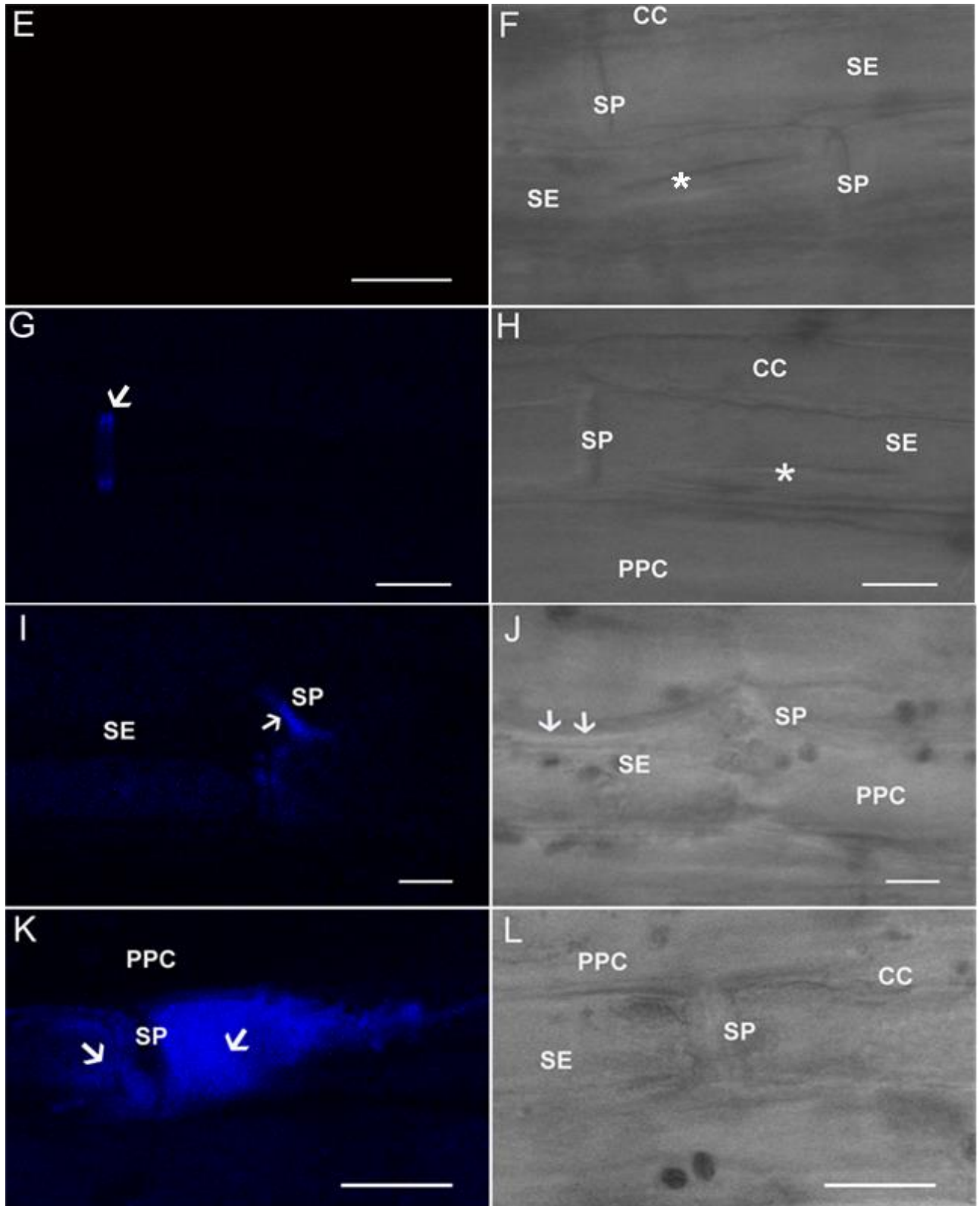
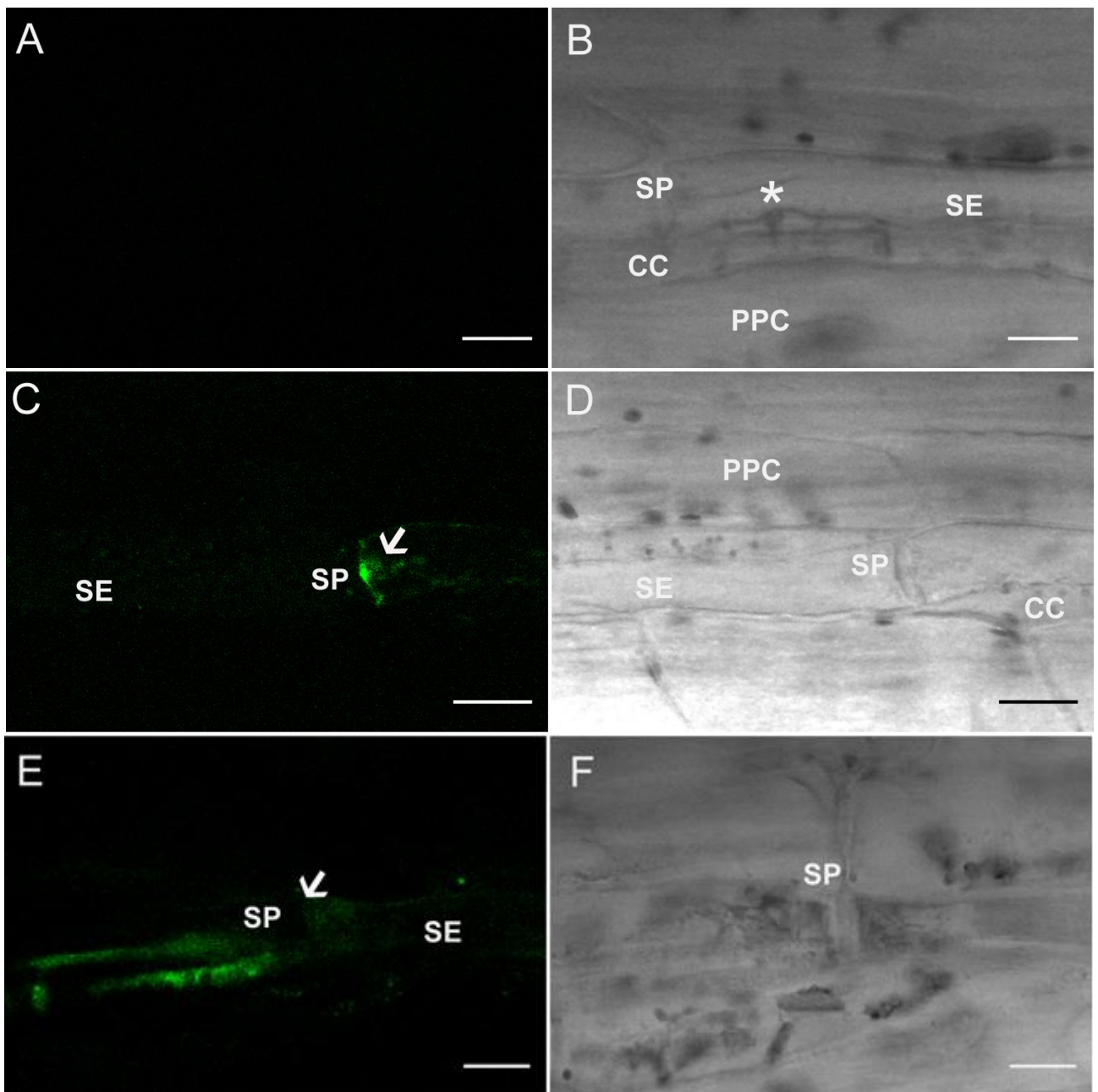


Figure 21: CLSM of phloem tissue in intact healthy (upper part of the panel) and FD-infected (lower half) *V. faba* plants stained with aniline blue. Phloem tissue after aniline blue treatment, specific for callose detection in intact sieve tubes, observed at wavelength of 405 nm (E,G,I,K) and under transmission light (F,H,J,L). In healthy sieve elements, callose was not detectable (E) or deposited in small amounts at the sieve-plate margins (G). In infected plants, aniline blue staining indicated large callose depositions along the sieve elements in particular in the vicinity of the sieve plates (I) through to plug formation (K). Note that forisomes were invisible in sieve elements of infected plants. CC: companion cell, SE: sieve-element, PPC: phloem parenchyma cell, SP: sieve plate. In F and H asterisk indicated forisome, in I and K arrows indicate callose/aniline fluorescence, in J arrows indicate thickened sieve-element walls, in G arrow indicate the sieve plate. Bars correspond to 10 μ m.

Results

Upon Ca^{2+} -binding, the fluorescence intensity of the cell-permeant dye Oregon Green BAPTA-1 (1,2-bis(o-aminophenoxy)ethane-N,N,-N',N'-tetraacetic acid, OGB-1) increases (Furch *et al.* 2009). The dye was used as a qualitative indicator of Ca^{2+} concentration inside the sieve elements (Fig. 22). No fluorescent signals were detected in intact sieve elements of uninfected *V. faba* plants (Fig. 22 A). The identical optical section observed under transmission light showed unstressed sieve elements as inferred by the presence of condensed forisomes (Fig. 22 B, asterisk). In the phloem of diseased plants, OGB-1 fluorescence was often intense with strong signals at the sieve plates (Fig. 22 E and G).



Results

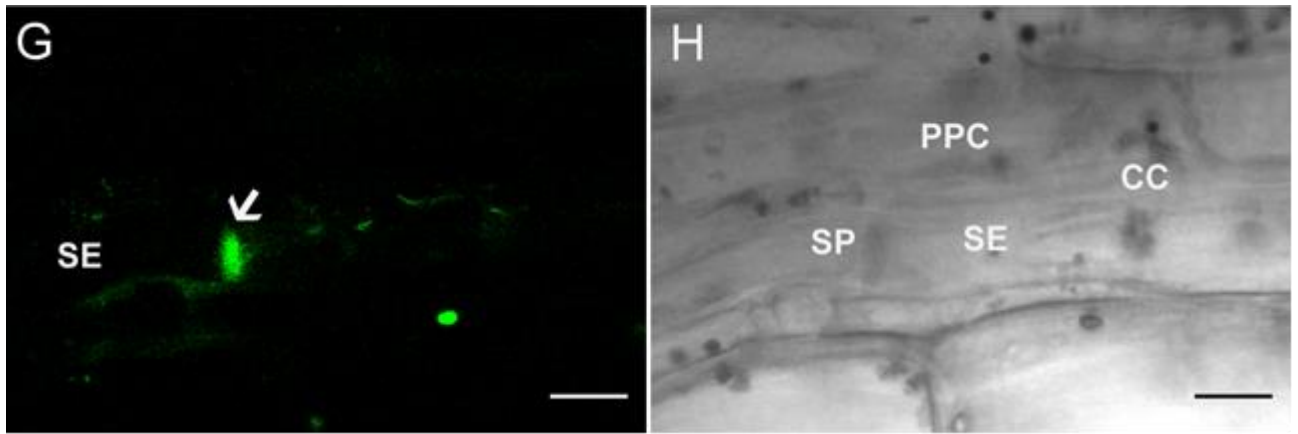


Figure 22: CLSM images of phloem tissue in intact healthy (upper part of the panel) and FD-infected (lower half) *V. faba* plants stained with OGB-1. Phloem after OGB-1 staining, observed at wavelength of 488 nm (A,C,E,G) and under transmission light (B,D,F,H). In healthy sieve elements, OGB-1 fluorescence was absent (A) or weakly present in the sieve plate region (C). In infected plants, the fluorescence signal was very strong along the sieve-element plasma membrane (E) particularly at the sieve plates (G). Note the dark undefined substances in sieve elements of FD-infected plants (F,H) and the transparent sieve-elements of healthy plants (B,D). CC: companion cell, SE: sieve-element, PPC: phloem parenchyma cell, SP: sieve plate. In B asterisk indicated forisome, in C, E and G arrows indicate sieve plates. Bars correspond to 10 µm.

Under transmission light, condensed forisomes did not occur (Fig. 22 F and H). Weak OGB-1 signals were sometimes found in healthy sieve elements that were mechanically stressed as a result of the preparation procedure as indicated by forisome dispersion (Fig. 22 C, arrow).

3.3. Ultrastructural analysis of plant-pathogen interaction

3.3.1. Plant materials and phytoplasma detection by PCR

To identify innate host-pathogen interaction *S. lycopersicum* plants were phytoplasma infected *via* grafting. Control plants showed regular growth without disease symptoms. In stolbur-diseased plants, typical symptoms, such as diffuse yellowing, leaf-size reduction, witches' brooms and stunting, emerged approximately 2 months after grafting (Fig. 23).

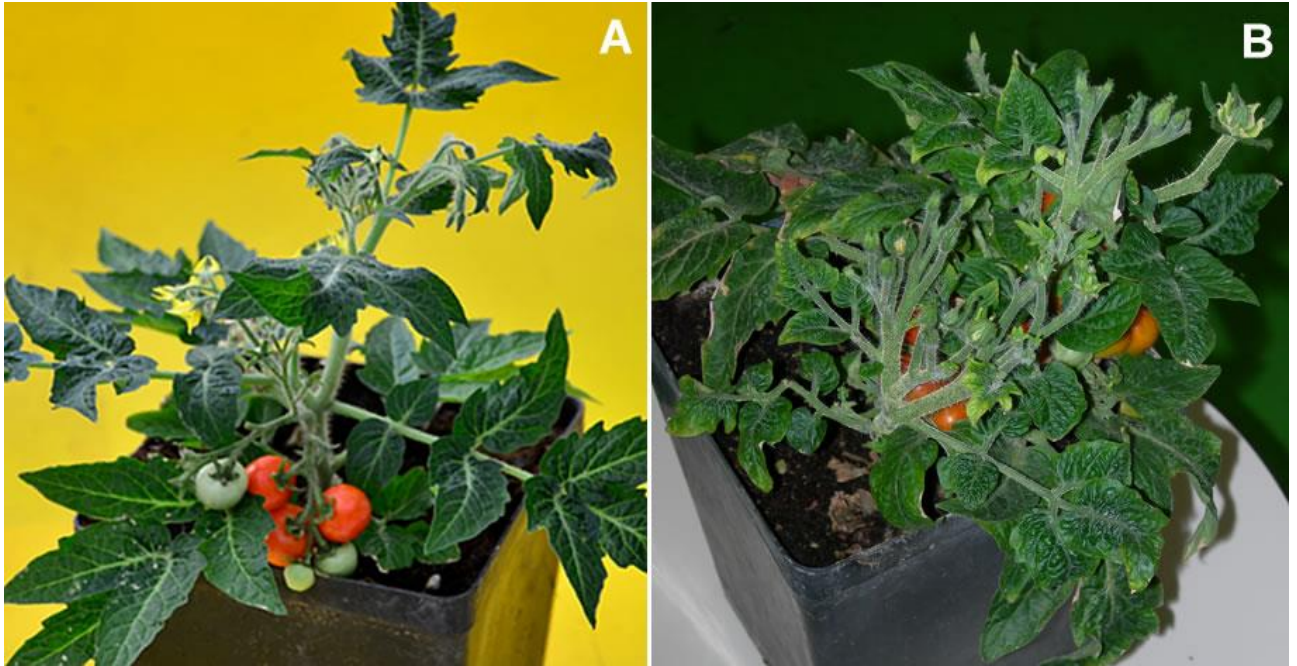


Figure 23: Images of healthy (left half of the panel) and stolbur-diseased (right half) *S. lycopersicum* Micro-Tom plants. Healthy *S. lycopersicum* plant showed regular growth, normal leaves and flowers are present (A). In stolbur-diseased plants diffuse symptoms were visible, such as leaf-size reduction and along with yellowing, witches' brooms and stunting (B).

Real time RT-PCR of 'Ca. *P. solani*' 16S rRNA confirmed the presence of phytoplasmas in leaf samples from stolbur-diseased *S. lycopersicon* before treatment for microscopic examination. Starting from 40 ng of total cDNA, stolbur phytoplasma 16SrRNA was detected in infected plants, whereas no amplification of the 16S rRNA gene was obtained in control plants (Supplemental table 2).

Observations were performed using four healthy and diseased *S. lycopersicum* plants, as soon as symptoms appeared on infected ones. Experiments were repeated on fifteen chosen leaf midrib segments, respectively from infected and healthy *S. lycopersicum* plants. For Light (LM), Epifluorescence (EFM) and Transmission Electron Microscopy (TEM) experiments several serial semithin and ultrathin sections of at least 100 samples from healthy and stolbur-diseased plants were collected and randomly chosen observed.

3.3.2. Imaging of phytoplasmas by Epifluorescence Microscopy

To visualize phytoplasmas in sieve elements of *S. lycopersicum* plants, longitudinal (Fig. 24 A to F), and cross sections (Fig. 24 G to J) from London Resin White (LRW)-embedded samples were cut, stained with the DNA specific marker DAPI (4',6-diamidino-2-phenylindole) and observed under the EFM.

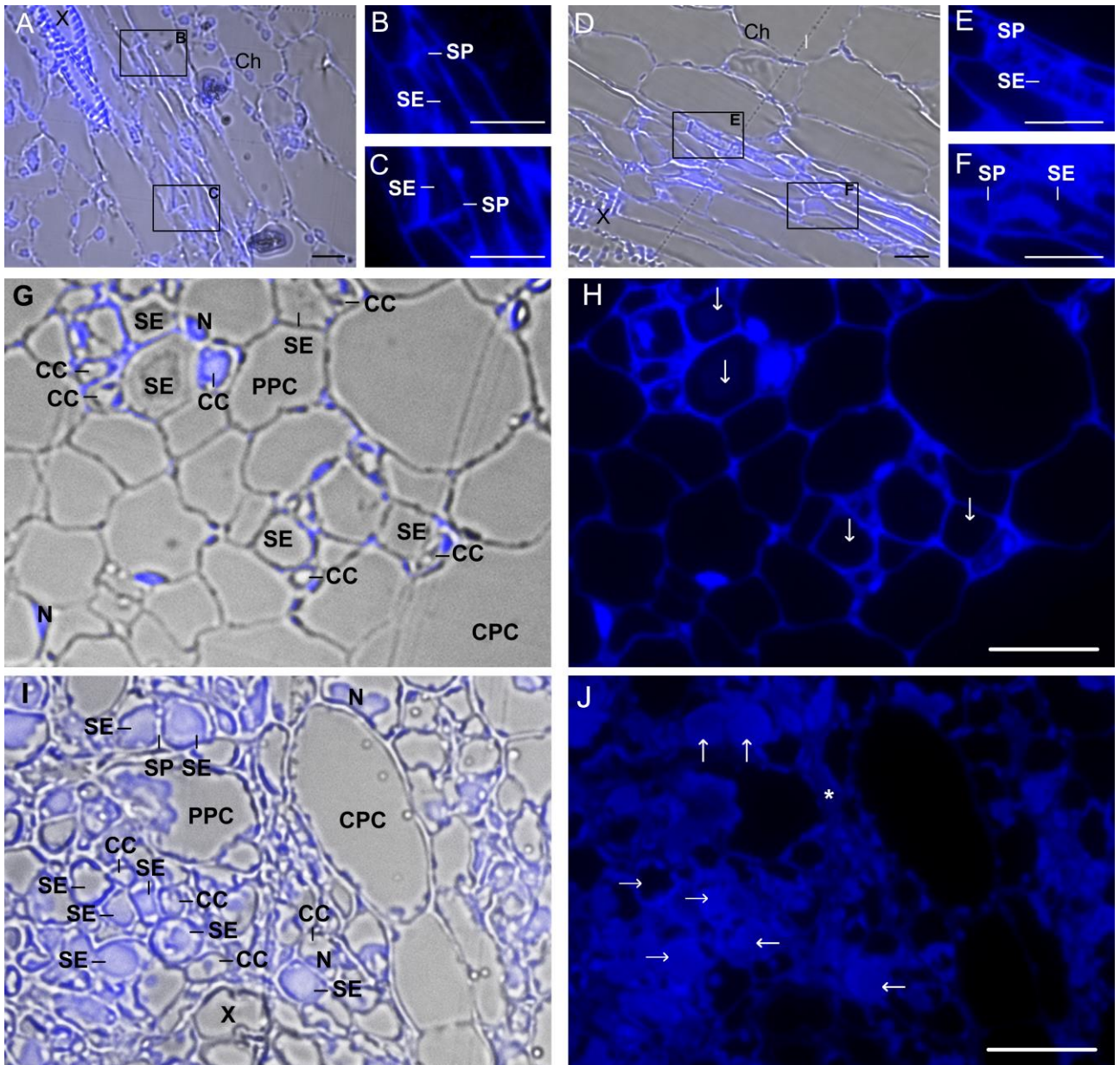


Figure 24: Light (LM) and Epifluorescence Microscopy (EFM) images from longitudinal and cross sections of main veins of healthy and stolbur-diseased *S. lycopersicum* leaves, stained with DAPI. In both longitudinal and cross-sections of phloem, autofluorescence of the chloroplasts (A and D) and unspecific signal of the cell walls was visible, the latter in particular in those of xylem vessels (A ,D) and close to the sieve plates (B,C,E,F). Fluorescence signals of the nuclei in companion cells and cortex parenchyma cells were discernible (G,H,I,J). In healthy leaves, fluorescent spots are absent inside sieve elements (A,B,C,G,H; arrows in H). In stolbur-diseased samples, fluorescent masses were accumulated along the sieve elements (D), in particular at the sieve plates (E,F), and fill up the lumina in some instances (I ,J; arrows in J). Transformation of sieve element structure and cell wall thickness occurred all along

Results

infected areas (I, asterisk). CC: companion cell, Ch: chloroplast, CPC: cortex parenchyma cells, N: nucleus, PPC: phloem parenchyma cell, SE: sieve element, SP: sieve plate, X: xylem vessel. Bars correspond to 10 μm .

In longitudinal leaf sections, DAPI fluorescence was absent in sieve elements of healthy samples (Fig. 24 A to C); only signals due to chloroplasts (Ch) in parenchyma cells (Fig. 24 A) as well as strong autofluorescence of the cell walls were detected (Fig. 24 B and C). In stolbur-diseased plants, fluorescent materials were accumulated all the way along the sieve elements (Fig. 24 D), in particular at the sieve plates (SP; Fig. 24 E and F). In cross-sections of healthy leaves, the vein structure was well preserved (Fig. 24 G) and no fluorescent signal was detectable inside sieve elements (Fig. 24 H). Nuclei (N) of companion cells (CC) and phloem parenchyma cells (PPC) were well discernible (Fig. 24 G and H). By contrast, infected samples showed several sieve elements filled with fluorescent masses (Fig. 24 I and J), indicating phytoplasma accumulation. In addition, cell-wall thickness and shape of the sieve elements were significantly altered and disorganized in affected areas (Fig. 24 I). Fluorescence signal associated with the nuclei was also discernible in companion cells and phloem parenchyma cells (Fig. 24 I and J), but not in non-vascular cells.

3.3.3. Sieve-element membrane network visualization by Epifluorescence Microscopy and Transmission Electron Microscopy

In order to visualize phytoplasma-related modification of phloem membrane system the fluorescent marker RH414 was used. In *S. lycopersicum* leaves the RH 414 (N-(3-triethylammoniumpropyl)-4-(4-(4-(diethylamino)phenyl)butadienyl)pyridinium dibromide) allowed imaging of the plasma membranes, nuclear membranes and organelles delimited by a double membrane (Fig. 25 A to F) as well as organism, like phytoplasmas, likewise bound by a double membrane. In healthy leaves, the fluorescent patterns showed a regular distribution of the membrane network and organelle arrangement (Fig. 25 A to C). As expected (e.g. Knoblauch and van Bel 1998), fluorescence was exclusively localized to the periphery of the sieve elements (Fig. 25 B and C). In companion cells, phloem parenchyma cells and in the cortex parenchyma cells (CPC), fluorescence signal from organelles like the nuclei and chloroplasts was visible (Fig. 25 A though C). In stolbur-diseased leaves, fluorescent signal in the sieve-element lumen indicated distortion of the membranes (Fig. 25 D to F).

Results

TEM images of healthy control leaves showed a strict alignment of the sieve-elements plasma membrane (PM) with the cell wall (Fig. 25 G). In infected tissue, the plasma membrane network of the vascular cells appeared contorted and undulated (Fig. 25 H to J). The sieve-element and the phytoplasma membranes appeared to be in close contact (Fig. 25 J). Together, they may have developed a membrane-bound corridor to secure the connection (Fig. 25 K to N). Even after detachment of the plasma membrane due to plasmolysis, the phytoplasmas remained attached to the host membrane (Fig. 25 L). The characteristic pleomorphism and the presence of ribosomes inside the bodies (Fig. 25 J) identified them without doubt as phytoplasmas (P), although size and position were similar to that of sieve-element plastids (SEP; see Fig. 27 H and Ehlers *et al.* 2000).

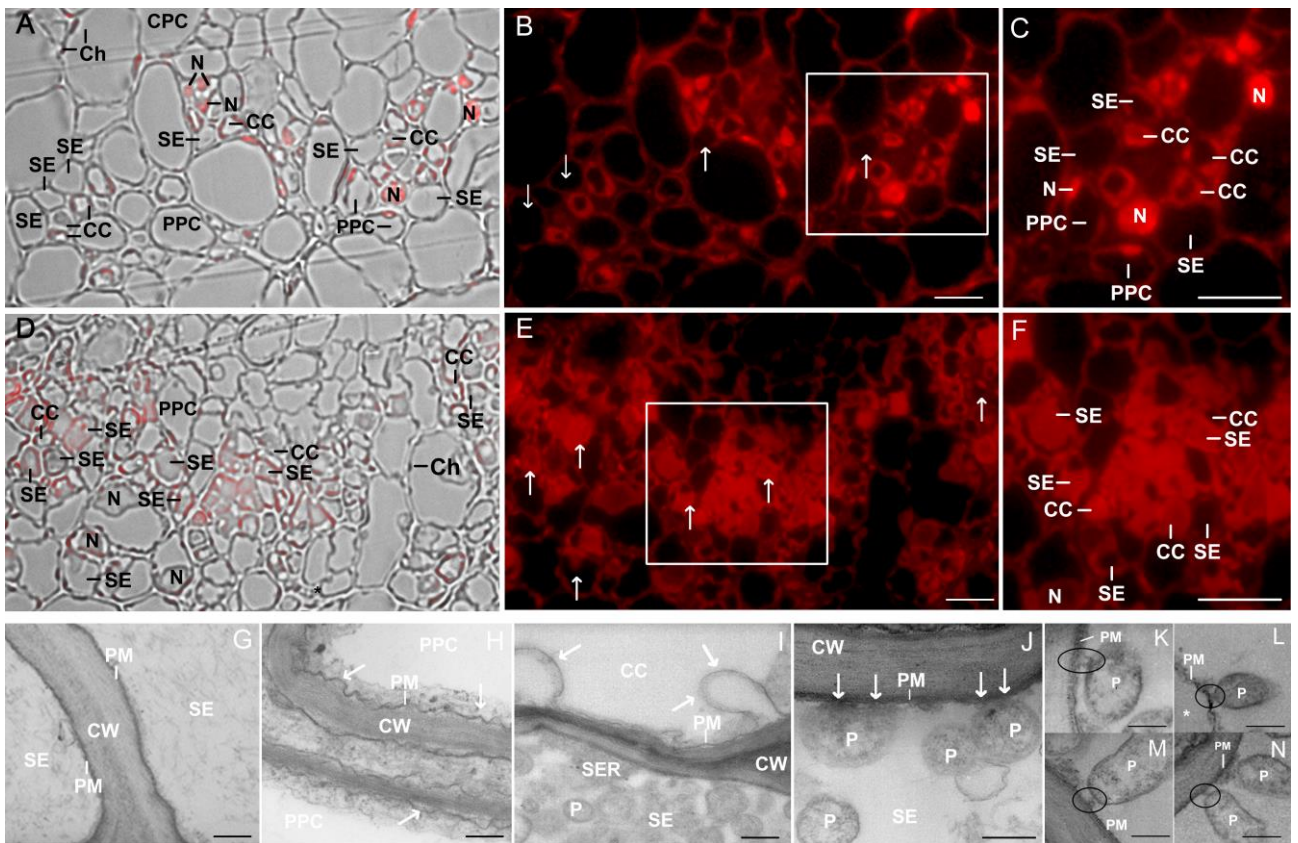


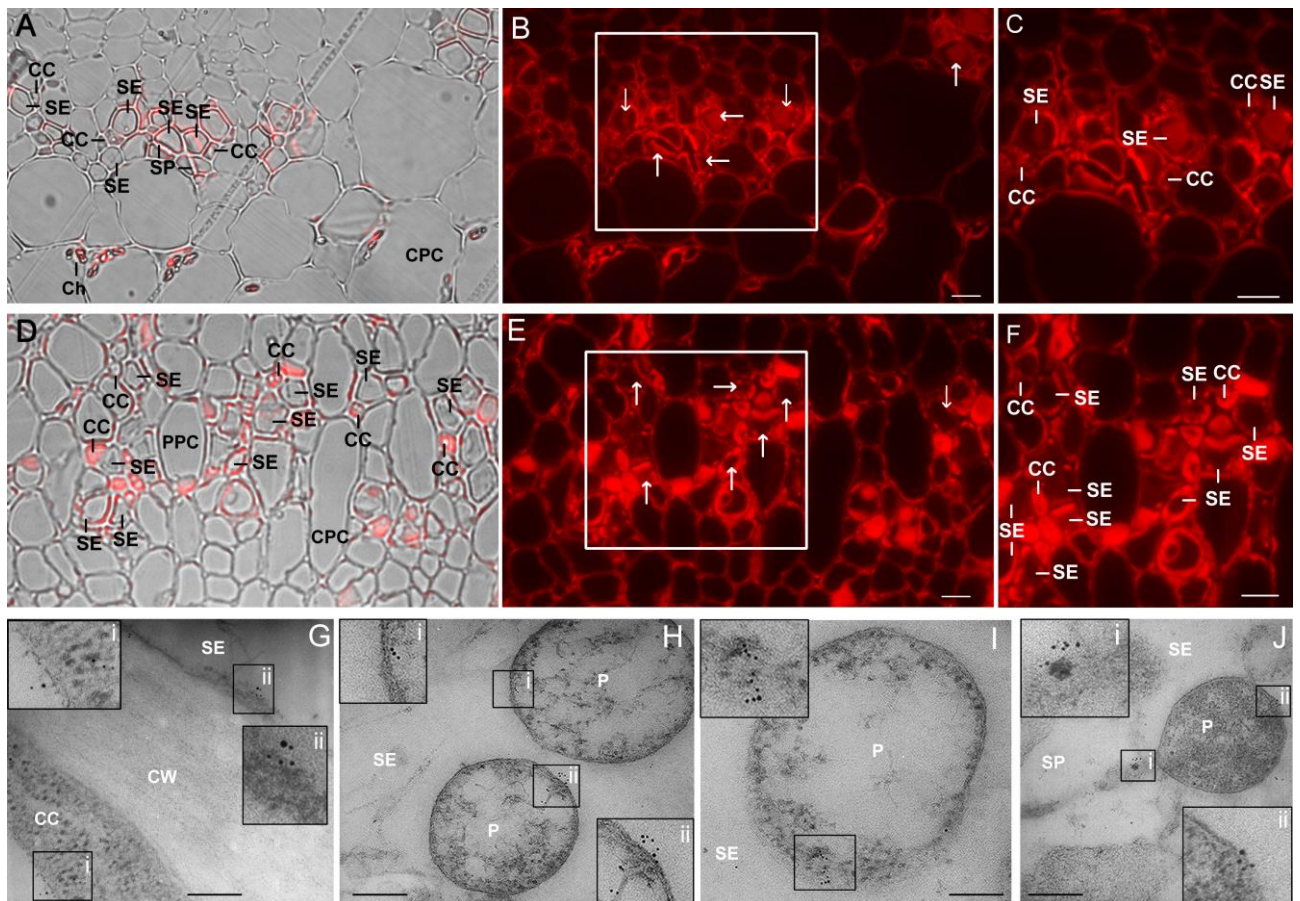
Figure 25: LM and EFM micrographs from cross-sections of main veins of healthy and stolbur-diseased *S. lycopersicum* leaves stained with RH 414. In healthy leaves (A,B,C), fluorescent signals were closely appressed to the sieve element cell wall (A,B; arrows in B) or aggregated around nuclei (A,B, C) and organelles, like chloroplast (A), that were delimited by a double membrane. The sieve-element lumen remained unlabeled (B,C; arrows in B). In stolbur-diseased leaves, the plasma membrane appeared distorted (D,E,F) with a stronger fluorescence inside the sieve element than in healthy plants (E,F; arrows in E). G to N: Attachment of phytoplasma body to sieve-element plasma membrane was demonstrated by Transmission Electron Microscopy (TEM). TEM observations from uninfected *S. lycopersicum* leaves (G) showed the sieve-element plasma membrane closely aligned to the cell wall. In stolbur-diseased *S. lycopersicum* leaves (H,N) the plasma membranes of phloem parenchyma and companion cells were rippled (H, arrows) or bulge (I, arrows). In sieve elements, plasma membrane modifications conferred an intimate association between phytoplasma and host membrane (J, arrows). A string-like structure seemed to connect phytoplasma and sieve-element plasma membrane (K to N, black circles). Even

Results

after detachment of the sieve-element plasma membrane due to plasmolysis (L, asterisk) the bacteria remained connected to the sieve-element plasma membrane (black circle). CC: companion cell, Ch: chloroplast, CPC: cortex parenchyma cells, CW: cell wall, N: nucleus, P: phytoplasma, PM: plasma membrane, PPC: phloem parenchyma cell, SE: sieve element, X: xylem vessel. Bars correspond to EFM = 10 μ m; TEM (H,I,J,K,L,M,N) = 200 nm; TEM (G) = 400 nm; Insets (C and F) represent enlarged regions of interest of B and E, respectively.

3.3.4. Sieve-element actin and SER network visualization and connections with phytoplasma cells

The modification of actin structures (Fig. 26) in *S. lycopersicum* sieve elements was visualized using α -actin-Texas Red-conjugated (TR) antibodies. Control samples, incubated without primary antibody did not showed signals (Supplementary Fig. 4 E and F). In healthy tissue the signal intensity differed among the diverse plant tissues. In contrast to the high signal intensity in sieve elements, the level of fluorescence was low in cortex parenchyma cells (Fig. 26 A to C). In comparison to the controls, the TR distribution in stolbur-diseased sieve elements (Fig. 26 D to F) changed radically, suggesting a re-arrangement of actin organizations in sieve elements of infected tissue. The sieve elements edges showed scattered signal distribution and actin structures appeared partly present in the sieve-element lumen (Fig. 26 E and F).



Results

Figure 26: LM and EFM micrographs from cross-sections main veins of healthy and stolbur-diseased *S. lycopersicum* leaves stained with an α -actin-Texas Red-conjugated antibody. In healthy samples (A,B,C) the fluorescence pattern indicates that actin structures network was localized at the periphery of the sieve elements (B,C; arrows in B). Intensity of TR fluorescence increased in sieve elements of stolbur-diseased plants (D,E,F), which appeared to be clustered around the sieve element periphery and in the lumen (E,F; arrows in E). G to J: Arrangement of sieve-element actin in relation to the phytoplasma cells evidenced by TEM-immunogold technique. In healthy plants gold particles were always distributed at the margins of the sieve elements (G, i, ii, iii). In infected tissue, gold particles were clustered in the sieve-element lumen in association with the phytoplasma membrane surface (H,I), forming groups mainly at one side of bacterial body (insets). Co-occurrence of gold particles was visible at the sieve pores and on phytoplasma membrane (J and insets). CC: companion cell, Ch: chloroplast, CPC: cortex parenchyma cells, CW: cell wall, P: phytoplasma, PPC: phloem parenchyma cell, SE: sieve element, SP: sieve pore, X: xylem vessel. Bars correspond to EFM = 10 μ m; Scale bars TEM = 200 nm; Insets (C and F) represent enlarged regions of interest of B and E, respectively.

The spatial relationship between actin structures and phytoplasma bodies was presented by labeling using α -actin-gold-conjugated antibodies (Fig. 26 G to J). In agreement with a recent report (Hafke *et al.* 2013), actin was localized at the periphery of the sieve elements in control samples (Fig. 26 G). In stolbur-diseased samples ultrastructural images showed that gold particles in the sieve element lumen were associated with phytoplasma cells, invariably clustered at one side of the phytoplasma membrane surface (Fig. 26 H to J).

To identify alteration of ER in infected sieve elements the reticulum marker ER Tracker Green was applied. Like actin filaments, the sieve-element reticulum (SER) network (Fig. 27) showed a re-organization after phytoplasma infection. Compared to healthy controls (Fig. 27 A to C) fluorescence intensity of the sieve-element ER Tracker Green increased in infected tissue (Fig. 27 D to F). Moreover structural modification of the sieve-element reticulum in infected tissue led to a difference in signal distribution. ER Tracker Green signal was aggregated at the edges of the sieve element and evident in sieve-element lumen after infection (Fig. 27 F).

Sieve-element reticulum stacks were mostly oriented in parallel to the sieve-element plasma membrane in healthy samples (Fig. 27 G and H), whereas the sieve-element reticulum seems to be contorted in stolbur-diseased samples (Fig. 27 I to L). In stolbur-diseased sieve elements, phytoplasma cells were in close proximity of the sieve-element reticulum (Fig. 27 I and K), but attachment structures jointing phytoplasma membrane and sieve-element reticulum *via* minute anchors were not observed. In infected plants, sieve-element reticulum stacks frequently appeared fragmented into lobes and vesicles, protruding into the sieve-element lumen (Fig. 27 L).

Results

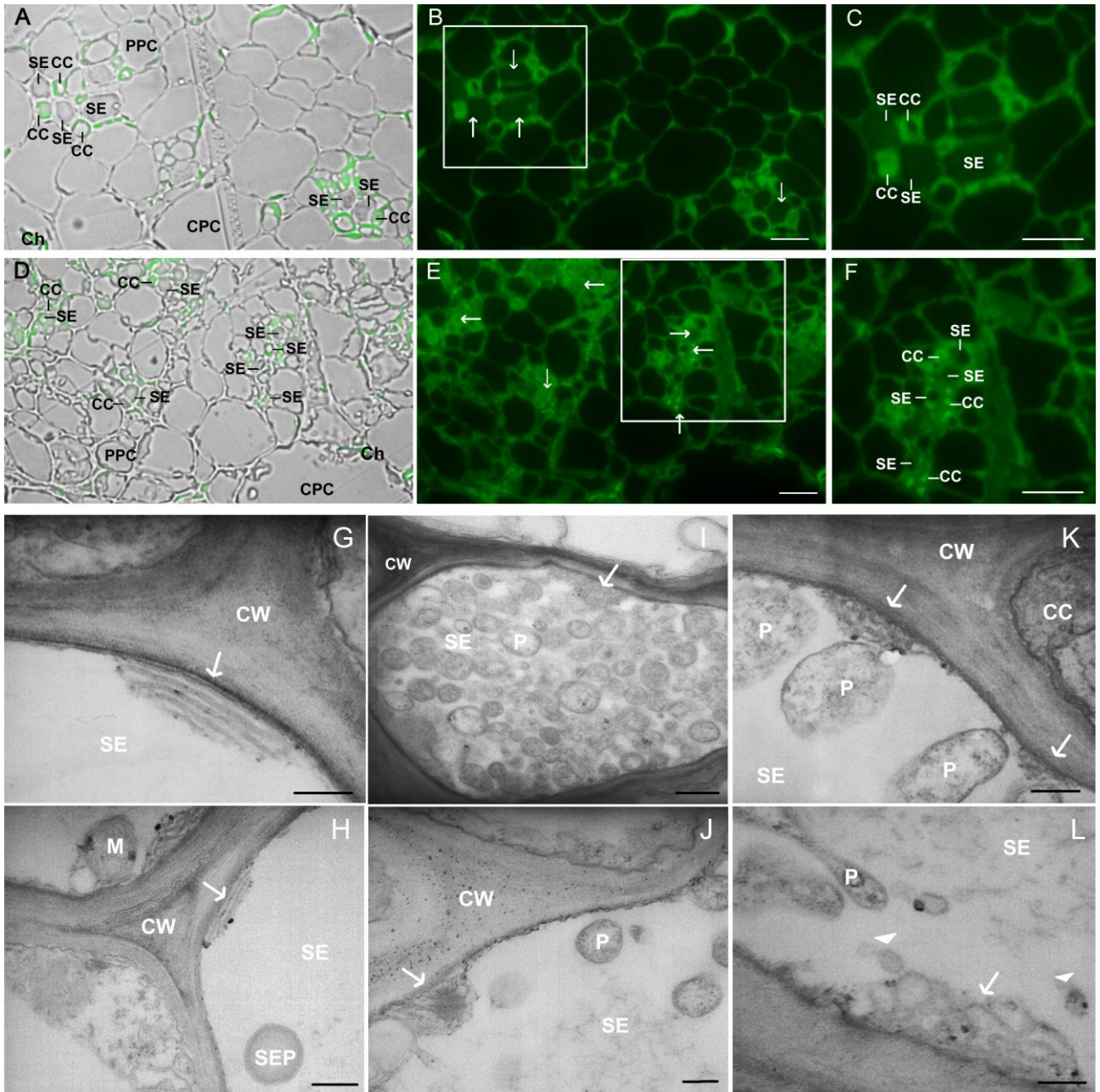


Figure 27: LM and EFM micrographs from cross-sections of the main veins of healthy and stolbur-diseased *S. lycopersicum* leaves stained with ER Tracker Green. In control leaves (A,B,C), fluorescence was localized to the periphery of sieve elements. In infected samples, fluorescence intensity had increased and distribution changed in sieve elements. (D,E,F). The sieve elements were “empty” in healthy samples (B,C; arrows in B) and appeared “filled” after infection (E,F; arrows in E). G to L: TEM pictures suggested an association between sieve-element reticulum and the phytoplasma body. In the healthy control samples, sieve-element reticulum network was organized in regular stacks, mostly parallel to the plasma membrane and closely associated with the plasma membrane (G,H, arrows). In stolbur-diseased tissues, sieve-element reticulum stacks were contorted (I,K,J, arrows) and in close contact with phytoplasmas (P in K). Fragmented sieve-element reticulum stacks also appeared as lobes and vesicles protruding into the sieve-element lumen (L, arrowheads). CC: companion cell, Ch: chloroplast, CPC: cortex parenchyma cells, CW: cell wall, M: mitochondria, N: nucleus, P: phytoplasma, PPC: phloem parenchyma cell, PM: plasma membrane, SE: sieve element, SEP: sieve-element plastid. Bars correspond to EFM = 10 μ m; Scale bars TEM (G,H,J,K,L) = 200 nm; TEM (I) = 400 nm; Insets (C and F) represent enlarged regions of interest of B and E, respectively.

4. Observation of phloem immune response to bacterial invasion

Systemic signaling *via* vascular bundles is essential for plant development and adaptation to environmental changes including biotic stress imposed by plant pathogens (Durrant and Dong 2004; Grant and Lamb 2006). The phloem system is involved in short- and long-distance transport of signal molecules. Signaling *via* diverse RNA-species (Hannapel *et al.* 2013; Kehr 2013), carbohydrates (Koch 2004; Müller *et al.* 2011), proteins (Le Hir and Bellini 2013; Pallas and Gomez 2013), oxygen species (Durner and Klessig 1999), secondary metabolite (Lee *et al.* 2007) and phytohormones (Golan *et al.* 2013) as well as electrical signals (Fromm *et al.* 2013) are supposed to be integral parts of induced systemic resistance response of plants (van Bel and Gaupels 2004). Moreover, reversible disruption of the mass flow in the phloem is assumed to be one of the first traits in plant immune defense (Schulz 1998; van Bel 2003). Rapid sieve-element occlusion due to callose and protein accumulation (Furch *et al.* 2007) might form a physical barrier to stop uncontrolled loss of phloem sap, to restrict pathogen invasion and to accumulate defense and signal molecules. Its reversibility ensures a systemic spread of signals. Finally, dynamics of cytoskeleton and rapid endomembrane reorganization in response to stress may enhance the delivery of pathogen defense-related components, such as toxins and pathogen-degrading enzymes, facing pathogen invasion (Opalski *et al.* 2005; Hardham *et al.* 2007; Tian *et al.* 2009).

In fact, information about the effect of phloem on initiation and first reaction to microbial invasion as well as on structural modification, including sieve-element occlusion, during bacterial infection lacks so far. The profound knowledge about the impact of biotic stress on plant, especially on the sensible and essential phloem system, defense and signaling mechanisms are fundamental for a better understanding of the physiology of plants. In this work an integrated approach of diverse plant species and techniques was investigated to gain a detailed understanding of plant immunity inside the phloem, which impacts the sieve-element function and morphology.

To explore the involvement of phloem cells on initiation of immune responses, bacterial elicitor was precisely applied and phloem reaction was directly observed using diverse (non)-invasive microscopy techniques. Long-term impact of bacterial infection on phloem physiology was studied using the intimate plant-phytoplasma interaction.

4.1. Distant flagellin-triggered signal induces Ca²⁺-mediated phasic sieve-element occlusion

Bacterial invasion into host tissue causes various diseases in plants (Jackson 2009). But plants do not surrender to pathogen infection without a struggle. Initiated immune responses, such as pattern-triggered immunity (PTI) or effector-triggered immunity (ETI), face bacteria to restrict growth and reproduction (Jones and Dangl 2006). Next to local biochemical and structural defense-related mechanisms (Mauch *et al.* 1988; Greenberg and Yao 2004; Naito *et al.* 2008; Coll *et al.* 2010; Bednarek and Osbourn 2009; Ding and Voinnet 2007; Zhang *et al.* 2007), systemic induced immune responses are known to occur during plant-pathogen interaction (Ryals *et al.* 1996; Durrant and Dong 2004; Mishina and Zeier 2007; Dempsey and Klessig 2012). Because of the capability of long-distance trafficking, the phloem plays a critical role in the transduction of SAR signals (Jenks and Kuc 1979; Guedes *et al.* 1980; Tuzun and Kuc 1985; van Bel and Gaupels 2004).

However, many studies focusing on molecules and mechanism of signal transduction in the phloem after pathogen attack (van Bel and Gaupels 2004), the specification of phloem-based immunity in response to bacterial infection are poorly understood.

Perception of bacterial invaders, among others trigger membrane depolarization (Jeworutzki *et al.* 2010) leading to an increase in cytosolic Ca²⁺ (Ranf *et al.* 2011). Increased Ca²⁺ concentration inside the plant cells are sensed by calcium-dependent protein kinases (CDPKs), known to initiate distinct immune reactions (Harmon *et al.* 2000; Harper and Harmon 2005). Among others, CDPKs can act, together or beside the mitogen-activated protein kinase (MAPK) cascade, to regulate reactive oxygen species (ROS) production (Kobayashi *et al.* 2007). Because of its chemical property to diffuse between cells, the membrane-permeable hydrogen peroxide (H₂O₂), a representative ROS, is assumed to propagate the initiated immune signal from cell to cell (Dubiella *et al.* 2013). Furthermore, plasma membrane depolarization can directly induce electrical signals (Davies 2004). Even if the propagation of such signals is limited (Overall and Gunning 1982), Ca²⁺ influx can trigger action potentials that induces self-amplification of electro potential waves (EPW) in adjacent cells (Davies and Stankovic 2006). Transmission of electric signals is known to generate local and distant immune reaction in response to mechanical and herbivore wounding (Mousavi *et al.* 2013).

Discussion

It seems reasonable that ROS as well as EPWs might reach the sieve elements and leading to Ca^{2+} burst (Mori and Schroeder 2004; Felle and Zimmermann 2007), known to be affecting phloem physiology (Furch *et al.* 2007). Functional modulation of sieve-tube performance might provide physical barriers and accumulation of antimicrobial compounds and signal molecules to restrict pathogen growth and distribution.

Indeed, many studies focus on direct defense reaction to abiotic stress (Furch *et al.* 2007; 2010; Thorpe *et al.* 2010) but the identification of structural and functional changes during biotic interactions is insufficiently understood so far. Furthermore, information about the involvement of phloem in initiation of immune responses lacks and seems speculative, since sieve-element cells do not contain significant organelles like nuclei, chloroplasts or the Golgi-apparatus (Knoblauch and van Bel 1998) essential for initiation of most plant immune responses.

Knowledge about the phloem-dependent immunity, signal transduction as well as physiological interference, are essential for a classification of phloem immune responses in accordance with complex bacterial-plant interaction.

In the first part of the present work diverse preparation techniques, such *in vivo* observation, fresh hand sectioning as well as protoplast studies were used to investigate flagellin-triggered plant immune response. Observations of Light Microscopy and Confocal Laser Scanning Microscopy (CLSM) provide information on phloem defense mechanism imposed by bacterial infection. In particular, we focused on the effect of bacterial elicitor on phloem-based initiation of immune responses and on physiological modification of phloem cells during initiate immune responses.

Techniques to study the phloem are difficult (Truernit *et al.* 2014), since phloem is sensible to even slightly injury and thus are covered by protective cell layers. Since differentiation of intended and accidental phloem reaction is problematic, a careful handling and preparation of plants material is essential for phloem analysis. Adequate approaches used for the present work can be divided into three parts:

(1) The non-destructive phloem *in vivo* technique provides observation of intact plants (Knoblauch and van Bel 1998). After exposing the phloem by careful removal of the cells covering the phloem tissue, the plants were recovered for at least 30 min, avoiding misinterpretation due to injury reaction. Furthermore, the possibility to verify the vitality of

Discussion

the plants by the presence of condensed forisomes, improved the validity of observed results.

(2) Ultrathin sections are laborious and time-consuming, and only small portions of fixed and embedded tissue of interest can be examined. Fast and precise fresh-hand sectioning of plant tissue avoid the use of tissue fixation and embedding. The necessity to kill plant tissues causes instantaneous, irreversible and massive reactions of sieve elements to wounding (van Bel 2003), which may lead to pieces of misleading information and erroneous interpretations.

(3) The use of sieve-element protoplasts provides the possibility to study membrane biology, including receptor-based reactions (Davey *et al.* 2005). Again, protoplasts were recovered after the last preparation step for at least 30 min and vitality of the sieve-element protoplast was verified by the presence of condensed forisomes.

Based on Light Microscopy and CLSM analysis, phloem immune reaction of broadbean (*Vicia faba*) and mouse-ear cress (*Arabidopsis thaliana*) stimulated by application of synthetic flagellin was observed.

Summarized we could demonstrate that (1) application of bacterial elicitor lead to Ca^{2+} -mediate forisome reaction and (2) receptor-based sieve-element occlusion. In addition, we could demonstrate that (3) immune reactions, including phloem responses, were not initiated along the sieve-element cells, confirming previous assumption.

4.1.1. Flagellin-triggered Ca²⁺ influx leading to forisome reaction

Forisomes are giant, crystalloid phloem proteins, which reversibly changes between a condensed, spindle-shaped form and a dispersed state (Knoblauch and van Bel 1998). A major difference between the two states is the increased volume of the dispersed protein. After a certain Ca²⁺ threshold is achieved inside the sieve-elements (Furch *et al.* 2009; Hafke *et al.* 2009) the forisome volume increase up to 6-folds (Knoblauch *et al.* 2003; 2012), leading to a sealing of the sieve pores (Knoblauch and van Bel 1998). Ca²⁺ influx can be triggered by diverse abiotic stimuli such as heat or cold shock (Furch *et al.* 2007; 2009; Thorpe *et al.* 2010) as well as biotic stimuli, such as fungal elicitor and phytohormones (Gaupels *et al.* 2008).

Observation of more than 1000 forisomes in unstimulated phloem of *V. faba* revealed the forisomes not to be randomly distributed. In accordance with earlier studies on smaller sample size (Furch *et al.* 2009) forisomes can be classified into 12 different positions (Fig. 6). Considering the absolute frequency of the various locations and positions (Fig. 7), more than 80% of the forisomes in intact and unstressed plants were located at the downstream side of the sieve tube (Fig. 7 A) in close contact to the sieve plate and the plasma membrane of the neighboring cells (Fig. 7 B). About 30% of the forisomes shows a contact with the sieve-element side facing the companion cell (Figs. 4, 5). Since the common interface between sieve element and companion cell amounts about 30% of the total sieve-element inner surface in transport phloem (van Bel 1996; 2003), there seems no preference for forisome contacts with the sieve-element side facing the companion cell.

Despite the regular mass flow in intact sieve tubes, some forisomes are located either at the center (Fig. 7 C) or the upstream side of the sieve tubes (Fig. 7 D), contradicting the forisomes to be floating inside the phloem tissue. Apparently, forisomes seem to be attached to sieve-element structures (Furch *et al.* 2009), to clear constant downstream pressure due to mass flow direction. Anchoring, like phloem plastids and endoplasmic reticulum (Ehlers *et al.* 2000), of forisomes to the sieve-element frame suggest that forisomes are not free-floating inside the sieve elements which opens the perspective that forisome can be regulated in position and thus possibly in function (Furch *et al.* 2009).

Comparing the forisome position and the phloem morphology, forisomes position is most likely connected to the places of high calcium storage (Kauss 1987; Gilroy *et al.* 1993; Sanders *et al.* 2002). Because high Ca²⁺ concentrations, necessary to trigger forisome reaction, cannot be reached in the whole sieve element due to the limited mobility range of Ca²⁺ ions (Gilroy *et al.* 1993), forisomes are facing structures which contain high abundance of Ca²⁺ channel (Fig. 7). Clustered Ca²⁺ channels in membranes as those of

Discussion

endoplasmic reticulum and the plasma membrane generate kind of calcium hotspots, capable to initiate forisome reaction (Furch *et al.* 2009; Hafke *et al.* 2009; Hafke and van Bel 2013).

Considering the reactivity of forisomes with respect to their location inside the sieve element, it is striking that, although the response time is not affected, the frequency of forisome reaction differs between the positions (Fig. 8). Whereas nearly three quarters of basal forisomes respond to application of heat stimuli, less than one half of the other positioned forisomes dispersed (Fig. 8 A). This is probably due to the fact that Ca^{2+} -permeable channels are more densely clustered at the downstream side of the sieve plate (Furch *et al.* 2009). Furthermore, increased reactivity of forisomes is associated with extended sieve-element contact (Fig. 8 B). This again renders credence to the view that contact of the forisome tips to Ca^{2+} hotspots, like in endoplasmic reticulum and the plasma membrane, are required for dispersion (Hafke *et al.* 2009).

The high concurrency and reactivity of forisomes at the downstream side with close contact to the sieve element supports the conclusion, these forisomes to be the most reactive once. In a kind of ground stage, these forisomes regulate mass flow by rapid all-or-nothing reaction due to Ca^{2+} influx into the phloem following the all-or-none principle of action potential (Fromm and Spanswick 1993). The regulatory properties of forisomes are consequently linked to the position inside the phloem. This becomes even more considerably regarding the forisome position prior to dispersion and after recondensation (Fig. 9). Forisomes seems to change the position from the high reactive ground stage (Fig. 9 A) to a not as reactive position without contact to the sieve element (Fig. 9 C). While it is not as noticeable as in *Phaseolus vulgaris*, where forisomes even change their location from basal to apical (Furch *et al.* unpublished), it is striking that forisomes in *V. faba* only move back to their reactive ground stage after a recovery time of several minutes (Fig. 9 D). This kind of movement inside the functioning mass flow again point to the theory of forisome anchoring (Furch *et al.* 2009), preferably in the vicinity of Ca^{2+} hotspots (van Bel *et al.* 2014).

The regulation of mass flow not only guarantees fast defense response but, at the same time, prevents nutrient deficiency due to exceeding of impaired mass flow. Forisome-based sieve-element occlusion thus might represent a monitoring tool for plant defense.

Discussion

Flagellin, as a part of the bacterial flagellum, is known to act as bacterial elicitor to activate plant immune responses (Felix *et al.* 1999; Gómez-Gómez *et al.* 1999). Perception of microbial-associated molecular patterns (MAMPs) *via* pattern-recognition receptors (Boller and Felix 2009) provokes several downstream defense responses resulting in pattern-triggered immunity (PTI) to restrict pathogen growth and distribution through structural barriers and providing antimicrobials (Dangl and Jones 2001; Boller and Felix 2009). Triggered by MAMP perception, plant immunity generates local immune responses, such as Ca^{2+} burst (Dodd *et al.* 2010) and reactive oxygen species (ROS) burst (Kobayashi *et al.* 2007), suggested to induce local chemical and electrical signals.

Local phloem reaction in response to bacterial interaction, imitated by artificial flagellin, strongly depends on the diverse flagellin concentrations (Fig. 10). Prior to stimulus, the spindle-shaped forisome was typically observed to be closely associated with the sieve plate and the plasma membrane as normal for unstressed phloem (Fig. 10 A, F, K and P). The dispersion starts invariably at the forisome ends subsequent to detachment from the plasma membrane (Fig. 10 B, G and L), recondensation inversely starts from the center (Fig. 10 D; I and N). While flagellin concentration higher than 1 μM almost invariably triggers forisome reaction (Fig. 10 A to E and F to J), concentration of 0.1 μM rarely triggers forisome dispersion (Fig. 10 K to O). Only one quarter of the irritated sieve elements show forisome reaction confirming that the conformational change is concentration-dependent. Furthermore, performing application of 0.01 μM flagellin, no phloem reaction occurred (Fig. 10 P to R).

Although forisome dispersion triggered by abiotic stress seems to underlie the all-or-nothing principle due to action potential wave characteristics (Fromm and Spanswick 1993), forisome reaction triggered by bacterial elicitor seems to be more complex. Average dispersion time seems, as the reaction itself, to be dose-dependent. Still the process of all-or nothing expires, the higher the flagellin concentration is, the faster the dispersion and the slower the recondensation proceed (Fig. 10 A to O). This indicates again the regulatory properties of phloem reaction. Also characterized by the fact that, even if the elicitor remains continuous on the exposed plant tissue the forisome dispersion reflects partial defense response (Fig. 10), either by non-permanent signal transduction or active control through the phloem.

We could show that reversible Ca^{2+} -mediate forisome reaction occurs during bacterial infection, that might reflect regulation of defense mechanism, by fast accumulation of defense signal and in turn by systemically signal transduction. Furthermore, forisome-

Discussion

based occlusion might represent the first line of rapid barricade to prevent uncontrolled pathogen movement inside the phloem tissue. Thus, sieve-element occlusion imposed by bacterial infection seems to be initiated during host immune responses.

Since the involvement of forisomes in sieve-tube sealing are harshly discusses (Peters *et al.* 2006; Knoblauch *et al.* 2014) and second line of sieve-element occlusion by other components, like callose or other phloem proteins, might occur, invisible in this procedure, further techniques were used to monitored the phloem immune responses, including sieve element occlusion.

4.1.2. Flagellin-induced biphasic sieve-element occlusion

There are evidences that callose (Furch *et al.* 2007; 2009), as well as phloem proteins (Ernst *et al.* 2012; Knoblauch *et al.* 2012) are involved in Ca^{2+} -mediate sieve-tube occlusion due to sieve-pore sealing (Hong *et al.* 2001; Knoblauch *et al.* 2003). The time-shifted effect of sieve-element occlusion, first by protein subsequently followed by callose (Furch *et al.* 2007; 2009), is most likely based on the Ca^{2+} concentrations-dependent activity of protein and callose reaction inside the phloem (Colombani *et al.* 2004; Furch *et al.* 2009; Hafke *et al.* 2009). In addition, callose deposition is based on defense-related synthesis due to Glucan Synthase-Like 7 activity (Barratt *et al.* 2011; Xie *et al.* 2011), while protein plugging is based on agglutination of existing components (Knoblauch and van Bel 1998). Both together reflect a sufficient interaction in defense reaction (van Bel *et al.* 2011) to seal the connection between the separate sieve elements. Reversibility of sieve-element occlusion, most likely due to removal of Ca^{2+} from the sieve tubes (Huda *et al.* 2013) ensures survival.

We could show that application of bacterial flagellin to *A. thaliana* leads to abrupt mass flow impairment (Fig. 11). Through photobleaching effect and the subsequent transport of fluorescent mass flow inside the phloem, sieve-element occlusion is indicated 10 minutes (Fig. 11 G) and 180 minutes (Fig. 11 I) after flagellin application. While phloem proteins are known to have a rapid and short-term impact on phloem mass flow (Ernst *et al.* 2012; Knoblauch *et al.* 2012), the comparative long occlusion period, more than 30 min, is most likely based on callose deposition inside the phloem (Furch *et al.* 2007; 2009). In between the bi-phasic occlusion effect the mass flow seems to function regular (Fig. 11 H). Furthermore, subsequently to the last occlusion phase the phloem occlusion lifted permanent providing a regular mass flow (Fig. 11 J). The phasic characteristics of

Discussion

occlusion event might be related to the bi-phasic ROS production (Baker and Orlandi 1995) or degradation and new the synthesis of flagellin receptor (Smith *et al.* 2014).

Again, the reversibility of sieve-element occlusion might ensure systemic spread of signals and prevent nutrient deficiency. The hypothesis of sieve-element occlusion function as a barrier to restrict pathogen invasion now seems rather questionable, since reopening of the sieve elements would allow a systemic distribution of phloem-pathogens. More likely, sieve-tube sealing ensures local accumulation of defense-related molecules and reversibility ensures signal spread.

Perception of bacterial elicitor flagellin is mediated by the transmembrane receptor FLS2 (Gómez-Gómez and Boller 2000). Based on the recognition of a single stretch of 22 amino acid residues in the N-terminus of flagellin (Felix *et al.* 1999) activates downstream defense events to provides basal defense responses in plants (Jones and Dangl 2006). In turn, plant carrying mutations in FLS2 show enhanced susceptibility to bacterial infection (Bauer *et al.* 2001; Zipfel *et al.* 2004).

We could show, that in flagellin insufficient *A. thaliana* mutants, no sieve-element occlusion takes place (Fig. 12). This indicated the occlusion event to be part of the receptor-mediated plant immunity. During plant immune responses to bacterial perception, sieve-element occlusion might be initiated as downstream defense responses. Sealing the sieve tube system may prevent invasion of pathogens and released effectors/elicitors, redirect nutrient flows and enrich signal and defense molecules.

4.1.3. Remote flagellin perception and signal transduction trigger phloem immune response

Compared to the results obtained in *in vivo* experiments with abiotic stimuli (Furch *et al.* 2007; 2009; Thorpe *et al.* 2010) the forisome reaction triggered by flagellin occurs delayed and slower (Fig. 10). Slow dispersion initiated from forisome tip raises the question about flagellin perception and signaling translocation. It was long been assumed that the phloem is not directly involved in the introduction of immune response. While recognition of pathogen elicitor and effector proteins can occur extracellular and intracellular (Bent and Mackey 2007), respectively, initiation of phloem-associated immune reaction seems unlikely, since the sieve-element cells do not contain indispensable organelles, related to plant immune responses (Knoblauch and van Bel 1998). Probably, recognition occurs not directly in the sieve elements but most likely in the neighboring cells. Remote signaling in

Discussion

nearby cells in turn enters the phloem cells to initiate immune responses affecting plant development (Hoshi *et al.* 2009).

Surveillance of isolated *V. faba* sieve-element protoplasts in response to flagellin treatment, confirms the assumption that the sites of flagellin perception and response are spatially separated (Fig. 13). Compromised perception of flagellin in the sieve-element cells (Fig. 13) but not in mesophyll protoplast (Fig. 13 and 14) supports the conclusion that sieve-element cells are not involved in initiation of plant immune responses by bacterial infection.

Presumably, phloem cells evolutionary have not developed systems for recognition of pathogen-associated molecular patterns, based on the fact that infection of plant, with the exception of vector-mediated transmission, does not primary infects the vascular tissue. The protective position of phloem tissue inside the plant corpus might not require autonomous perception of bacterial invasion, subsequently these infection are mainly associated with injury of the outer plant layer. Latter would initiate plant immune responses that reach the vascular bundle.

Summarized, our finding shows the first time a phloem-based immune reaction initiated by bacterial invasion. The present studies provide evidence that pathogen elicitor triggers defense signals in cortex cells that reaches the phloem to set physiological reactions, including sieve-element occlusion, in affected sieve tubes.

Together, the analysis revealed insights into the plant responses to bacterial infection but raise numerous questions. In particular, it remains unclear which signals and sieve-element components are exactly involved in phloem-based defense reactions. Temporal and spatial correlation between ROS burst (Wi *et al.* 2012) and sieve-element occlusion might favor ROS as the major signal in phloem based immunity. Furthermore, the rapid and long-lasting effect of sieve-element occlusion indicated that both, callose and phloem proteins, are involved in sealing the sieve tubes (Furch *et al.* 2007; 2009).

Above all, one can only speculate about the importance of impaired mass flow in plant immunity. Since the phloem is not directly part of the initiation of plant immune responses, the involvement of phloem-based immunity seems to be a downstream event of general plant immunity. Beside the possible function in signaling and defense, molecule

Discussion

accumulation, due to metabolically active companion cells, the sieve-element occlusion in direct pathogen restriction seems to be unlikely. Even in case of phloem-restricted pathogens the reversibility of occlusion mechanism seems, at first sight, counterproductive. But reopening of barred sieve tubes might appear essential for survival to facilitate the systemic spread of defense signals rather than the systemic spread of pathogens.

Investigations on sieve-element insufficient mutants would give a substantial progress in studies on phloem-based immunity. One consequence of insufficient control mechanism of sieve tubes (signaling and nutrient distribution) might be, probably based on alteration in signal transduction, a decreased resistance to different pathogens. Phloem reaction to local immune responses, like pattern-triggered-immunity and effector-triggered immunity, as well as systemic responses, like systemic acquired resistance, triggered by different pathogens need to be investigated in sieve-element occlusion insufficient mutants. Infection of such plants might help to develop a concept of plant immunity, including phloem-based responses.

4.2. Phytoplasma infection leads to Ca²⁺-mediate alteration of phloem morphology and transport

Phytoplasmas are obligate, phloem-restricted phytopathogens that are disseminated by phloem-sap sucking insects (Christensen *et al.* 2005). There are evidences that symptoms, such as growth disturbance and flower abortion, are initiated during pathogen-host specific interaction (Hogenhout *et al.* 2008). Next to impaired mass flow, subsequent expansion of the disease symptoms can not only based on phytoplasmas plugging the sieve elements, but it implies the involvement of phytoplasma-secreted effector proteins on plant cells morphology and function (Hogenhout *et al.* 2008; Bai *et al.* 2009). Phytoplasmas produce effector proteins that are known to interact and depredate host immune system (Hoshi *et al.* 2009; MacLean *et al.* 2011; Sugio *et al.* 2011) to increase bacterial motility (Suzuki *et al.* 2006; Galetto *et al.* 2011; Boonrod *et al.* 2012) as well as vector (Sugio *et al.* 2011) and pathogen fitness (Lu *et al.* 2014) leading to typical phytoplasma-related symptoms (Hoshi *et al.* 2009; MacLean *et al.* 2011).

Even if many studies focused on macromolecular modulation of phytoplasma-related host symptoms, the identification of essential modifications on host tissue triggered by phytoplasma infection has been poorly understood (Rudzińska-Langwald and Kamińska 2001; Santi *et al.* 2013). Furthermore, the studies lack to specify the structures involved in host-pathogen interaction. A part many effector-based symptoms, among others, carbohydrate redistribution (Lepka *et al.* 1999) and impaired mass flow (Kartte and Seemüller 1991) seem to be induced by deficiency of sieve-tube performance, so it seems reasonable that massive changes in phloem physiology can occur. Effector-based targeted modulation of phloem cells could be triggered by remote signaling, induced mainly in neighboring cells to interfere with phloem processes of defense and development. Cytological relationships between phytoplasmas and sieve elements are essential for the establishment of phytopathogenic activity in the host (Christensen *et al.* 2005), but identification of structural and functional changes during infection has not been investigated to date. Knowledge about the phytoplasma-interaction capability to modify sieve elements morphology, signaling and transport is essential for understanding the phytoplasma-host relationships.

In the present work diverse microscopic techniques, such as Light-, Epifluorescence- (EFM) as well as Confocal Laser Scanning Microscopy (CLSM) and Transmission Electron Microscopy (TEM) were used to give new insight to phytoplasma-host interaction.

Discussion

Observation of both, fresh and embedded tissue provides information on structural and biochemical modifications in sieve elements following phytoplasma infection. In particular, we focused on the effects of phytoplasma infection on phloem mass-flow performance and structural modification.

The analysis can be divided into two parts:

(1) Methods to study phytoplasma-induced alteration of host structures thus far provoked massive, native occlusion artifacts in sieve tubes. Hence, phytoplasma-phloem relationships were investigated in intact host plants. Computerized image-processing and -analysis by CLSM using an array of vital target specific fluorescent probes appear the appropriate tool for *in vivo* investigation (Knoblauch and van Bel 1998). Phloem-specific phytoplasmas and their interactions with the plant host (Reichel and Beachy 1998) were investigated using healthy and phytoplasma-infected broadbean (*Vicia faba*) plants, used as hosts of '*Candidatus* Phytoplasma vitis' ('Ca. P. vitis'), the phytoplasma in nature associated to Flavescence Dorée (FD) disease of grapevines.

(2) In conventional microscopy studies either ultrastructural analysis by TEM or identification of structures by EFM can be reached. To combine both analysis using serial semithin and ultrathin sections, hence, structural relationships between phytoplasmas and the sieve-element plasma membrane-ER-actin network was investigated using resin-embedded leaf sections of healthy and phytoplasma-infected tomato (*Solanum lycopersicon*) plants, used as hosts of the '*Candidatus* Phytoplasma solani' ('Ca. P. solani'), the pathogen associated to stolbur disease. Combination of both, TEM immunogold-labeling and EFM (immuno)fluorescence-staining (Musetti *et al.* 2002; Bell *et al.* 2013), was used to achieve precise localization and identification of cellular targets.

Summarized we could show that (1) apparently, phytoplasma infection brings about Ca^{2+} influx into sieve tubes leading to sieve-plate occlusion by callose deposition and/or protein plugging. In addition, Ca^{2+} influx may confer cell wall thickening of conducting elements. In conclusion, phytoplasma-triggered sieve-element occlusion presumptive has dramatic effects on phytoplasma spread and nutrition distribution. Furthermore, we could demonstrate that (2) a drastic re-organization of sieve-element membrane structures in infected tissues occurs. The plasma membrane becomes undulated and the ER stacks are distorted and protruded toward sieve-element lumen. The actin aggregates on the phytoplasma surface provide evidence in favors of a coupling between phytoplasmas and

Discussion

sieve-element cytoskeleton. Probably, all these modification have dramatic effects on phytoplasma fitness and host symptoms.

4.2.1. Phytoplasmas trigger Ca^{2+} influx leading to sieve-element occlusion

The DNA-specific dye DAPI (4',6-diamidino-2-phenylindole) was used to detect phytoplasmas in diseased plants (Loi *et al.* 2002) and to identify phytoplasmas inside sieve elements *in vivo* (Fig. 17). Use of DAPI in living cells, as well as the fact that it does not affect cell viability, is well documented in literature, both for animal and plant cells (Subramaniam *et al.* 2001; Cai *et al.* 2008; Ocarino *et al.* 2008).

Phytoplasmas were found to be distributed along the sieve elements, particularly in the vicinity of the sieve plates (Fig. 17 G). In the enucleate sieve elements (van Bel 2003), no interference with nuclear staining can occur (Fig. 17 E). Theoretically, sieve-element plastids, which are of the same size as phytoplasmas, may become stained as well, but there is no overlap between the location of the plastids and the DAPI-stained dots inside the sieve elements (Fig. 17 G and H).

Environmental changes, such as burning (Furch *et al.* 2009) or cooling (Thorpe *et al.* 2010) can trigger sieve-element occlusion, one of the first local responses to stress. In contrast to abiotic stress, knowledge about phloem reaction to biotic stress, such as pathogen attack, is insufficient. Some studies have reported nitric oxide production in the companion cells of the phloem following application of fungal elicitor leading to some dispersion (Gaupels *et al.* 2008) indicating a sieve-tube occlusion (Knoblauch and van Bel 1998).

In diseased plants (Fig. 16 D), mass flow was significantly reduced as compared to the healthy ones (Fig. 16 B), and, in most cases, had fully ceased. Thereby the effect of mass flow rate coincides with the presence of phytoplasma in infected sieve element (Fig. 18 K and L; Fig. 19 O and P). Sealing the sieve-tube system may prevent the invasion of pathogens and/or their released effectors/elicitors, redirect nutrient flows, and/or enrich signal and defense molecules. In addition, sieve-element occlusion might represent an important source of accumulated nutrition and energy for successful development of phytoplasma inside the phloem (Lepka *et al.* 1999).

It is important to underline that even though sieve elements of infected tissue often seem collapsed and dysfunctional (Fig. 22 F and H) companion cell of the diseased plants still appears to be functional (Fig. 18 L; Fig. 19 O) indicating that the companion cell activity is not totally impaired by infection, which could be important for phytoplasma survival. After having lost nuclei and most of their organelles during their ontogeny, sieve-elements rely on the metabolic activities of companion cells (van Bel *et al.* 2002) and may fail to fully nourish phytoplasmas. Companion cells are metabolically active and provide all the

Discussion

compounds essential for sieve-element maintenance. As phytoplasmas lack many genes indispensable for cell metabolism (Christensen *et al.* 2005), compounds provided by companion cells might be an important source of nutrition for these pathogens or rather might represent the central position of host immunity inside the phloem.

Although phytoplasma aggregates may be able to plug the sieve pores, it is more likely that phytoplasma-induced sealants are responsible for sieve-tube occlusion. One common observed mechanism for sieve-tube narrowing is *via* extracellular deposition of callose inside the sieve elements, mainly aggregated at the sieve plates and the plasmodesmata (Koh *et al.* 2012).

Severe phytoplasma infection is inextricably bound up with callose deposition. Intensive accumulations of callose occur in the vicinity of the sieve plates of phytoplasma-infected tissue (Fig. 21 I and K) and sometimes in the adjacent zones, while only insignificant signal is emitted in healthy *V. faba* plants (Fig. 21 E and G).

Next to sieve-tube constriction by callose, sieve pores can be blocked by phloem proteins (Furch *et al.* 2007). To repress further translocation phloem proteins are released from the parietal position and agglutinate at the sieve plates (Knoblauch and van Bel 1998). In contrast to traditional phloem proteins, in Fabaceae, phloem proteins are aggregated in giant protein bodies called forisomes (Knoblauch *et al.* 2001). In response to different stresses, reversible conformational change from a condensed to a dispersed state enable to plug the sieve plates and prevents loss of photoassimilates (Knoblauch and van Bel 1998; Knoblauch *et al.* 2001; Furch *et al.* 2007; Thorpe *et al.* 2010).

In phytoplasma-diseased *V. faba* plants, spindle-shaped forisomes are dispersed (Fig. 20 D; Fig. 21 J and L) and, hence, become invisible under the light microscope. Moreover, in infected plants high amounts of unidentified protein structures (Fig. 20 C) are visible at the sieve plate while, except the forisomes, only a minor amount of parietal proteinous aggregation at the sieve-element of healthy plants occurs (Fig. 20 A).

Both, protein agglomeration and callose deposition are Ca^{2+} -dependent (King and Zeevaart 1974; Thonat *et al.* 1993; Knoblauch *et al.* 2001) and are likely triggered by release of Ca^{2+} into the sieve element lumen (Furch *et al.* 2009; Hafke *et al.* 2009).

In diseased plants, the Ca^{2+} concentration in the sieve elements was markedly elevated (Fig. 22 E and G) as compared to the healthy ones (Fig. 22 A and C). Especially at the

Discussion

sieve-plate region, a significant increase of Ca^{2+} concentration seems to occur in phytoplasma-infected sieve elements.

It appears that phytoplasma infection, possibly by secretion of phytoplasma effectors (Sugio *et al.* 2011), induces Ca^{2+} influx into the sieve elements. The scattered distribution of Ca^{2+} ions inside the sieve elements and callose deposition along the longitudinal walls indicates that phytoplasma do not only activate Ca^{2+} channels near the sieve plates, but also at other Ca^{2+} hotspots such as the pore-plasmodesma units between sieve elements and companion cells (Furch *et al.* 2009; Hafke *et al.* 2009). Recovery of the occlusion phenomena after a certain time demonstrated that occlusion can be reversed following Ca^{2+} extrusion (Furch *et al.* 2007; 2010). It seems, however, that in phytoplasma infected *V. faba*, phytoplasmas impose continuous gating of the Ca^{2+} channels given the permanent occlusion of infected sieve elements.

In addition to sieve-plate occlusion, the sieve-element path may also be narrowed in diseased plants by thickening of the walls as revealed by recent observations. Increased sieve-element wall thickness and enhanced total phenolics have been reported for phytoplasma-diseased plants (Musetti *et al.* 2000; Choi *et al.* 2004). This would be consistent with accumulation of phenolic materials, probably by companion cells, since a Golgi system is absent in sieve elements, against the sieve-element walls. It has been demonstrated that a Ca^{2+} signal is required to induce phenylalanine ammonia-lyase (PAL) activity (Messiaen *et al.* 1993), a key enzyme of the phenol synthesis pathway, as well as PAL gene expression (Long and Jenkins 1998). This would add an interesting side-effect of Ca^{2+} influx on phytoplasma restriction.

4.2.2. Phytoplasma infection is associated with re-organization of plasma membrane-ER network and actin structure in sieve elements

The DNA-specific fluorescent dye DAPI was extensively used to detect phytoplasmas in fresh-sectioned plant materials (Loi *et al.* 2002) and is suitable for the identification of phytoplasmas *in situ* (see results above). Here, DAPI was used to detect phytoplasmas in LRW-embedded infected leaf samples. Although the signal was not as strong as in freshly sectioned material, the DNA fluorescence was sufficient to assess phytoplasma presence in both longitudinal and cross-sections (Fig. 24).

Discussion

Adherence to host membranes is an established factor in pathogenesis (Razin *et al.* 1998) of several cultivable *Mollicutes* infecting humans and animals. It is largely unknown if phytoplasmas interact in such a fashion with host plants. In infected sieve element, phytoplasmas appear to be attached to the plasma membrane (Marcone 2010), although unambiguous proof of adherence to host membranes has not been given. However, several studies demonstrated the presence of a subset of adhesin-like membrane proteins in most phytoplasmas (for review see Kube *et al.* 2012).

A drastic ultrastructural re-arrangement of membranes in stolbur-diseased sieve tubes (Fig. 25 D, E and F) is indicated by alteration of signal distribution in infected areas and by an increase in fluorescent signal in the sieve-element lumina. TEM images of stolbur-diseased vascular areas reveal the signal alteration to be due to host membrane remodeling (Fig. 25 H and I) and phytoplasma presence (Fig. 25 J). High-resolution images (Fig. 25 K, L, M and N) disclosed intimate and strong connections between phytoplasma cells and the sieve-element plasma membrane, in the form of membrane junctions or overlays. This cytological observation correlates to what has been reported on pathogenic mycoplasmas, even if the latter have an extracellular localization (Razin *et al.* 1998). Contact between the mycoplasma and host cell membrane may result in local, transient fusion of the two membranes or exchange of membrane components. Diverse proteases, involved in the breakdown of host proteins, are encoded in the phytoplasma genomes (Kube *et al.* 2012) and many of them are supposedly linked to phytoplasma virulence. Phytoplasma membrane proteases might be responsible for phloem impairment (Seemüller *et al.* 2013), a major effect of phytoplasma infection (Fig. 18 and 19).

It has been extensively reported that pathogens actively modulate the host cytoskeleton for successful invasion (Rottner *et al.* 2005; Pizarro-Cerdá and Cossart 2006) and movement inside host cells (Tilney and Portnoy 1989; Sansonetti 1993; Opalski *et al.* 2005). Interaction of phytoplasma with the plant host cytoskeleton is inferred by the presence of phytoplasma antigenic membrane proteins (AMP or IMP), which are able to dock onto the vector cytoskeleton (Suzuki *et al.* 2006; Galetto *et al.* 2011) or plant-host actin filaments (Boonrod *et al.* 2012).

Our study indeed reveals a spatial overlap of invader pathogen and host sieve-element actin structures (Fig. 26 H and I). It is important to note that the unilateral binding between actin and phytoplasma indicates a polarity of phytoplasma body as has been extensively reported for other prokaryotic microorganisms (Lybarger and Maddock 2001; Dworkin 2009). In particular, gram-positive intracellular pathogenic bacteria (i.e. *Listeria*

Discussion

monocytogenes) have evolved a mode of motility dependent on the unipolar polymerization of host actin (Lybarger and Maddock 2001). This actin-based motility facilitates cell-to-cell spread of pathogens *via* bacterial projections delivering the bacteria into adjacent host cells (Lybarger and Maddock 2001). Phytopathogenic phytoplasmas may induce a similar asymmetric polymerization of host actin allowing pleomorphic changes in phytoplasma corpus (Rudzińska-Langwald and Kaminska 1999) to enable active movement in sieve elements as indicated by concurrent gold labeling near sieve plates and phytoplasmas (Fig. 26 J). The ability to bind to actin may enable phytoplasmas to spread along plant actin filaments in sieve element, especially through the narrow sieve pores. The sieve-pore diameters are mostly smaller (e.g. van Bel 2003) than the size of the phytoplasmas (Hogenhout *et al.* 2008). In plant cells, organelles, like plastids, frequently move along the interface between cytoskeleton and ER (Schattat *et al.* 2011). This raises the question if this also holds for phytoplasmas having a similar size.

part from a role in pathogen movement, membrane fusion associated with actin-controlled events may open up a corridor for nutrient supply by delivery of vesicles and protein complexes from host to phytoplasmas (Mathur and Hülskamp 2002; Vantard and Blanchoin 2002). Increased intensity and modified distribution of the actin signals in sieve element following stolbur disease point to a large-scale remodeling of actin filaments in *S. lycopersicum* phloem. While actin in healthy sieve element is distributed along the periphery of the cell (Fig. 26 B and C; Hafke *et al.* 2013), the probable formation of new filaments (indicated by the increase in TR fluorescence) and/or re-organization of existing ones result in actin aggregation at the edges and in the sieve-element cell lumen, especially in severely infected areas (Figs. 26 E and F).

Furthermore, the cytoskeleton supports numerous cellular processes including rapid reaction to abiotic and biotic stresses (Day *et al.* 2011), to protect the cell against destructive processes (Morelli *et al.* 1998; Wang and Riechmann 2007; Wang *et al.* 2010). Host actin remodeling and increase in actin filament abundance indicate that the cytoskeleton is a key element in plant defense (Opalski *et al.* 2005; Hardham *et al.* 2007; Tian *et al.* 2009) and thus may also play a role in pattern-triggered immunity (PTI) (Henty-Ridill *et al.* 2013). Cytoskeleton re-arrangement and related increase in actin expression and distribution in stolbur-diseased *S. lycopersicum* may be involved in plant immunity as shown for other biotrophic interactions (Jin *et al.* 1999).

Sieve-element endoplasmic reticulum also plays a part in the complex interaction between phytoplasmas and sieve elements. During differentiation of sieve element (Thorsch and

Discussion

Esau 1981), endoplasmic reticulum usually becomes aggregated in regular stacks (cisternae) close to the plasma membrane along the lateral sieve-element walls (Sjolund and Shih 1983). The cisternae lie either parallel (Evert 1990) or perpendicular (Ehlers *et al.* 2000) to the plasma membrane. The sieve-element reticulum stacks are tethered to the plasma membrane and to each other by anchors of unknown nature (Ehlers *et al.* 2000) to prevent dragging by mass flow and potential clogging of sieve pores. Structural and functional relationships between phytoplasmas and the endoplasmic reticulum are not well documented so far. Rudzińska-Langwald and Kaminska (2001) reported that endoplasmic reticulum is often situated in the lumen of sieve elements of Aster Yellows-infected *Limonium sinuatum* being detached from the plasma membrane and in close connection with phytoplasmas.

We could show that closely connected to the actin, sieve-element reticulum shows re-organization in infected areas (Fig. 27 D, E and F) accompanied by a contortion of the endoplasmic reticulum stacks (Fig. 27 J and K). Increased intensity and modified distribution of the ER signals following stolbur disease point to a large-scale clustering of ER network in *S. lycopersicum* sieve elements. As actin filaments are often aligned with the reticulum stacks (Boevink *et al.* 1998), sieve-element reticulum network may act as a second track for the bacterial movement with so far unknown connectors between sieve-element reticulum and phytoplasmas. Beside this, the sieve-element reticulum expansion observed in the stolbur-diseased sieve elements, due to the formation of lobes as well as to the fragmentation into vesicles (Fig. 27 L), might be correlated to the requirement of increasing the reticulum surface thus providing a greater area for defense protein distribution into the lumen of the sieve elements, as demonstrated to happen in animal cells (Watson and Stephens 2005; Strating and Martens 2009). Finally, ER stacks are important cellular compartments for Ca²⁺ storage in sieve elements (Sjolund and Shih 1983). Actin pulling may activate Ca²⁺ release from the ER system in sieve elements following phytoplasma infection (Rudzińska-Langwald and Kamińska 2001) as demonstrated above. Persistent connection between sieve-element reticulum and ER of the companion cells (Martens *et al.* 2006) may increase the potential calcium signaling in the phloem of infected plants.

Discussion

In conclusion, our finding shows the first time that phytoplasma infection results in a significant re-organization of sieve-element structure in phloem tissue as well as almost completely breakdown of sieve-element function. The present studies provide evidence that infection of plants with phytoplasma leads to abnormalities in the sieve-element plasma membrane, sieve-element endoplasmic reticulum as well as actin network. Furthermore, Ca^{2+} -mediated sieve-element occlusion due to sieve plate sealing by callose and proteins point to a complex interplay of host and invader during phytoplasma infection.

Collectively, the analysis revealed insights into the host responses to phloem-restricted bacteria but raise numerous questions with one of the leading themes. One can only speculate about the importance of the contact between phytoplasmas and sieve-element structures and reduced mass flow concerning symptoms appearance and initiator.

Macroscopical symptoms (Fig. 15 and 23) can either be induced by the phytoplasma impairing the mass flow and ultrastructural modification of phloem cells or rather represent phloem independent alteration due to effector-based targeting in distant tissue.

Furthermore, phytoplasmas may induce a targeted modulation by release of effector proteins, which initiate response, mainly in phloem associated cells since, as above mentioned in the results, the sieve elements not involved in response initiation. Phytoplasma bind to host structure to enable nutrient supply and systemically spread inside the sieve elements, which permits a fast distribution and proliferation of bacteria in the host plant. On the other hand, focal orientation of phloem substructures in the direction of the stress imposed by phytoplasma infection seems to reflect defense response of the plant. In addition, sieve-element occlusion is known to be initiated during host immune response but might be driven by the phytoplasma to permit accumulation of nutrients.

Even if it still remains unclear whether structural alteration is based on insufficient host defense response inside/outside the sieve element or “willfully” induced by phytoplasmas hijacking and/or suppressing host immunity, the recent work give a novel view inside the complex phytoplasma-host interaction.

The latter approach is favored by the fact that the symptoms mostly include an increment of vegetative plant tissues thereby generating a more extended phloem network for phytoplasma replication (Hogenhout and Šeruga Musić 2010) and accumulation of nutrition (Christensen *et al.* 2005) seems to be beneficial for phytoplasmas. All in all, phytoplasmas seem to induce changes in the expression of genes chiefly involved in hormone metabolism, stress response, electron transport, and protein modification or

Discussion

degradation (Jagoueix-Eveillard *et al.* 2001; Pracros *et al.* 2006; Margaria and Palmano 2011). It seems that the phytoplasmas win evolutionary arm race, to turn the host into a *Zombie* (Arduengo 2014) that provides board and lodging for the phytoplasma parasite.

The discovery of phytoplasma effector proteins (Sugio *et al.* 2011) could give a boost to studies on the initial mechanisms involved in phloem/phytoplasma interactions. Application of phytoplasma effectors to intact plants might help to establish the time-course of the events involved in phloem reactions to infection.

List of references

- Abramovitch, R. B., Anderson, J. C., and Martin, G. B. 2006. Bacterial elicitation and evasion of plant innate immunity. *Nat. Rev. Mol. Cell Biol.* 7:601-611.
- Alvarez, M. E., Pennell, R. I., Meijer, P. J., Ishikawa, A., Dixon, R. A., and Lamb, C. 1998. Reactive oxygen intermediates mediate a systemic signal network in the establishment of plant immunity. *Cell* 92:773-784.
- Andersen, M. T., Liefing, L. W., Havukkala, I., and Beever, R. E. 2013. Comparison of the complete genome sequence of two closely related isolates of '*Candidatus* Phytoplasma australiense' reveals genome plasticity. *BMC Genomic* 14:529.
- Arduengo, M. 2014. Plant biologists take the lead on elucidating zombie genetics. Promega Corporation.
- Attaran, E., Zeier, T. E., Griebel, T., and Zeier, J. 2009. Methyl salicylate production and jasmonate signaling are not essential for systemic acquired resistance in *Arabidopsis*. *Plant Cell* 21:954-971.
- Bai, X. D., Correa, V. R., Toruno, T. Y., Ammar, E. D., Kamoun, S., and Hogenhout, S. A. 2009. AY-WB phytoplasma secretes a protein that targets plant cell nuclei. *Mol. Plant Microbe Interact.* 22:18-30.
- Bai, X., Zhang, J., Ewing, A., Miller, S. A., Radek, A. J., Shevchenko, D. V., Tsukerman, K., Walunas, T., Lapidus, A., Campbell, J. W., *et al.* 2006. Living with genome instability: the adaptation of phytoplasmas to diverse environments of their insect and plant hosts. *J. Bacteriol.* 188:3682-3696.
- Baker, C. J., and Orlandi, E. W. 1995. Active oxygen in plant pathogenesis. *Annu. Rev. Plant Pathol.* 33:299-321.
- Barbara, D. J., Morton, A., Clark, M. F., and Davies, D. L. 2001. Molecular variation in immunodominant membrane proteins from phytoplasmas. *Acta. Hort.* 550:405-408.
- Barratt, D. H. P., Kolling, K., Graf, A., Pike, M., Calder, G., Findlay, K., Zeeman, S. C., and Smith, A. M. 2011. Callose synthase GLS7 is necessary for normal phloem transport and inflorescence growth in *Arabidopsis*. *Plant Physiol.* 155:328-341.
- Baskin, T. I., Busby, C. H., Fowke, L. C., Sammut, M., and Gubler, F. 1992. Improvements in immunostaining samples embedded in methacrylate: Localization of microtubules and other antigens throughout developing organs in plants of diverse taxa. *Planta* 187:405-413.
- Bauer, Z., Gómez-Gómez, L., Boller, T., and Felix, G. 2001. Sensitivity of different ecotypes and mutants of *Arabidopsis thaliana* toward the bacterial elicitor flagellin correlates with the presence of receptor-binding sites. *J. Biol. Chem.* 276:45669-45676.
- Bednarek, P., and Osbourn, A. 2009. Plant-microbe interactions: chemical diversity in plant defense. *Science* 324:746-748.
- Behmer S., Olszewski N., Sebastiani J., Palka S., Sparacino G., and Grebenok R. J. 2013. Plant phloem sterol contents: forms, putative functions, and implications for phloem-feeding insects. *Front. Plant Sci.* 4:370.
- Behnke, H. D., and Sjolund, R. D. 1990. Sieve elements. Comparative structure, induction and development. H. D. Behnke and R.D. Sjolund, eds., Springer Verlag, Berlin, Germany.
- Bell, K., Mitchell, S., Paultre, D., Posch, M., and Oparka, K. 2013. Correlative imaging of fluorescent proteins in resin-embedded plant material. *Plant Physiol.* 161:1595-1603.
- Bellomo, C., Carraro, L., Ermacora, P., Pavan, F., Osler, R., Frausin, C., and Governatori, G. 2007. Recovery phenomena in grapevines affected by grapevine yellows in Friuli Venezia Giulia. *Bul. Insectol.* 60:235-236.
- Bent, A. F., and Mackey, D. 2007. Elicitors, effectors, and R genes: the new paradigm and a lifetime supply of questions. *Annu. Rev. Phytopathol.* 45:399-436.
- Berg, M., Davis, D. L., Clark, M. F., Vetten, H. J., Maier, G., Marccone, C.,

List of references

- and Seemüller, E. 1999. Isolation of the gene encoding an immunodominant membrane protein of the apple proliferation phytoplasma, and expression and characterization of the gene product. *Microbiol.* 145:1937-1943.
- Berg, M., and Seemüller, E. 1999. Chromosomal organization and nucleotide sequence of the elongation factors G and Tu of the apple proliferation phytoplasma. *Gene* 226:103-109.
- Bertaccini, A. 2007. Phytoplasmas, diversity, taxonomy, and epidemiology. *Front. Biosci.* 12:673-689.
- Bertaccini, A., and Duduk, B. 2009. Phytoplasma and phytoplasma diseases: a review of recent research. *Phytopath mediterranean* 48:355-378.
- Bertamini, M., Grando, M. S., Muthuchelian, K., and Nedunchezian, N. 2002a. Effect of phytoplasmal infection on photosystem II efficiency and thylakoid membrane protein changes in field grown apple (*Malus pumila*) leaves. *Physiol. Mol. Plant Pathol.* 61:349-356.
- Bertamini, M., Grando, M. S., and Nedunchezian, N. 2004. Effects of Phytoplasma Infection on pigments, chlorophyll-protein complex and photosynthetic activities in field grown apple leaves. *Biologia Plantarum* 47:237-242.
- Bertamini, M., and Nedunchezian, N. 2001. Effect of phytoplasma [stolbour-subgroup (Bois noir-BN)] of photosynthetic pigments, saccharides, ribulose-1,5-bisphosphate carboxylase, nitrate and nitrite reductases and photosynthetic activities in field-grow grapevine (*Vitis vinifera* L.cv. Chardonnay) leaves. *Photosynthetica* 39:119-122.
- Bertamini, M., Nedunchezian, N., Tomasi, F., and Grando, M. S. 2002b. Phytoplasma [Stolbur-subgroup (Bois Noir-BN)] infection inhibits photosynthetic pigments, ribulose-1,5-bisphosphate carboxylase and photosynthetic activities in field grown grapevine (*Vitis vinifera* L. cv. Chardonnay) leaves. *Physiol. Mol. Plant Pathol.* 61:357-366.
- Block, A., Li, G., Fu, Z. Q., and Alfano, J. R. 2008. Phytopathogen type III effector weaponry and their plant targets. *Curr. Opin. Plant. Biol.* 11:396-403.
- Boevink, P., Oparka, K., Santa Cruz, S., Martin, B., Betteridge, A., and Hawes, C. 1998. Stacks on tracks: the plant Golgi apparatus traffics on an actin/ER network. *Plant J.* 15:441-447.
- Boller, T., and Felix, G. 2009. A renaissance of elicitors: perception of microbe-associated molecular patterns and danger signals by pattern-recognition receptors. *Annu. Rev. Plant Biol.* 60:379-406.
- Boller, T., and He, S. Y. 2009. Innate immunity in plants: an arms race between pattern recognition receptors in plants and effectors in microbial pathogens. *Science* 324:742-744.
- Boonrod, K., Munteanu, B., Jarausch, B., Jarausch, W., and Krczal, G. 2012. An immunodominant membrane protein (Imp) of 'Candidatus Phytoplasma mali' binds to plant actin. *Mol. Plant Microbe Interact.* 25:889-895.
- Borgo, M., and Angelini, E. 2002. Diffusione della flavescenza dorata della vite in Italia e relazioni con vitigni, pratiche agronomiche e materiali di propagazione. *Atti Gior. Fitopatol.* 1:35-50.
- Braccini, P., and Nasca, M. 2008. Influence of some environmental factors on the phenomenon of recovery in Bois noir affected vines. *Petria* 18:363-365.
- Braun, E. J., and Sinclair, W. A. 1976. Translocation in phloem necrosis-diseased American elm seedlings. *Phytopathol.* 68:1733-1737.
- Cai, J., Zhang, X., Wang, X., Li, C., and Liu, G. 2008. *In vivo* MR imaging of magnetically labeled mesenchymal stem cells transplanted into rat liver through hepatic arterial injection.
- Carraro, L., Ermacora, P., Loi, N., and Osler, R. 2004. The recovery

List of references

- phenomenon in apple proliferation infected apple trees. *J. Plant Pathol.* 86:141-146.
- Caudwell, A. 1961. Les phenomenes de retablissement chez la Flavescence doree de la vigne. *Ann. Epiphytes* 12:347-354.
- Chanda, B., Xia, Y., Mandal, M. K., Yu, K., Sekine, K. T., Gao, Q. M., Selote, D., Hu, Y., Stromberg, A., Navarre, D., Kachroo, A., and Kachroo, P. 2011. Glycerol-3-phosphate is a critical mobile inducer of systemic immunity in plants. *Nat. Genet.* 43:421-427.
- Chaturvedi, R., Venables, B., Petros, R. A., Nalam, V., Li, M., Wang, X., Takemoto, L. J., and Shah, J. 2012. An abietane diterpenoid is a potent activator of systemic acquired resistance. *Plant J.* 71:161-172.
- Chen, W., Li, Y., Wang, Q., Wang, N., and Wu, Y. 2014. Comparative genome analysis of wheat blue dwarf phytoplasma, an obligate pathogen that causes wheat blue dwarf disease in China. *PLoS One* doi:10.1371/journal.pone.0096436.
- Choi, Y. H., Casas Tapias, E., Kim, H. K., Lefeber, A. W. M., Erkelens, C., Verhoeven, J. Th. J., Brzin, J., Zel, J., and Verpoorte, R. 2004. Metabolic discrimination of *Catharanthus roseus* leaves infected by phytoplasma using ¹H-NMR spectroscopy and multivariate data analysis. *Plant Physiol.* 135:2398-2410.
- Christensen, N. M., Axelsen, K. B., Nicolaisen, M., and Schulz, A. 2005. Phytoplasmas and their interactions with hosts. *Trends Plant Sci.* 10:526-535.
- Coll, N. S., Vercammen, D., Smidler, A., Clover, C., Van Breusegem, F., Dangl, J. L., and Epple, P. 2010. Arabidopsis type I metacaspases control cell death. *Science* 330:1393-1397.
- Colombani, A., Djerbi, S., Bessueille, L., Blomqvist, K., Ohlsson, A., Berglund, T., Teeri, T. T., and Bulone, V. 2004. *In vitro* synthesis of (1-3)- β -D-glucan (callose) and cellulose by detergent extracts of membranes from cell suspension cultures of hybrid aspen. *Cellulose* 11:313-327.
- Contaldo, N., Bertaccini, A., Paltrinieri, S., Windsor, H. M., and Windsor, G. D. 2012. Axenic culture of plant pathogenic phytoplasmas. *Phytopathol. Med.* 51:607-617.
- Cronshaw, J., and Sabnis, D. D. 1990. Phloem proteins. Pages 255-383 in: Sieve elements. Comparative Structure, Induction and Development. H. D. Behnke and R.D. Sjolund. eds., Springer Verlag, Berlin, Germany.
- Curković Perica, M. 2008. Auxin-treatment induces recovery of phytoplasma-infected periwinkle. *J. Appl. Microbiol.* 105:1826-1834.
- Dafalla, G. A., and Cousin, M. T. 1988. Fluorescence and electron microscopy of *Cynodon dactylon* affected with a white leaf disease in Sudan. *J. Phytopathol.* 122:25-34.
- D'Amelio, R., Massa, N., Gamalero, E., D'Agostino, G., Sampò, S., Berta, G., Faoro, F., Iriti, M., Bosco, D., and Marzachi, C. 2007. Preliminary results on the evaluation of the effects of elicitors of plant resistance on chrysanthemum yellows phytoplasma infection. *Bul. Insectol.* 60:317-318.
- Dangl, J. L., and Jones, J. D. 2011. Plant pathogens and integrated defence responses to infection. *Nature* 6839:826-833.
- Davey, M. R., Anthony, P., Power, J. B., and Lowe, K. C. 2005. Plant protoplasts: status and biotechnological perspectives. *Biotechnol. Adv.* 23:131-171.
- Davies, E. 2004. New functions for electrical signals in plants. *New Phytol.* 161:607-610.
- Davies, E., and Stankovic, B. 2006. Electrical signals, the cytoskeleton, and gene expression: a hypothesis on the coherence of the cellular responses to environmental insult. Pages 309-320 in: Communication in Plants – Neuronal Aspects of Plant Life. F. Baluska, S. Mancuso and D. Volkmann. eds., Springer Verlag, Berlin, Germany.

List of references

- Day, B., Henty, J. L., Porter, K. J., and Staiger, C. J. 2011. The pathogen-actin connection: A platform for defense signaling in plants. *Ann. Phytopathol. Soc. Jpn.* 49:489-506.
- de Beer, A., and Vivier, M. A. 2011. Four plant defensins from an indigenous South African Brassicaceae species display divergent activities against two test pathogens despite high sequence similarity in the encoding genes. *BMC Res. Notes* 4:459.
- Dempsey, D. A., and Klessig, D. F. 2012. SOS - too many signals for systemic acquired resistance? *Trends Plant Sci.* 17:538-545.
- Ding, S. W., and Voinnet, O. 2007. Antiviral immunity directed by small RNAs. *Cell* 130:413-426.
- Dodd, A. N., Kudla, J., and Sanders, D. 2010. The language of calcium signaling. *Annu. Rev. Plant Biol.* 61:593-620.
- Doi, Y., Teranaka, M., Yora, K., and Asuyama, H. 1967. Mycoplasma or PLT grouplike microorganisms found in phloem elements of plants infected with mulberry dwarf, potato witches' broom, aster yellows, or Paulownia witches' broom.
- Doyle, J. J., and Doyle, J. L. 1990. Isolation of plant DNA from fresh tissue. *Focus* 12:13-15.
- Du, T., Wang, Y., Hu, Q. S., Chen, J., Liu, S., Huang, W. J., and Lin, M. L. 2005. Transgenic Paulownia expressing shiva-1 gene has increased resistance to Paulownia witches' broom disease. *J. Integrative Plant Biol.* 47:1500-1506.
- Dubiella, U., Seybold, H., Durian, G., Komander, E., Lassig, R., Witte, C. P., Schulze, W. X., and Romeis, T. 2013. Calcium-dependent protein kinase/NADPH oxidase activation circuit is required for rapid defense signal propagation. *Natl. Acad. Sci. U.S.A.* 110:8744-8749.
- Durner, J., and Klessig, D. F. 1999. Nitric oxide as a signal in plants. *Curr. Opin. Plant Biol.* 2: 369-374.
- Durrant, W. E., and Dong, X. 2004. Systemic acquired resistance. *Annu. Rev. Phytopathol.* 42:185-209.
- Dworkin, J. 2009. Cellular polarity in prokaryotic organisms. *Cold Spring Harb Perspect Biol.* doi:10.1101/cshperspect.a003368.
- Economou, A. 1999. Following the leader: bacterial protein export through the Sec pathway. *Trends Microbiol.* 7:315-320.
- Ehlers, K., Knoblauch, M., and van Bel, A. J. E. 2000. Ultrastructural features of well-preserved and injured sieve elements: minute clamps keep the phloem transport conduits free for mass flow. *Protoplasma* 214:80-92.
- Ehya, F., Monavarfeshani, A., Mohseni Fard, E., Karimi Farsad, L., Khayam Nekouei, M., Mardi, M., and Salekdeh, G. H. 2013. Phytoplasma-Responsive microRNAs modulate hormonal, nutritional, and stress signalling pathways in Mexican lime trees. *PLoS One* 8:e66372.
- Endeshaw, S. T., Murolo, S., Romanazz, G., and Neri, D. 2012. Effects of Bois noir on carbon assimilation, transpiration, stomatal conductance of leaves and yield of grapevine (*Vitis vinifera*) cv. Chardonnay. *Physiol. Plant* 145:286-295.
- Ernst, A. M., Jekat, S. B., Zielonka, S., Müller, B., Neumann, U., Rüping, B., Twyman, R. M., Krzyzanek, V., Prüfer, D., and Noll, G. 2012. Sieve element occlusion (SEO) genes encode structural phloem proteins involved in wound sealing of phloem. *Proc. Natl. Acad. Sci. U.S.A.* 106:1980-1989.
- Ernst, A. M., Rüping, B., Jekat, S. B., Nordzieke, S., Reineke, A. R., Müller, B., and Bornberg-Bauer, E., Prüfer, D., and Noll, G. A. 2011. The sieve element occlusion gene family in dicotyledonous plants. *Plant Signal. Behav.* 6:151-153.
- Esau, K. 1969. The Phloem. *Encyclopedia of Plant Anatomy*, Gebrüder Borntraeger, Berlin, Stuttgart, Germany.
- Esau, K., and Cheadle, V. I. 1958. Wall thickening in sieve elements. *Proc. Natl. Acad. Sci. U.S.A.* 44:546-443.

List of references

- Evert, R. F. 1990. Dicotyledons. Pages 103-137 in: Sieve Elements. Comparative Structure, Induction and Development. H. D. Behnke and R. D. Sjolund. eds., Springer Verlag, Berlin, Germany.
- Faoro, F. 2005. Perché è così difficile osservare al microscopio elettronico i fitoplasmi della vite? *Petria* 15:99-101.
- Felix, G., Duran, J. D., Volko, S., and Boller, T. 1999. Plants have a sensitive perception system for the most conserved domain of bacterial flagellin. *Plant J.* 18:265-276.
- Felle, H. H., and Zimmermann, M. R. 2007. Systemic signalling in barley through action potentials. *Planta* 226:203-214.
- Fraser, C. M., Gocayne, J. D., White, O., Adams, M. D., Clayton, R. A., Fleischmann, R. D., Bult, C. J., Kerlavage, A. R., Sutton, G., Kelley, J. *et al.* 1995. The minimal gene complement of *Mycoplasma genitalium*. *Science* 270:397-403.
- Fromm, J., Hajirezaei, M. R., Becker, V. K., and Lautner, S. 2013. Electrical signaling along the phloem and its physiological responses in the maize leaf. *Front Plant Sci.* 4:239.
- Fromm, J., and Spanswick, R. 1993. Characteristics of action potential in willow (*Salix viminalis* L). *J. Ex. Bot.* 44:1119-1125.
- Furch, A. C. U., Hafke, J. B., Schulz, A., and van Bel, A. J. E. 2007. Ca²⁺-mediated remote control of reversible sieve tube occlusion in *Vicia faba*. *J. Exp. Bot.* 58:2827-2838.
- Furch, A. C. U., van Bel, A. J. E., Fricker, M. D., Felle, H. H., Fuchs, M., and Hafke, J. B. 2009. Sieve-element Ca²⁺ channels as relay stations between remote stimuli and sieve-tube occlusion in *Vicia faba*. *Plant Cell* 21:2118-2132.
- Furch, A. C. U., Zimmermann, M. R., Will, T., Hafke, J. B., and van Bel, A. J. E. 2010. Remote-controlled stop of phloem mass flow by biphasic occlusion in *Cucurbita maxima*. *J. Exp. Bot.* 61:3697-3708.
- Gai, Y. P., Li, Y. Q., Guo, F. Y., Yuan, C. Z., Mo, Y. Y., Zhang, H. L., Wang, H., and Ji X. L. 2014. Analysis of phytoplasma-responsive sRNAs provide insight into the pathogenic mechanisms of mulberry yellow dwarf disease. *Sci. Rep.* doi:10.1038/srep05378.
- Galetto, L., Bosco, D., Balestrini, R., Genre, A., Fletcher J., and Marzachi, C. 2011. The major antigenic membrane protein of '*Candidatus Phytoplasma asteris*' selectively interacts with ATP synthase and actin of leafhopper vectors. *PLoS ONE* 6:e22571.
- Galetto, L., Bosco, D., Fletcher J., and Marzachi, C. 2007. Production of polyclonal and monoclonal antibodies specific against membrane proteins of "*Candidatus Phytoplasma asteris*", chrysanthemum yellows isolate. *Bulletin of Insectol.* 60:211-212.
- Gatineau, F., Jacob, N., Vautrin, S., Larrue, J., Lherminier, J., Richard-Molard, M., and Boudon-Padieu, E. 2002. Association with the syndrome "basses richesses" of sugar beet of a phytoplasma and a bacterium-like organism transmitted by a *Pentastiridius sp.* *Phytopathol.* 92:384-392.
- Gaupels, F., Furch, A. C. U., Will, T., Mur, L. A., Kogel, K. H., and van Bel, A. J. E. 2008. Nitric oxide generation in *Vicia faba* phloem cells reveals them to be sensitive detectors as well as possible systemic transducers of stress signals. *New Phytol.* 178:634-646.
- Gaupels, F., and Ghirardo, A. 2013. The extrafascicular phloem is made for fighting. *Front. Plant Sci.* 4:187.
- Gilroy, S., Bethke, P. C., and Jones, R. L. 1993. Calcium homeostasis in plants. *J. Cell Sci.* 106:453-462.
- Glazebrook, J. 2005. Contrasting mechanisms of defense against biotrophic and necrotrophic pathogens. *Annu. Rev. Phytopathol.* 43:205-2027.
- Gohre, V., Spallek, T., Haweker, H., Mersmann, S., Mentzel, T., Boller, T., de Torres, M., Mansfield, J. W., and

List of references

- Robatzek, S. 2008. Plant pattern-recognition receptor FLS2 is directed for degradation by the bacterial ubiquitin ligase AvrPtoB. *Curr. Biol.* 18:1824-1832.
- Golan, G., Betzer, R., and Wolf, S. 2013. Phloem-specific expression of a melon Aux/IAA in tomato plants alters auxin sensitivity and plant development. *Front. Plant Sci.* 4:329.
- Gómez-Gómez, L., and Boller, T. 2000. FLS2: an LRR receptor-like kinase involved in the perception of the bacterial elicitor flagellin in *Arabidopsis*. *Mol. Cell.* 5:1003-1011.
- Gómez-Gómez, L., Felix, G., and Boller, T. 1999. A single locus determines sensitivity to bacterial flagellin in *Arabidopsis thaliana*. *Plant J.* 18:277-284.
- Goodwin, P. B., Shepherd, V., and Erwee, M. G. 1990. Compartmentation of fluorescent tracers injected into the epidermal cells of *Egeria densa* leaves. *Planta* 181:129-136.
- Grant, M., and Lamb, C. 2006. Systemic immunity. *Curr. Opin. Plant Biol.* 9:414-420.
- Greenberg, J.T., and Yao, N. 2004. The role and regulation of programmed cell death in plant-pathogen interactions. *Cell. Microbiol.* 6:201-211.
- Guedes, M. E. M., Richmond, S., and Kuc, J. 1980. Induced systemic resistance to anthracnose in cucumber as influenced by the location of the inducer inoculation with *Colletotrichum lagenarium* and the onset of flowering and fruiting. *Physiol. Plant Pathol.* 17:229-233.
- Guo, M., Tian, F., Wamboldt, Y., and Alfano, J. R. 2009. The majority of the type III effector inventory of *Pseudomonas syringae* pv. tomato DC3000 can suppress plant immunity. *Mol. Plant Microbe Interact.* 22:1069-1080.
- Hafke, J. B., Ehlers, K., Föllner, J., Höll, S. R., Becker, S., and van Bel, A. J. E. 2013. Involvement of the sieve element cytoskeleton in electrical responses to cold shocks. *Plant Physiol.* 162:707-719.
- Hafke, J. B., Furch, A. C. U., Fricker, M. D., and van Bel, A. J. E. 2009. Forisome dispersion in *Vicia faba* is triggered by Ca²⁺ hotspots created by concerted action of diverse Ca²⁺ channels in sieve elements. *Plant Signal. Behav.* 4:968-972.
- Hafke, J. B., Furch, A. C. U., Reitz, M. U., and van Bel, A. J. E. 2007. Functional sieve element protoplasts. *Plant Physiol.* 145:703-711.
- Hafke, J. B., van Amerongen, J. K., Kelling, F., Furch, A. C. U., Gaupels, F., and van Bel, A. J. E. 2005. Thermodynamic battle for photosynthate acquisition between sieve tubes and adjoining parenchyma in transport phloem. *Plant Physiol.* 138:1527-1537.
- Hafke, J. B., and van Bel, A. J. E. 2013. Cellular basis of electrical potential waves along the phloem and impact of coincident Ca²⁺ fluxes. Pages 122-140 in: *Phloem. Molecular cell biology, systemic communication, biotic interactions.* G.A. Thompson, A.J.E. van Bel. eds., Wiley-Blackwell, Chichester, U.K.
- Hannapel D. J., Sharma P., and Lin, T. 2013. Phloem-mobile RNAs and root development. *Front. Plant Sci.* 4:257.
- Hardham, A. R., Jones, D. A., and Takemoto, D. 2007. Cytoskeleton and cell wall function in penetration resistance. *Curr. Opin. Plant Biol.* 10:342-348.
- Harmon, A. C., Gribskov, M., and Harper, J. F. 2000. CDPKs: a kinase for every Ca²⁺ signal? *Trends Plant Sci.* 5:154-159.
- Harper, J. F., and Harmon, A. 2005. Plants, symbiosis and parasites: a calcium signalling connection. *Nat. Rev. Mol. Cell Biol.* 6:555-566.
- Henty-Ridilla, J. L., Shimono, M., Li, J., Chang, J. H., Day, B., and Staiger, C. J. 2013. The plant actin cytoskeleton responds to signals from microbe-associated molecular patterns. *PLoS Pathog.* 9:e1003290.
- Himeno, M., Kitazawa, Y., Yoshida, T.,

List of references

- Maejima, K., Yamaji, Y., Oshima, K., and Namba, S. 2014. Purple top symptoms are associated with reduction of leaf cell death in phytoplasma-infected plants. *Sci. Rep.* 4:4111.
- Hogenhout, S. A., and Loria, R. 2008. Virulence mechanisms of gram-positive plant pathogenic bacteria. *Curr. Opin. Plant Biol.* 11:449-456.
- Hogenhout, S. A., Oshima, K., Ammar, E., Kakizawa, S., Kingdom, H. N., and Namba, S. 2008. Phytoplasmas: bacteria that manipulate plants and insects. *Mol. Plant Pathol.* 9:403-423.
- Hogenhout, S. A., and Šeruga Musić, M. 2010. Phytoplasma genomics, from sequencing to comparative and functional genomics – What have we learnt? Pages 19-36 in: *Phytoplasmas: genomes, plant hosts and vectors*. P. Weintraub and P. Jones. eds., CABI publishing, Oxfordshire, U.K.
- Hong, Z., Delauney, A. J., Verma, D. P. S. 2001. A cell-plate specific callose synthase and its interaction with phragmoplastin. *Plant Cell* 13: 755-768.
- Hoshi, A., Oshima, K., Kakizawa, S., Ishii, Y., Ozeki, J., Hashimoto, M., Komatsu, K., Kagiwada, S., Yamaji, Y., and Nambam, S. 2009. A unique virulence factor for proliferation and dwarfism in plants identified from a phytopathogenic bacterium. *Proc. Natl. Acad. Sci. U.S.A.* 106:6416-6421.
- Huda, K. M. K., Banu, M. S. A., Tuteja, R., and Tuteja, N. 2013. Global calcium transducer P-type Ca^{2+} -ATPases open new avenues for agriculture by regulating stress signalling. *J. Ex. Bot.* 64:3099-3109.
- Hwang, I., and Sheen, J. 2001. Two-component circuitry in Arabidopsis signal transduction. *Nature* 413:383-389.
- Imlau, A., Truernit, E., and Sauer, N. 1999. Cell-to-cell and long-distance trafficking of the green fluorescent protein in the phloem and symplastic unloading of the protein into sink tissues. *Plant Cell* 11:309-322.
- IRPCM Phytoplasma/Spiroplasma Working Team – Phytoplasma taxonomy group. 2004. *Int. J. Syst. Evol. Microbiol.* 54:1243-1255.
- Jackson, R. W. 2009. Plant-Pathogenic Bacteria: Genomics and Molecular Biology. *Biotech. J.* 4:1497.
- Jagoueix-Eveillard, S., Tarendeau, F., Guolter, K., Danet, J. L., Bové, J. M., and Garnier, M. 2001. *Catharanthus roseus* genes regulated differentially by mollicute infections. *Mol. Plant Microbe Interact.* 14:225-233.
- Jain, A., Poling, M. D., Karthikeyan, A. S., Blakeslee, J. J., Peer, W. A., Titapiwatanakun, B., Murphy, A. S., and Raghothama, K. G. 2007. Differential effects of sucrose and auxin on localized phosphate deficiency-induced modulation of different traits of root system architecture in Arabidopsis. *Plant Physiol.* 144:232-247.
- Jekat, S. B., Ernst, A. M., von Bohl, A., Zielonka, S., Twyman, R. M., Noll, G. A., and Prüfer, D. 2013. P-proteins in Arabidopsis are heteromeric structures involved in rapid sieve tube sealing. *Front. Plant Sci.* 4:225.
- Jenns, A. E., and Kuc, J. 1979. Graft transmission of systemic resistance of cucumbers to anthracnose induced by *Colletotrichum lagenarium* and tobacco necrosis virus. *Phytopathol.* 69:753-756.
- Jeworutzki, E., Roelfsema, M. R., Anschütz, U., Krol, E., Elzenga, J. T., Felix, G., Boller, T., Hedrich, R., and Becker, D. 2010. Early signaling through the Arabidopsis pattern recognition receptors FLS2 and EFR involves Ca-associated opening of plasma membrane anion channels. *Plant J.* 62:367-378.
- Jin, S., Xu, R., Wei, Y., and Goodwin, P. H. 1999. Increased expression of a plant actin gene during a biotrophic interaction between round-leaved mallow, *Malva pusilla*, and *Colletotrichum gloeosporioides f. sp. malvae*. *Planta* 209:487-494.

List of references

- Jones, J. D., and Dangl, J. L. 2006. The plant immune system. *Nature* 444:323-259.
- Jung, H. W., Tschaplinski, T. J., Wang, L., Glazebrook, J., and Greenberg, J. T. 2009. Priming in systemic plant immunity. *Science* 324:88-91.
- Kakizawa, S., Oshima, K., Jung, J. H., Suzuki, S., Nishigawa, H., Arashida, R., Miyata, S., Ugaki, M., Kishino, H., and Namba, S. 2006. Positive selection acting on a surface membrane protein of the plant-pathogenic phytoplasmas. *J. Bacteriol.* 188:3424-3428.
- Kakizawa, S., Oshima, K., Nishigawa, H., Jung, H. Y., Wei, W., Suzuki, S., Tanaka, M., Miyata, S., Ugaki, M., and Namba, S. 2004. Secretion of immunodominant membrane protein from onion yellows phytoplasma through the Sec protein-translocation system in *Escherichia coli*. *Microbiol.* 150:135-142.
- Kartte, S., and Seemüller, E. 1991. Histopathology of apple proliferation in *Malus* taxa and hybrids of different susceptibility. *J. Phytopathol.* 131:149-160.
- Kauss, H. 1987. Some aspects of calcium-dependent regulation in plant metabolism. *Annu. Rev. Plant Physiol.* 38:47-72.
- Kehr, J. 2013. Systemic regulation of mineral homeostasis by micro RNAs. *Front. Plant Sci.* 4:145.
- King, R. W., and Zeevaart, J. A. D. 1974. Enhancement of phloem exudation from cut petioles by chelating agents. *Plant Physiol.* 12:96-103.
- Kirkpatrick, B. C. 1992. Mycoplasma-like organisms: plant and invertebrate pathogens. Pages 4050-4067 in: *The Prokaryotes*. A. Balows, H. G. Trüper, M. Dworkin, W. Harder and K. H. Schleifer. 2nd eds., Springer, New York, U.S.A.
- Knoblauch, M., Froelich, D. R., Pickard, W. F., and Peters, W. S. 2014. SEORious business: structural proteins in sieve tubes and their involvement in sieve element occlusion. *J. Exp. Bot.* 65:1879-1893.
- Knoblauch, M., Noll, G. A., Müller, T., Prüfer, D., Schneider-Hüther, I., Scharner, D., van Bel, A. J. E., and Peters, W. S. 2003. ATP-independent contractile proteins from plants. *Nat. Mater.* 2:600-603.
- Knoblauch, M., Peters, W. S., Ehlers, K., and van Bel, A. J. E. 2001. Reversible calcium-regulated stopcocks in legume sieve tubes. *Plant Cell* 13:1221-1230.
- Knoblauch, M., Stubenrauch, M., van Bel, A. J. E., and Peters, W. S. 2012. Forisome performance in artificial sieve tubes. *Plant, Cell Environ.* 15:1419-1427.
- Knoblauch, M., and van Bel, A. J. E. 1998. Sieve tubes in action. *Plant Cell* 10:35-50.
- Kobayashi, M., Ohura, I., Kawakita, K., Yokota, N., Fujiwara, M., Shimamoto, K., Doke, N., and Yoshioka, H. 2007. Calcium-dependent protein kinases regulate the production of reactive oxygen species by potato NADPH oxidase. *Plant Cell* 19:1065-1080.
- Koch, K. 2004. Sucrose metabolism: regulatory mechanisms and pivotal roles in sugar sensing and plant development. *Curr. Opin. Plant Biol.* 7:235-246.
- Koh, E. J., Zhou, L., Williams, D. S., Park, J., Ding, N., Duan, Y. P., and Kang, B. H. 2012. Callose deposition in the phloem plasmodesmata and inhibition of phloem transport in citrus leaves infected with "*Candidatus Liberibacter asiaticus*". *Protoplasma* 249:687-697.
- Köhle, H., Jeblick, W., Poten, F., Blascheck, W., and Kauss, H. 1985. Chitosan-elicited callose synthesis in soybean cells as a Ca²⁺-dependent process. *Plant Physiol.* 77: 544-551.
- Koui, T., Natsuaki, T., and Okuda, S. 2003. Phylogenetic analysis of elongation factor Tu gene of phytoplasmas from Japan. *J. Gen. Plant Pathol.* 69:316-319.
- Kube, M., Mitrovic, J., Duduk, B., Rabus, R., and Seemüller, E. 2012. Current view on phytoplasma genomes and

List of references

- encoded metabolism. *Scientific World J.* doi:10.1100/2012/185942.
- Kuc, J. 1987. Translocated signals for plant immunization. *Ann. NY. Acad. Sci.* 494:221-223.
- Kudla, J., Batistic, O., and Hashimoto, K. 2010. Calcium signals: the lead currency of plant information processing. *Plant Cell* 22:541-563.
- Lattanzio, G., Andaluz, S., Matros, A., Calvete, J. J., Kehr, J., Abadía, A., Abadía, J., and López-Millán, A. F. 2013. Protein profile of *Lupinus texensis* phloem sap exudates: searching for Fe- and Zn-containing proteins. *Proteomics* 13:2283-2296.
- Lee, I. M., Davis, R. E., and Gundersen-Rindal, D. E. 2000. Phytoplasma: phytopathogenic mollicutes. *Annu. Rev. Microbiol.* 54:221-255.
- Lee, I. M., Martini, M., Marcone, C., and Zhu, S. F. 2004. Classification of phytoplasma strains in the elm yellows group (16SrV) and proposal of '*Candidatus Phytoplasma ulmi*' for the phytoplasma associated with elm yellows. *Intern. J. Syst. Evol. Microbiol.* 54:337-347.
- Lee, I. M., Pastore, M., Vibio, M., Danielli, A., Attathorn, S., Davis, R. E., and Bertaccini, A. 1997. Detection and characterization of a phytoplasma associated with annual blue grass (*Poa annua*) white leaf disease in southern Italy. *Eur. J. Plant Pathol.* 103:251-254.
- Lee, M. J., Pate, J. S., Harris, D. J., Atkins, C. A. 2007. Synthesis, transport and accumulation of quinolizidine alkaloids in *Lupinus albus* L. and *L. angustifolius* L. *J. Exp. Bot.* 58:935-946.
- Lee, I. M., Zhao, Y., and Bottner, K. D. 2006. SecY gene sequence analysis for finer differentiation of diverse strains in the aster yellows phytoplasma group. *Mol. Cell. Probes* 20:87-91.
- Le Gall, F., Bove, J. M., and Garnier, M. 1998. Engineering of a single-chain variable-fragment (scFv) antibody specific for the stolbur phytoplasma (Mollicute) and its expression in *Escherichia coli* and tobacco plants. *Appl. Environ. Microbiol.* 64:4566-4572.
- Le Hir, R., and Bellini, C. 2013. The plant-specific dof transcription factors family: new players involved in vascular system development and functioning in *Arabidopsis*. *Front Plant Sci.* 4:164.
- León, R., Santamaría, J. M., Alpizar, L., Escamilla, J. A., and Oropeza, C. 1996. Physiological and biochemical changes in shoots of coconut palms affected by lethal yellowing. *New Phytol.* 134:227-234.
- Lepka, P., Stitt, M., Moll, E., and Seemüller, E. 1999. Effect of phytoplasmal infection on concentration and translocation of carbohydrates and amino acids in periwinkle and tobacco. *Physiol. Mol. Plant Pathol.* 55:59-68.
- Lherminier, J., Benhamou, N., Larrue, J., Milet, M. L., Boudon-Padieu, E., Nicole, M., and Blein, J. P. 2003. Cytological characterization of elicitor induced protection in tobacco plants infected by *Phytophthora parasitica* or phytoplasma. *Phytopathol.* 93:1308-1319.
- Lingua, G., D'Agostino, G., Massa, N., Antosiano, M., and Berta, G. 2002. Mycorrhiza-induced differential response to a yellows disease in tomato. *Mycorrhiza* 12:191-198.
- Loebenstein, G., Thottappilly, G., Fuentes, S., and Cohen, J. 2009. Virus and phytoplasma diseases. Pages 105-134 in: *The sweetpotato*. G. Loebenstein, G. Thottappilly. eds., Springer Verlag, Berlin, Germany.
- Loi, N., Ermacora, P., Carraro, L., Osler, R., and Chen, T. A. 2002. Production of monoclonal antibodies against apple proliferation phytoplasma and their use in serological detection. *Eur. J. Plant Pathol.* 108:81-86.
- Long, J. C., and Jenkins, G. I. 1998. Involvement of plasma membrane redox activity and calcium homeostasis in the UV-B and UV-A/blue light induction of gene expression in *Arabidopsis*. *Plant Cell* 10:2077-2086.

List of references

- Lu, Y. T., Li, M. Y., Cheng, K. T., Tan, C. M., Su, L. W., Lin, W. Y., Shih, H. T., Chiou, T. J., and Yang, J. Y. 2014. Transgenic plants that express the phytoplasma effector SAP11 show altered phosphate starvation and defense responses. *Plant Physiol.* 164:1456-1469.
- Lucas, W. J., Yoo, B. C., and Kragler, F. 2001. RNA as a long-distance information macromolecule in plants. *Nat. Rev. Mol. Cell Biol.* 2:849-857.
- Lybarger, S. R., and Maddock, J. R. 2001. Polarity in action: asymmetric protein localization in bacteria. *J. Bacteriol.* 183:3261-3267.
- MacLean, A. M., Orlovskis, Z., Kowitwanich, K., Zdziarska, A. M., Angenent, G. C., Immink, R. G., and Hogenhout, S. A. 2014. Phytoplasma effector SAP54 hijacks plant reproduction by degrading mads-box proteins and promotes insect colonization in a RAD23-dependent manner. *PLoS Biol.* 12:e1001835.
- MacLean, A. M., Sugio, A., Makarova, O. V., Findlay, K. C., Grieve, V. M., Tóth, R., Nicolaisen, M., and Hogenhout, S. A. 2011. Phytoplasma effector SAP54 induces indeterminate leaf-like flower development in arabidopsis plants. *Plant Physiol.* 157:831-841.
- Maghuly, F., Khan, M. A., Borroto Fernandez, E., Druart, P., Bernard Watillon, B., and Laimer, M. 2008. Stress regulated expression of the GUS-marker gene (*uidA*) under the control of plant calmodulin and viral 35S promoters in a model fruit tree rootstock: *Prunus incisa x serrula*. *J. Biotechnol.* 135:105-116.
- Malamy, J., Carr, J. P., Klessig, D. F., and Raskin, I. 1990. Salicylic Acid: a likely endogenous signal in the resistance response of tobacco to viral infection. *Science* 250:1002-1004.
- Marcone, C. 2010. Movement of phytoplasmas and the development of disease in the plant. Pages 114-131 in: *Phytoplasmas: genomes, plant hosts and vectors*. P. Jones and P. Weintraub. eds., CABI Publishing, Wallingford, U.K.
- Marcone, C., Neimark, H., Ragozzino, A., Lauer, U., and Seemüller, E. 1999. Chromosome sizes of phytoplasmas composing major phylogenetic groups and subgroups. *Phytopathol.* 89:805-810.
- Margaria, P., and Palmano, S. 2011. Response of the *Vitis vinifera* L. cv. 'Nebbiolo' proteome to Flavescence dorée phytoplasma infection. *Proteomics* 11:212-224.
- Martens, H. J., Roberts, A. G., Oparka, K. J., and Schulz, A. 2006. Quantification of plasmodesmatal endoplasmic reticulum coupling between sieve elements and companion cells using fluorescence redistribution after photobleaching. *Plant Physiol.* 142:471-480.
- Mathur, J., and Hülskamp, M. 2002. Microtubules and microfilaments in cell morphogenesis in higher plants. *Curr. Biol.* 12:669-676.
- Matsubayashi, Y. 2011. Small post-translationally modified Peptide signals in Arabidopsis. *Arabidopsis Book* 9:e0150.
- Matteoni, J. A., and Sinclair, W. A. 1983. Stomatal closure in plants infected with mycoplasma-like organisms. *Phytopathol.* 73:398-402.
- Mauch, F., Mauch-Mani, B., and Boller, T. 1988. Antifungal hydrolases in pea tissue II. Inhibition of fungal growth by combinations of chitinase and β -1, 3-glucanase. *Plant Physiol.* 88:936-942.
- Maust, B. E., Espadas, F., Talavera, C., Aguilar, M., Santamaria, J. M., and Oropeza, C. 2003. Changes in carbohydrate metabolism in coconut palms infected with the lethal yellowing phytoplasma. *Phytopathol.* 93:976-981.
- Messiaen, J., Read, N. D., van Cutsem, P., and Trewavas, A. J. 1993. Cell wall oligogalacturonides increase cytosolic free calcium in carrot protoplasts. *J. Cell Sci.* 104:365-371.
- Métraux, J. P., Signer, H., Ryals, J., Ward, E., Wyss-Benz, M., Gaudin, J., Raschdorf, K., Schmid, E., Blum, W.,

List of references

- and Inverardi, B. 1990. Increase in salicylic acid at the onset of systemic acquired resistance in cucumber. *Science* 250:1004-1006.
- Milkus, B., Clair, D., Idir, S., Habili, N., and Boudon-Padieu, E. 2004. First detection of stolbur phytoplasma in grapevines (*Vitis vinifera* cv. Chardonnay) affected with grapevine yellows in the Ukraine. *New Disease Reports* 10:12.
- Mishina, T. E., and Zeier, J. 2007. Pathogen-associated molecular pattern recognition rather than development of tissue necrosis contributes to bacterial induction of systemic acquired resistance in *Arabidopsis*. *Plant J.* 50:500-513.
- Mitton, F. M., Pinedo, M. L., and de la Canal, L. 2009. Phloem sap of tomato plants contains a DIR1 putative ortholog. *J. Plant Physiol.* 166:543-547.
- Morelli, J. K., Zhou, W., Yu, J., Lu, C., and Vayda, M. E. 1998. Actin depolymerization affects stress-induced translational activity of potato tuber tissue. *Plant Physiol.* 116:1227-1237.
- Mori, I. C., and Schroeder, J. I. 2004. Reactive oxygen species activation of plant Ca^{2+} channels. A signaling mechanism in polar growth, hormone transduction, stress signaling, and hypothetically mechanotransduction. *Plant Physiol.* 135:702-708.
- Mousavi, S. A. R., Chauvin, A., Pascaud, F., Kellenberger, S., and Farmer, E. E. 2013. Glutamate receptor-like genes mediate leaf-to-leaf wound signalling. *Nature* 500:422-426.
- Müller, B., Pantin, F., Genard, M., Turc, O., Freixes, S., Piques, M., and Gibon, Y. 2011. Water deficits uncouple growth from photosynthesis, increase C content, and modify the relationships between C and growth in sink organs. *J. Exp. Bot.* 62:1715-1729.
- Münch, E. 1930. *Die Stoffbewegung in der Pflanze*. Gustav Fischer Verlag, Jena, Germany.
- Munyaneza, J. E., Lemmetty, A., Nissinen, A. I., Sengoda, V. G., Fisher, T. W. 2011. Molecular detection of aster yellows phytoplasma and "*Candidatus Liberibacter solanacearum*" in carrots affected by the psyllid *Trioza apicalis* (Hemiptera: Triozidae) in Finland. *J. Plant Pathol.* 93:697-700.
- Musetti, R. 2006. Patogeni e piante di interesse agronomico: un approccio morfologico. Pages 325-334 in: 50 anni di Microscopia in Italia tra storia, progresso ed evoluzione. D. Quaglino, E. Falcieri, M. Catalano, A. Diaspro, A. Montone, P. Mengucci and C. Pellicciari. eds., PLME Editrice, Palvia, Italy.
- Musetti, R. 2010. Biochemical changes in plants infected by phytoplasmas. Pages 132-146 in: Phytoplasmas genomes, plant hosts and vectors. P.G. Weintraub and P. Jones. eds., CABI publishing, Oxfordshire, U.K.
- Musetti, R., Carraro, L., Loi, N., and Ermacora, P. 2002. Application of immunoelectron microscopy techniques in the diagnosis of phytoplasma diseases. *Microsc. Res. Tech.* 56:462-464.
- Musetti, R., and Favali, M. A. 1999. Histological and ultrastructural comparative study between *Prunus* varieties of different susceptibility to plum leptonecrosis. *Cytobios* 99:73-82.
- Musetti, R., Favali, M. A., and Pressacco, L. 2000. Histopathology and polyphenol content in plants infected by phytoplasmas. *Cytobios* 102:133-147.
- Musetti, R., Grisan, S., Polizzotto, R., Martini, M., Paduano, C., and Osler, R. 2011. Interactions between '*Candidatus Phytoplasma mali*' and the apple endophyte *Epicoccum nigrum* in *Catharanthus roseus* plants. *J. Appl. Microbiol.* 110:746-756.
- Musetti, R., Paolacci, A., Ciaffi, M., Tanzarella, O. A., Polizzotto, R., Tubaro, F., Mizzau, M., Ermacora, P., Badiani, M., and Osler, R. 2010. Phloem cytochemical modification and gene expression following the recovery

List of references

- of apple plants from apple proliferation disease. *Phytopathol.* 100:390-399.
- Musetti, R., Polizzotto, R., Grisan, S., Martini, M., Borselli, S., Carraro, L., and Osler, R. 2007. Effects induced by fungal endophytes in *Catharanthus roseus* tissues infected by phytoplasmas. *Bull. Insectol.* 60:293-294.
- Musetti, R., Sanità di Toppi, L., Ermacora, P., and Favali, M. A. 2004. Recovery in apple trees infected with the apple proliferation phytoplasma: an ultrastructural and biochemical study. *Phytopathol.* 94:203-208.
- Musetti, R., Sanità di Toppi, L., Martini, M., Ferrini, F., Loschi, A., Favali, M. A., and Osler, R. 2005. Hydrogen peroxide localization and antioxidant status in the recovery of apricot plants from european stone fruit yellows. *Eur. J. Plant. Pathol.* 112:53-61.
- Musetti, R., Tubaro, F., Polizzotto, R., Ermacora, P., and Osler, R. 2008. Il "Recovery" da apple proliferation in melo è associato all' aumento della concentrazione dello ione calcio nel floema. *Petria* 18:380-383.
- Nacry, P., Canivenc, G., Muller, B., Azmi, A., Van Onckelen, H., Rossignol, M., and Dumas, P. 2005. A role for auxin redistribution in the responses of the root system architecture to phosphate starvation in *Arabidopsis*. *Plant Physiol.* 138:2061-2074.
- Naito, K., Taguchi, F., Suzuki, T., Inagaki, Y., Toyoda, K., Shiraishi, T., and Ichinose, Y. 2008. Amino acid sequence of bacterial microbe-associated molecular pattern flg22 is required for virulence. *Mol. Plant Microbe Interact.* 21:1165-1174.
- Navarro, L., Dunoyer, P., Jay, F., Arnold, B., Dharmasiri, N., Estelle, M., Voinnet, O., and Jones, J. D. 2006. A plant miRNA contributes to antibacterial resistance by repressing auxin signaling. *Science* 312:436-439.
- Navarro, L., Zipfel, C., Rowland, O., Keller, I., Robatzek, S., Boller, T., and Jones, J. D. 2004. *Plant Physiol.* 135:1113-1128.
- Nürnberg, T., Brunner, F., Kermmerling, B., and Piater, L. 2004. Innate immunity in plants and animals: striking similarities and obvious differences. *Immunol. Rev.* 198:249-226.
- Ocarino, N. M., Bozzi, A., Pereira, R. D. O., Breyner, N. M., Silva, V. L., Castanheira, P., Goes, A. M., and Serakides, R. 2008. Behavior of mesenchymal stem cells stained with 4', 6-diamidino-2-phenylindole dihydrochloride (DAPI) in osteogenic and non osteogenic cultures. *Biocell* 32:175-183.
- O'Mara, J., Bauernfeind, R., Stevens, A., Gast, K., and Steven, S. 1993. Aster Yellows. Cooperative Extension Service, Kansas State University.
- Opalski, K., Schultheiss, H., Kogel, K. H., and Hüchelhoven, R. 2005. The receptor-like MLO protein and the RAC/ROP family G-protein RACB modulate actin reorganization in barley attacked by the biotrophic powdery mildew fungus *Blumeria graminis* f.sp. *hordei*. *Plant J.* 41:291-303.
- Oparka, K. J., and Cruz, S. S. 2000. The great escape: Phloem transport and unloading of macromolecules. *Annu. Rev. Plant Physiol. Plant Mol. Biol.* 51:323-347.
- Oparka, K. J., Duckett, C. M., Prior, D. A. M., and Fisher, D. B. 1994. Real-time imaging of the phloem unloading in the root tip of *Arabidopsis*. *Plant J.* 6:759-766.
- Oshima, K., Kakizawa, S., Nishigawa, H., Jung, H. Y., Wei, W., Suzuki, S., Arashida, R., Nakata, D., Miyata, S., Ugaki, M., *et al.* 2004. Reductive evolution suggested from the complete genome sequence of a plant-pathogenic phytoplasma. *Nat. Genet.* 36:27-29.
- Osler, R., Carraro, L., Ermacora, P., Ferrini, F., Loi, N., Loschi, A., Martini, M., Mutton, P. B., and Refatti, E. 2003. Roguing: a controversial practice to eradicate grape yellows caused by phytoplasmas. Extended abstracts 14th Meeting of ICVG, Locorotondo 68.

List of references

- Osler, R., Carraro, L., Loi, N., and Refatti, E. 1993. Symptom expression and disease occurrence of a yellows disease of grapevine in northeastern Italy. *Plant Disease* 77:496-498.
- Osler, R., Loi, N., Carraro, L., Ermacora, P., and Refatti, E. 1999. Recovery in plants affected by phytoplasmas. Pages 496-498 in: *Proceedings of the 5th Congress of the European Foundation for Plant Pathology*, Taormina, Italy.
- Overall, R. L., and Gunning, B. E. S. 1982. Intercellular communication in *Azolla* roots: II Electric coupling. *Protoplasma* 11:151-160.
- Pallas, V., and Gómez, G. 2013. Phloem RNA-binding proteins as potential components of the long-distance RNA transport system. *Front Plant Sci.* 4:130.
- Park, S., Rancour, D. M., and Bednarek, S. Y. 2007. Protein domain-domain interactions and requirements for the negative regulation of Arabidopsis CDC48/p97 by the plant ubiquitin regulatory X (UBX) domain-containing protein, PUX1. *J. Biol. Chem.* 282:5217-5224.
- Pelissier, H. C., Peters, W. S., Collier, R., van Bel, A. J. E., and Knoblauch, M. 2008. GFP tagging of sieve element occlusion (SEO) proteins results in green fluorescent forisomes. *Plant Cell Physiol.* 49:1699-1710.
- Rennie, E. A., and Turgeon, R. 2009. A comprehensive picture of phloem loading strategies. *Proc. Natl. Acad. Sci. U.S.A.* 106:14162-14167.
- Pérez-Torres, C. A., López-Bucio, J., Cruz-Ramírez, A., Ibarra-Laclette, E., Dharmasiri, S., Estelle, M., and Herrera-Estrella, L. 2008. Phosphate availability alters lateral root development in Arabidopsis by modulating auxin sensitivity via a mechanism involving the TIR1 auxin receptor. *Plant Cell* 20:3258-3272.
- Peters, W. S., van, Bel A. J. E., and Knoblauch, M. 2006. The geometry of the forisome-sieve element-sieve plate complex in the phloem of *Vicia faba* L. leaflets. *J. Ex. Bot.* 57:3091-3098.
- Pickard B. 1973. Action potentials in plants. *Bot. Rev.* 39:172-201.
- Pizarro-Cerdá, J., and Cossart, P. 2006. Subversion of cellular functions by *Listeria monocytogenes*. *J. Pathol.* 208:215-223.
- Pracros, P., Renaudin, J., Eveillard, S., Mouras, A., and Hernould, M. 2006. Tomato flower abnormalities induced by stolbur phytoplasma infection are associated with changes of expression of floral development genes. *Mol. Plant Microbe Interact.* 19:62-68
- Quaglino, F., Zhao, Y., Casati, P., Bulgari, D., Bianco, P. A., Wei, W., and Davis, R. E. 2013. '*Candidatus* Phytoplasma solani', a novel taxon associated with stolbur and bois noir related diseases of plants. *Int. J. Syst. Evol. Microbiol.* 63:2879-2894.
- Ranf, S., Eschen-Lippold, L., Pecher, P., Lee, J., and Scheel, D. 2011. Interplay between calcium signalling and early signalling elements during defence responses to microbe- or damage-associated molecular patterns. *Plant J.* 68:100-113.
- Razin, S., Yogev, D., and Naot, Y. 1998. Molecular biology and pathogenicity of mycoplasmas. *Microbiol. Mol. Biol. Rev.* 62:1094-1156.
- Reichel, C., and Beachy, R. N. 1998. Tobacco mosaic virus infection induces severe morphological changes of the endoplasmic reticulum. *Proc. Natl. Acad. Sci. U.S.A.* 95:11169-11174.
- Reynolds, E. S. 1963. The use of lead citrate at high pH as an electron-opaque stain in electron microscopy. *J. Cell Biol.* 17:208-212.
- Rizzitello, A. E., Harper, J. R., and Silhavy, T. J. 2001. Genetic evidence for parallel pathways of chaperone activity in the periplasm of *Escherichia coli*. *J. Bacteriol.* 183:6794-6800.
- Robert-Seilaniantz, A., MacLean, D., Jikumaru, Y., Hill, L., Yamaguchi, S., Kamiya, Y., and Jones, J. D. G. 2011. The microRNA miR393 re-directs secondary metabolite biosynthesis

List of references

- away from camalexin and towards glucosinolates. *Plant J.* 67:218-231.
- Romanazzi, G., D'Ascenzo, D., and Murolo, S. 2009. Field treatment with resistance inducers for the control of grapevine bois noir. *J. Plant Pathol.* 91:677-682.
- Romanazzi, G., and Murolo, S. 2008. '*Candidatus* Phytoplasma ulmi' causing yellows in *Zelkova serrata* newly reported in Italy. *New Disease Report* 17:2008-2026.
- Rosebrock, T. R., Zeng, L., Brady, J. J., Abramovitch, R. B., Xiao, F., and Martin, G. B. 2007. A bacterial E3 ubiquitin ligase targets a host protein kinase to disrupt plant immunity. *Nature* 448:370-374.
- Rottner, K., Stradal, T. E., and Wehland, J. 2005. Bacteria-host-cell interactions at the plasma membrane: stories on actin cytoskeleton subversion. *Develop. Cell* 9:3-17.
- Rudzińska-Langwald, A., and Kamińska, M. 1999. Cytopathological evidence for transport of phytoplasma in infected plants. *Acta Soc. Bot. Pol.* 68:261-266.
- Rudzińska-Langwald, A., and Kamińska, M. 2001. Ultrastructural changes in Aster Yellows Phytoplasma affected *Limonium sinuatum* Mill. plants. I. Pathology of conducting tissues. *Acta Soc. Bot. Pol.* 70:173-180.
- Rudzińska-Langwald, A., and Kamińska, M. 2003. Changes of ultrastructure and cytoplasmic free calcium in *Gladiolus x hybridus* Van Houtte roots infected by aster yellows phytoplasma. *Acta Soci. Bot. Pol.* 72:269-282.
- Rüping, B., Ernst, A.M., Jekat, S. B., Nordzieke, S., Reineke, A. R., Müller, B., Bornberg-Bauer, E., Prüfer, D., and Noll, G. A. 2010. Molecular and phylogenetic characterization of the sieve element occlusion gene family in Fabaceae and non-Fabaceae plants. *BMC Plant Biol.* 10:219.
- Ryals, J. A., Neuenschwander, U. H., Willits, M. G., Molina, A., Steiner, H. Y., and Hunt, M. D. 1996. Systemic acquired resistance. *Plant Cell* 8:1809-1819.
- Sanders, D., Pelloux, J., Brownlee, C., and Harper, J. F. 2002. Calcium at the crossroads of signaling. *Plant Cell* 14:401-417.
- Sansonetti, P. J. 1993. Bacterial pathogens, from adherence to invasion: comparative strategies. *Med. Microbiol. Immunol.* 182:223-232.
- Santi, S., Grisan, S., Pierasco, A., De Marco, F., and Musetti, R. 2013. Laser microdissection of grapevine leaf phloem infected by stolbur reveals site-specific gene responses associated to sucrose transport and metabolism. *Plant, Cell Environ.* 36:343-355.
- Schattat, M., Barton, K., Baudisch, B., Klösgen, R. B., and Mathur, J. 2011. Plastid stromule branching coincides with contiguous endoplasmic reticulum dynamics. *Plant Physiol.* 155:1667-1677.
- Schneider, B, Gibb, K., and Seemüller, E. 1997. Sequence and RFLP analysis of the elongation factor Tu gene used in differentiation and classification of phytoplasmas. *Microbiol.* 143:3381-3359.
- Schulz, A. 1998. The phloem. Structure related to function. *Prog. Bot.* 59:429-475.
- Schulz, A. 2005. Role of plasmodesmata in solute loading and unloading. Pages 135-161 in: *Plasmodesmata*. K. Oparka. eds., Blackwell Publishing, Oxford, U.K.
- Seemüller, E. 1990. Apple proliferation. In: *Compendium of apple and pear diseases*. Pages 67-68 in: A. L. Jones and H. S. Aldwinkle. eds., APS Press, St Paul, Minnesota, U.S.A.
- Seemüller, E., Sule, S., Kube, M., Jelkmann, W., and Schneider, B. 2013. The AAA+ ATPases and HflB/FtsH proteases of '*Candidatus* Phytoplasma mali': phylogenetic diversity, membrane topology, and relationship to strain virulence. *Mol. Plant Microbe Interact.* 26:367-376.
- Shalitin, D., Wang, Y., Omid, A., Gal-On, A., and Wolf, S. 2002. Cucumber mosaic virus movement protein affects sugar metabolism and transport in

List of references

- tobacco and melon plants. *Plant Cell Environ.* 25:989-997.
- Shalitin, D., and Wolf, S. 2000. Cucumber mosaic virus infection affects sugar transport in melon plants. *Plant Physiol.* 123:597-604.
- Sheen, J. 2001. Signal transduction in maize and *Arabidopsis* mesophyll protoplasts. *Plant Physiol.* 127:1466-1475.
- Shapiguzov, A., Vainonen, J. P., Wrzaczek, M., and Kangasjärvi, J. 2012. ROS-talk - how the apoplast, the chloroplast, and the nucleus get the message through. *Front Plant Sci.* 3:292.
- Shikata, M., Yamaguchi, H., Sasaki, K., and Ohtsubo, N. 2012. Overexpression of *Arabidopsis* miR157b induces bushy architecture and delayed phase transition in *Torenia fournieri*. *Planta* 236:1027-1035.
- Sjolund, R. D., and Shih, C. Y. 1983. Freeze-fracture analysis of phloem structure in plant tissue cultures. I. The sieve element reticulum. *J. Microsc. Ultrastr.* 82:111-121.
- Slewiniski, T. L., and Braun, D. M. 2010. Current perspectives on the regulation of whole-plant carbohydrate partitioning. *Plant Sci.* 178:341-349.
- Slewiniski, T. L., Zhang, C., and Turgeon, R. 2013. Structural and functional heterogeneity in phloem loading and transport. *Front Plant Sci.* 4:244.
- Smith, J. M., Salamango, D. J., Leslie, M. E., Collins, C. A., and Heese, A. 2014. Sensitivity to Flg22 is modulated by ligand-induced degradation and de novo synthesis of the endogenous flagellin-receptor flagellin-sensing2. *Plant Physiol.* 164:440-454.
- Strating, J. R. P. M., and Martens, G. J. M. 2009. The p24 family and selective transport processes at the ER-Golgi interface. *Biol. Cell* 101:495-509.
- Subramaniam, R., Desveaux, D., Spickler, C., Michnick, S. W., and Brisson, N. 2001. Direct visualization of protein interactions in plant cells. *Nature Biotechnol.* 19:769-772.
- Sugawara, K., Honma, Y., Komatsu, K., Himeno, M., Oshima, K., and Namba, S. 2013. The alteration of plant morphology by small peptides released from the proteolytic processing of the bacterial peptide TENGU. *Plant Physiol.* 162:2005-2014.
- Sugio, A., Kingdom, H. N., MacLean, A. M., Grieve, V. M., and Hogenhout, S. A. 2011. Phytoplasma protein effector SAP11 enhances insect vector reproduction by manipulating plant development and defense hormone biosynthesis. *Proc. Natl. Acad. Sci. U.S.A.* 108:1254-1263.
- Suzuki, S., Oshima, K., Kakizawa, S., Arashida, R., Jung, H. Y., Yamaji, Y., Nishigawa, H., Ugaki, M., and Namba, S. 2006. Interaction between the membrane protein of a pathogen and insect microfilament complex determines insect-vector specificity. *Proc. Natl. Acad. Sci. U.S.A.* 103:4252-4257.
- Tai, C. F., Lin, C. P., Sung, Y. C., and Chen, J. C. 2013. Auxin influences symptom expression and phytoplasma colonisation in periwinkle infected with periwinkle leaf yellowing phytoplasma. *Ann. Appl. Biol.* 3:420-429.
- Tao, Y., Xie, Z., Chen, W., Glazebrook, J., Chang, H. S., Han, B., Zhu, T., Zou, G., and Katagiri, F. 2003. Quantitative nature of *Arabidopsis* responses during compatible and incompatible interactions with the bacterial pathogen *Pseudomonas syringae*. *Plant Cell* 15:317-330.
- Tena, G., Asai, T., Chiu, W. L., and Sheen, J. 2001. Plant MAPkinase signaling cascades. *Curr. Opin. Plant Biol.* 4:392-400.
- Thonat, C., Boyer, N., Penel, C., Courduroux, J. C., and Gaspar, T. 1993. Cytological indication of the involvement of calcium and calcium-related proteins in the early responses of *Bryonia dioica* to mechanical stimulus. *Protoplasma* 176:133-137.
- Thorpe, M. R., Furch, A. C. U., Minchin, P. E. H., Föller, J., van Bel, A. J. E., and Hafke, J. B. 2010. Rapid cooling

List of references

- triggers for some dispersion just before phloem transport stops. *Plant Cell Environ.* 33:259-271.
- Thorsch, J., and Esau, K. 1981. Changes in the endoplasmic reticulum during differentiation of a sieve element in *Gossypium hirsutum*. *J. Ultrastr. Res.* 74:183-194.
- Tian, M., Chaudhry, F., Ruzicka, D. R., Meagher, R. B., Staiger, C. J., and Day, B. 2009. Arabidopsis actin-depolymerizing factor AtADF4 mediates defense signal transduction triggered by the *Pseudomonas syringae* effector AvrPphB. *Plant Physiol.* 150:815-824.
- Tilney, L. G., and Portnoy, D. A. 1989. Actin filaments and the growth, movements, and spread of the intracellular bacterial parasite *Lysteria monocytogens*. *J. Cell Biol.* 109:1597-1608.
- Tran-Nguyen, L. T., Kube, M., Schneider, B., Reinhardt, R., and Gibb, K. S. 2008. Comparative genome analysis of "*Candidatus* *Phytoplasma australiense*" (subgroup tuf-Australia I; rp-A) and "*Ca. Phytoplasma asteris*" Strains OY-M and AY-WB. *J. Bacteriol.* 190:3979-3991.
- Truernit, E. 2014. Phloem imaging. *J. Exp. Bot.* 65:1681-1688.
- Tsuda, K., and Katagiri, F. 2010. Comparing signaling mechanisms engaged in pattern-triggered and effector-triggered immunity. *Curr. Opin. Plant Biol.* 13:459-465.
- Tsuda, K., Sato, M., Stoddard, T., Glazebrook, J., and Katagiri, F. 2009. Network properties of robust immunity in plants. *PloS Genet.* doi:10.1371/journal.pgen.1000772.
- Turgeon R., and Ayre B. G. 2005. Pathways and mechanisms of phloem loading. Pages 45-67 in: *Vascular transport in plants*. N. M. Holbrook and M. A. Zwieniecki. eds., Elsevier Academic Press, New York, U.S.A.
- Tuzun, S., and Kuc, J. 1985. Movement of a factor in tobacco infected with *Peronospora tabacina* which systemically protects against blue mold. *Physiol. Plant Pathol.* 26:321-330.
- van Bel, A. J. E. 1993. Strategies of phloem loading. *Annu. Rev. Plant Physiol. Plant Mol. Biol.* 44:253-281.
- van Bel, A. J. E. 1996. Interaction between sieve element and companion cell and the consequences for photoassimilate distribution. Two structural hardware frames with associated software packages in dicotyledons? *J. Exp. Bot.* 47:1129-1140.
- Van Bel, A. J. E. 2003. The phloem, a miracle of ingenuity. *Plant Cell Environ.* 26:125-149.
- Van Bel, A. J. E., Ehlers, K., and Knoblauch, M. 2002. Sieve elements caught in the act. *Trends Plant Sci.* 7:126-132.
- van Bel, A. J. E., Furch, A. C. U., Will, T., Buxa, S. V., Musetti, R., and Hafke, J. B. 2014. Spread the news: systemic dissemination and local impact of Ca²⁺ signals along the phloem pathway. *J. Ex. Bot.* 65:1761-1787.
- Van Bel, A. J. E., and Gaupels, F. 2004. Pathogen resistance and alarm signals via the phloem. *Mol. Plant Pathol.* 5:495-504.
- van Bel, A. J. E., and Hess, P. 2003. Kollektiver Kraftakt zweier Exzentriker. *Biologie unserer Zeit* 4:220-230.
- van Bel, A. J. E., and Knoblauch, M. 2000. Sieve element and companion cell; the story of the comatose patient and the hyperactive nurse. *Austral. J. Plant Physiol.* 27:477-487.
- van Bel, A. J. E., Knoblauch, M., Furch, A. C. U, and Hafke, J. B. 2011. (Questions)ⁿ on phloem biology. 1. Electropotential waves, Ca²⁺ fluxes and cellular cascades along the propagation pathway. *Plant Sci.* 181:210-218.
- van Loon, L. C. 1985. Pathogen-related proteins. *Plant Mol. Biol.* 4:111-116.
- Van Loon, L. C., and Van Strien, E. A. 1999. The families of pathogenesis-related proteins, their activities, and comparative analysis of PR-1 type

List of references

- proteins. *Physiol. Mol. Plant Pathol.* 55:85-97.
- Vantard, M., and Blanchoin, L. 2002. Actin polymerization processes in plant cells. *Curr. Opin. Plant Biol.* 5: 502-506.
- Verdin, E., Salar, P., Danet, J. L., Choueiri, E., Jreijiri, F., El Zammar, S., Gélie, B., Bové, J. M., and Garnier, M. 2003. 'Candidatus *Phytoplasma phoenicium*', a novel phytoplasma associated with an emerging lethal disease of almond trees in Lebanon and Iran. *Int. J. Syst. Evol. Microbiol.* 53:833-838.
- Vitali, M., Chitarra, W., Galetto, L., Bosco, D., Marzachi, C., Gullino, M. L., Spanna, F., and Lovisolo, C. 2013. Flavescence dorée phytoplasma deregulates stomatal control of photosynthesis in *Vitis vinifera*. *Ann. Appl. Biol.* 3:335-346.
- Wahid, A., and Ghani, A. 2007. Varietal differences in mungbean (*Vigna radiata*) for growth, yield, toxicity symptoms and cadmium accumulation. *Ann. Appl. Biol.* 152:59-69.
- Wang, Y., and Riechmann, V. 2007. The role of the actomyosin cytoskeleton in coordination of tissue growth during *Drosophila oogenesis*. *Curr. Biol.* 7:1349-1355.
- Wang, H., Robinson, R. C., and Burtnick, L. D. 2010. The structure of native G-actin. *Cytoskeleton* 67:456-465.
- Watson, P., and Stephens, D. J. 2005. ER-to-Golgi transport: form and formation of vesicular and tubular carriers. *Biochim. Biophys. Acta* 1744:304-315.
- Weintraub, P. G., and Beanland, L. 2006. Insect vectors of phytoplasmas. *Annu. Rev. Entomol.* 51:91-111.
- Weisburg, W. G., Tully, J. G., Rose, D. L., Petzel, J. P., Oyaizu, H., Yang, D., Mandelco, L., Sechrest, J., Lawrence, T. G., and Van Etten, J. 1989. A phylogenetic analysis of the mycoplasmas: basis for their classification. *J. Bacteriol.* 171:6455-6467.
- Wellman, C. H., Osterloff, P. H., and Mohiuddin, U. 2003. Fragments of the earliest land plants. *Nature* 425:282-285.
- White, R. G., Badelt, K., Overall, R. L., and Vesik, M. 1994. Actin associated with plasmodesmata. *Protoplasma* 180:169-184.
- Wi, S. J., Ji, N. R., and Park, K. Y. 2012. Synergistic biosynthesis of biphasic ethylene and reactive oxygen species in response to hemibiotrophic *Phytophthora parasitica* in tobacco plants. *Plant Physiol.* 159:251-265.
- Will, T., Furch, A. C. U., and Zimmermann M. R. 2013. How phloem-feeding insects face the challenge of phloem-located defenses. *Front. Plant Sci.* 4:336.
- Xie, B., Wang, X., Zhu, M., Zhang, Z., and Hong, Z. 2011. *CaIS7* encodes a callose synthase responsible for callose deposition in the phloem. *Plant J.* 65:1-14.
- Yoo, B. C., Lee, J. Y., and Lucas, W. J. 2002. Analysis of the complexity of protein kinases within the phloem sieve tube system. *J. Biol. Chem.* 277:15325-15332.
- Zhang, J. Y., Broeckling, C. D., Sumner L. W., and Wang Z.Y. 2007. Heterologous expression of two *Medicago truncatula* putative ERF transcription factor genes, WXP1 and WXP2, in *Arabidopsis* led to increased leaf wax accumulation and improved drought tolerance, but differential response in freezing tolerance. *Plant Mol. Biol.* 64:265-278.
- Zhang, J., Shao, F., Li, Y., Cui, H., Chen, L., Li, H., Zou, Y., Long, C., Lan, L., Chai, J., *et al.* 2007b. A *Pseudomonas syringae* effector inactivates MAPKs to suppress PAMP-induced immunity in plants. *Cell Host Microbe* 1:175-185.
- Zhang, J., and Zhou, J. 2010. Plant immunity triggered by microbial molecular signatures. *Mol. Plant.* 3:783-793.
- Zhao, Y., Liu Q., and Davis R. E. 2004. Transgene expression in strawberries driven by a heterologous phloem-

List of references

- specific promoter. *Plant Cell Rep.* 23:224-230.
- Zhao, H., Sun, R., Albrecht, U., Padmanabhan, C., Wang, A., Coffey, M. D., Girke, T., Wang, Z., Close, T. J., Roose, M., *et al.* 2013. Small RNA profiling reveals phosphorus deficiency as a contributing factor in symptom expression for Citrus Huanglongbing disease. *Mol. Plant* 6:301-310.
- Zhong, B. X., and Shen, Y. W. 2004. Accumulation of pathogenesis-related type-5 like proteins in phytoplasma-infected garland chrysanthemum *Chrysanthemum coronarium*. *Acta Biochim. Biophys. Sin.* 36:773-779.
- Zipfel, C., Kunze, G., Chinchilla, D., Caniard, A., Jones, J. D., Boller, T., and Felix, G. 2006. Perception of the bacterial PAMP EF-Tu by the receptor EFR restricts *Agrobacterium*-mediated transformation. *Cell* 125:749-760.
- Zipfel, C., Robatzek, S., Navarro, L., Oakeley, E. J., Jones, J. D., Felix, G., and Boller, T. 2004. Bacterial disease resistance in *Arabidopsis* through flagellin perception. *Nature* 428:764-767.
- Zorloni, A., Scattini, G., Bianco, P. A., and Belli, G. 2002. Possible reduction of grapevine Flavescence doree by a careful winter pruning. *Petria* 12:407-408.

List of Figures and Tables

Introduction

Figure 1: Phloem defense response.	12
Figure 2: Vector-born phytoplasma transmission.	16

Material and Methods

Figure 3: Technical procedure of pressure infiltration.	27
Figure 4: Technical procedure of <i>in vivo</i> observation method.	29
Figure 5: Technical procedure of protoplast isolation.	30

Results

Distant flagellin-triggered signal induces Ca²⁺ mediated phasic sieve-element occlusion

Figure 6: Classification of <i>V. faba</i> forisome position based on 3-D analysis.	37
Figure 7: Absolute frequency of forisome relative to location and positions in the sieve element of <i>V. faba</i>	38
Figure 8: Forisome reaction of <i>V. faba</i> in response to heat stimuli.	40
Figure 9: Change of forisome position in <i>V. faba</i> due to distant stimulus.	41
Figure 10: Forisome reaction to application of various flagellin concentrations to intact sieve elements in <i>V. faba</i>	42
Figure 11: Observation of mass flow in sieve tubes after pressure infiltration of 1 μ M flg22 in the leaves of wild type <i>A. thaliana</i> (Col-0).	43
Figure 12: Observation of mass flow in sieve tubes after pressure infiltration of 1 μ M flg22 in the leaves of <i>A. thaliana</i> (<i>fls2</i>).	45
Figure 13: <i>V. faba</i> sieve -element protoplast reaction in response to application of flagellin and high mannitol concentration.	45
Figure 14: Observation of ROS production in isolated protoplasts.	46

Phytoplasmas trigger Ca²⁺ influx leading to sieve-element occlusion

Figure 15: Images of healthy (left half of the panel) and Flavescence Dorée (FD)-infected (right half) <i>V. faba</i> plants.	48
Figure 16: CLSM images of phloem tissue in intact healthy (upper part of the panel) and FD-infected (lower part) <i>V. faba</i> plants stained with CFDA.	49
Figure 17: CLSM images of phloem tissue in intact healthy (upper part of the panel) and FD-infected (lower part) <i>V. faba</i> plants stained with DAPI.	50
Figure 18: CLSM images of phloem tissue in intact healthy (upper part of the panel) and FD-infected (lower part) <i>V. faba</i> plants stained with DAPI and CFDA.	51
Figure 19: CLSM images of phloem tissue in intact healthy (upper part of the panel) and FD-infected (lower part) <i>V. faba</i> plants stained with CFDA and DAPI.	52
Figure 20: CLSM images of phloem tissue in intact healthy (upper part of the panel) and FD-infected (lower half) <i>V. faba</i> plants stained with CMEDA/CMFDA.	53
Figure 21: CLSM images of phloem tissue in intact healthy (upper part of the panel) and FD-infected (lower half) <i>V. faba</i> plants stained with aniline blue.	554

List of Figures and Tables

Figure 22: CLSM images of phloem tissue in intact healthy (upper part of the panel) and FD-infected (lower half) *V. faba* plants stained with OGB-1.55

Phytoplasma infection is associated with re-organization of plasma membrane-ER network and actin structure in sieve elements

Figure 23: Images of healthy (left half of the panel) and stolbur-diseased (right half) *S. lycopersicum* Micro-Tom plants.57

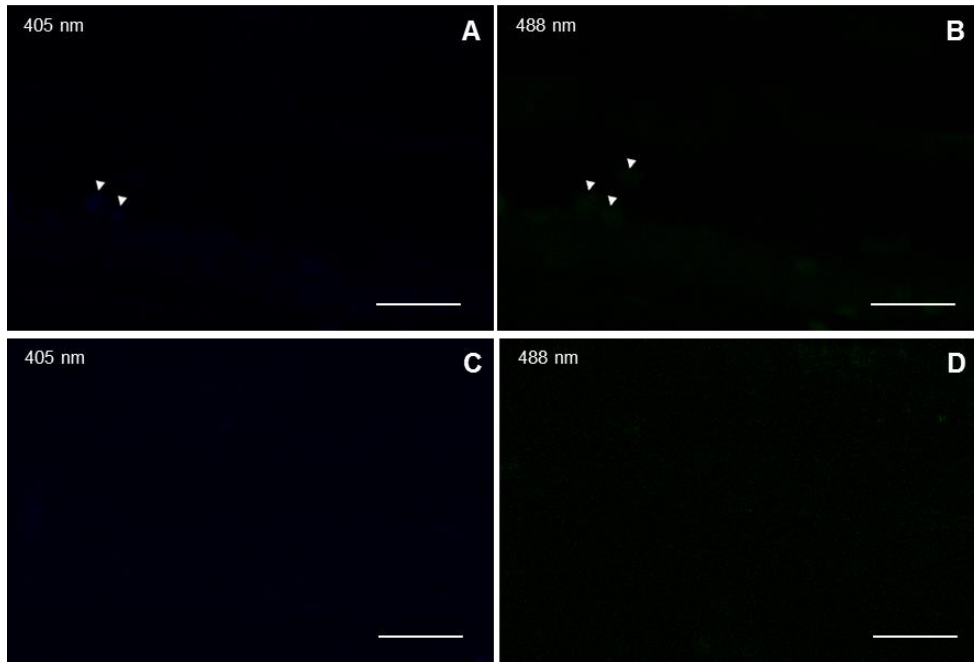
Figure 24: Light (LM) and Epifluorescence Microscopy (EFM) images from longitudinal and cross sections of main veins of healthy and stolbur-diseased *S. lycopersicum* leaves, stained with DAPI.58

Figure 25: LM and EFM micrographs from cross-sections of main veins of healthy and stolbur-diseased *S. lycopersicum* leaves stained with RH 414.60

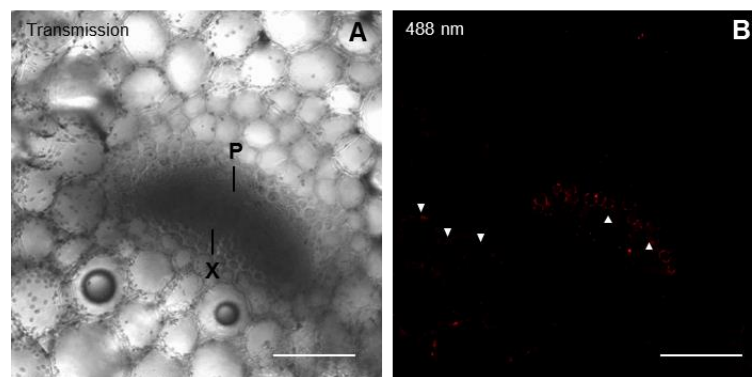
Figure 26: LM and EFM micrographs from cross-sections main veins of healthy and stolbur-diseased *S. lycopersicum* leaves stained with an α -actin-Texas Red-conjugated antibody.61

Figure 27: LM and EFM micrographs from cross-sections of the main veins of healthy and stolbur-diseased *S. lycopersicum* leaves stained with ER Tracker Green.63

Appendix

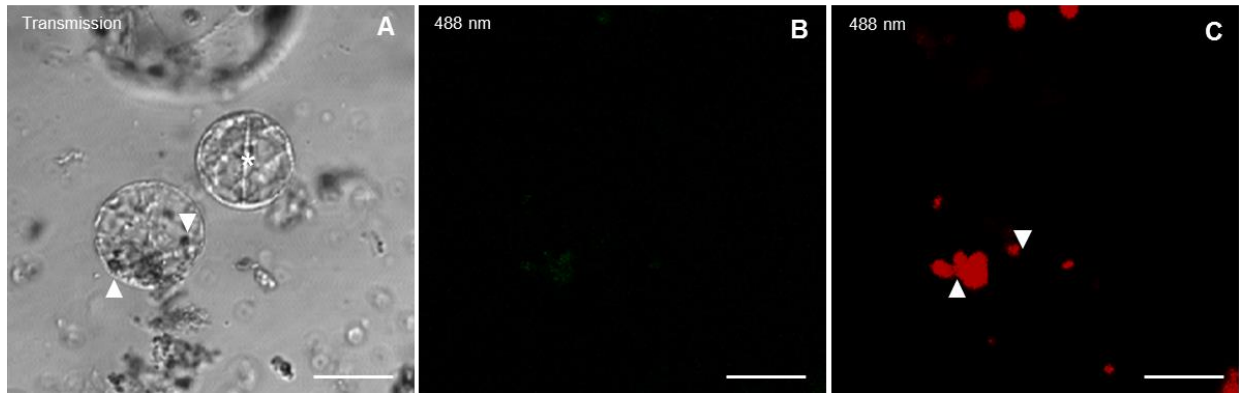


Supplemental Image 1: Autofluorescence images of unstained healthy (A,B) and FD-infected (C,D) *V. faba* phloem tissue. Sieve elements of healthy plants, using 405 nm (A), 488 nm (B) wavelength do not exhibit strong signals. Similar results were obtained for FD-infected sieve elements both at 405 nm (C) and 488 nm (D) wavelengths. In A and B arrowheads indicate autofluorescence of chloroplasts in the parenchyma cell above the sieve elements. CC, companion cell; PPC, phloem parenchyma cell; SE, sieve element; SP, sieve plate. Scale bars = 10 μ m.

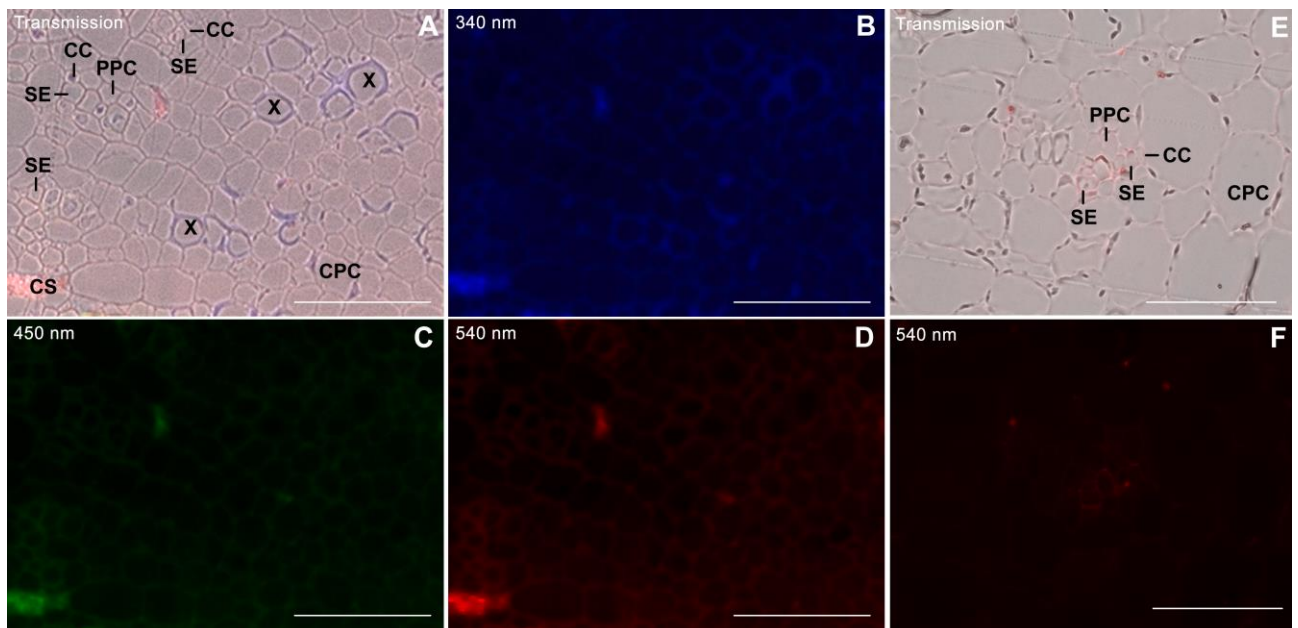


Supplemental Image 2: Autofluorescence and background images of unstained *A. thaliana* vascular tissue. Except signals from xylem and chloroplast (arrowheads), cross-sections excited to a wavelength of 488 nm do not show strong signals. P: phloem, X: xylem. Scale bars 20 μ m.

Appendix



Supplemental Image 3: Autofluorescence images of untreated protoplast from *V. faba* stem tissue. Except weak signal from chloroplast neither sieve-element nor mesophylls protoplasts show strong signal when excited by wavelength of 488 nm. To identify the green signal as emission from longer wavelength (point of reference) chlorophyll signal was collected simultaneously starting a wavelength of 600 nm (red signal). In A asterisk indicated forisome, in A and C arrowheads indicate chloroplast. Scale bars = 10 μm .



Supplemental Image 4: Autofluorescence and background images of untreated (A-D) and secondary antibody-only treated (E-F) *S. lycopersicum* tissue. Overlay (A) of bright-field image and images excited with a wavelength of 340 nm (B), 450 nm (C) or 540 nm (D) served as a staining control, respectively. Overlay (E) of bright-field image and sample treated with secondary antibody-only excited with a wavelength of 540 nm (F) showing non-specific secondary binding. CC, companion cell; CPC, cortex parenchyma cells; CS, crystalline structure; PPC, phloem parenchyma cell; SE, sieve element; X, xylem vessel. Scale bars = 50 μm .

Appendix

Well	Label	Primers	C(T)
F1	Vicia To1 FD	16SRT f1r1	18,25
F2	Vicia To2 FD	16SRT f1r1	19,70
F3	Vicia To3 FD	16SRT f1r1	21,41
F4	Vicia To4 FD	16SRT f1r1	18,55
F5	Vicia To5 FD	16SRT f1r1	17,95
F6	Vicia To6 FD	16SRT f1r1	17,18
F8	C. roseus FD+	16SRT f1r1	17,25
F9	Grapevine FD+	16SRT f1r1	19,20
F10	Vicia1C-22_03_12	16SRT f1r1	None
F12	H ₂ O	16SRT f1r1	None

F1 to F6: samples
 FD-infected *V. faba*
F8: positive control
 FD- infected *Catharanthus roseus*
F9: positive control
 FD-infected grapevine
F10: negative control
 healthy *V. faba*

Supplemental Table 1: Molecular detection of ‘*Candidatus Phytoplasma vitis*’ in *Vicia faba* plants. Flavescence Dorée phytoplasma 16S rRNA was detected in infected plants, whereas no amplification was obtained in control plants.

Well	Label	Primers	C(T)
F1	Stolbur-infected S. lyc 1	16SRT f2r3	17.98
F2	Stolbur-infected S. lyc 2	16SRT f2r3	19.38
F3	Stolbur-infected S. lyc 3	16SRT f2r3	17.54
F4	Stolbur-infected S. lyc 4	16SRT f2r3	16.10
F5	C. roseus Stol+	16SRT f2r3	17.55
F6	Grapevine Stol+	16SRT f2r3	23.50
F7	Tomato C-	16SRT f2r3	None
F8	H ₂ O	16SRT f2r3	None

F1 to F4: samples
 stolbur-infected *S. lycopersicon*
F5: positive control
 stolbur-infected *Catharanthus roseus*,
F6: positive control
 stolbur-infected grapevine
F7: negative control
 healthy *S. lycopersicon*

Supplemental Table 2: Molecular detection of ‘*Candidatus Phytoplasma solani*’ in *Solanum lycopersicon* plants. Stolbur phytoplasma 16S rRNA was detected in infected plants, whereas no amplification was obtained in control plants.

List of own publications

Present thesis is a condensed version of research results. Some of the detailed results have been summarized in following manuscripts, some of which are published:

Buxa, S. V., Zimmermann, M. R., Kogel, K. H., and Furch, A.C.U. 2011. PAMP triggered sieve-tube occlusion. Deutsche Botanikertagung (poster presentation), Freie Universität Berlin, Berlin, Germany.

Kang, H. G., Hyong, W. C., von Einem, S., Manosalva, P., Ehlers, K., Liu, P. P., **Buxa, S. V.**, Moreau, M., Mang, H. G., Kachroo, P., Kogel, K. H., and Klessig, . DF. 2012. CRT1 is a nuclear-translocated MORC endonuclease that participates in multiple levels of plant immunity. Nature Communication 3, 1297. Faculty of 1000*

Musetti, R.*, **Buxa, S. V.***, De Marco, F., Loschi, A., Polizzotto, R., Kogel, K. H., and van Bel, A. J. E. 2013. Phytoplasma-triggered Ca²⁺ influx is involved in sieve-tube blockage. Molecular Plant-Microbe Interactions 26, 379-386. *equally contributed

Buxa, S. V.*, van Bel, A. J. E., Hafke, J. B., Kogel, K. H., and Furch, A. C. U. FLS2 sensors located in cortex cells trigger electrical potential waves conferring Ca²⁺-mediated sieve-tube occlusion. 2013. Deutsche Botanikertagung (poster presentation), Eberhard Karls Universität Tübingen, Tübingen, Germany.

van Bel, A. J. E., Furch, A. C. U., Will, T., **Buxa, S. V.**, Musetti, R., and Hafke, J. B. 2014. Spread the news: systemic dissemination and local impact of Ca²⁺ signals along the phloem pathway. Journal of Experimental Botany 65, 1761-1787.

Buxa, S. V., Polizzotto, R., De Marco, F., Loschi, A., Kogel, K. H., van Bel, A.J.E., and Musetti, R. Stolbur disease in tomato is associated with the re-organization of plasma membrane-ER network and actin filaments in sieve elements. in process

Furch, A. C. U.* , **Buxa, S. V.***, and van Bel, A. J. E. Similar intracellular location and stimulus reactivity, but differential mobility of tailless and tailed forisomes in intact sieve tubes. in process *equally contributed

Buxa, S. V.*, van Bel, A. J. E., Hafke, J. B., Kogel, K. H., and Furch, A. C. U. FLS2 sensors located in cortex cells trigger electrical potential waves conferring Ca²⁺-mediated sieve-tube occlusion. in process

Affirmation

„Ich erkläre: Ich habe die vorgelegte Dissertation selbständig und ohne unerlaubte fremde Hilfe und nur mit den Hilfen angefertigt, die ich in der Dissertation angegeben habe. Alle Textstellen, die wörtlich oder sinngemäß aus veröffentlichten Schriften entnommen sind, und alle Angaben, die auf mündlichen Auskünften beruhen, sind als solche kenntlich gemacht. Bei den von mir durchgeführten und in der Dissertation erwähnten Untersuchungen habe ich die Grundsätze guter wissenschaftlicher Praxis, wie sie in der „Satzung der Justus-Liebig-Universität Gießen zur Sicherung guter wissenschaftlicher Praxis“ niedergelegt sind, eingehalten.“

“I hereby declare that the dissertation submitted for the degree of Doctor rerum naturalium at the Justus-Liebig University of Giessen was in all parts exclusively prepared on my own, and that other resources or other means, than those explicitly referred to, have not been utilized.”

Stefanie Vera Buxa

Giessen, 31. July 2014

Stefanie Vera Buxa

Stefanie-Vera-Buxa@gmx.de • +49 641 1314157 • +49 176 63141130
Weserstraße 5, 35390 Giessen, Germany

General Information

Academic title: Msc.
Current position/status: Ph.D. student
Institute address: Institute of Phytopathology and Applied Zoology
Justus Liebig University Giessen, Heinrich-Buff-Ring 26-32
D-35392 Giessen, Germany

Academic Education and Qualifications

02/2011 - 03/2014	Ph.D. Student at the Institute of Phytopathology and Applied Zoology, Justus Liebig University Giessen Thesis: " <i>MAMP-triggered sieve-element occlusion and systemic signaling in phloem of higher plants.</i> " Supervisor: Prof. Dr. Kogel
10/2008 - 02/2011	Master of Science in Biology at Justus Liebig University Giessen Major subject: Botany/ Genetics/ Ecology/ Cell Biology Master's thesis: " <i>Controlling the movement of forisomes in <i>Vicia faba</i> and <i>Phaseolus vulgaris</i>.</i> " Supervisor: Prof. Dr. van Bel; final mark: 1.6
10/2005 - 10/2008	Bachelor of Science in Biology at Justus Liebig University Giessen Major subject: Botany/ Didactics of Biology/ Plant Physiology Bachelor's thesis: " <i>Systemic signals mediate by calcium-binding proteins in response to leaf squashing.</i> " Supervisor: Prof. Dr. AJE van Bel; final mark: 1.6
08/2002 - 06/2005	German Abitur (equivalent to A level) at the Berufliche Schulen des Main-Kinzig-Kreises Gelnhausen; final mark: 2.2 Major subject: Emphasis on nutritional science and home economics

Professional Career and Experience

04/2014 - 05/2014	Executive assistant of Major Equipment Initiatives, Justus-Liebig University Giessen, Giessen, Germany
04/2011 - 03/2014	Giessen Graduate Centre for the Life Sciences (GGL) fellowship, Justus-Liebig University Giessen, Giessen, Germany
10/2013 - 01/2014	Teaching assistant, Institute for Phytopathology and Applied Zoology, Justus Liebig University Giessen, Giessen, Germany
01/2012 - 12/2013	Graduate fellow (Justus Doctoral Grant), Institute for Phytopathology and Applied Zoology, Justus Liebig University Giessen, Giessen, Germany
10/2013	Leica International Advanced Confocal Microscopy Course, Leica Confocal Imaging Center, Mannheim, Germany
09/2013	Participant in Deutsche Botanikertagung (poster presentation), Eberhard Karls Universität Tübingen, Tübingen, Germany

Curriculum Vitae

04/2013 - 09/2013	Supervision of Bachelor thesis at the Institute for Phytopathology and Applied Zoology, Justus Liebig University Giessen, Giessen, Germany
06/2013	Research stay abroad, Department of Agricultural and Environmental Sciences (DISA), University of Udine, Udine, Italy
08/2012 - 02/2013	Organizer and coordinator of Collaborative Research Centre 1067 (Communication at the Interface: mechanisms of root pathogenesis and systemic signaling) at the Justus Liebig University Giessen, Giessen, Germany
10/2012	Leica Microscopy Workshop, Institute of Cytobiology and Cytopathology, Philipps University Marburg, Germany
02/2012 - 08/2012	Supervision of Bachelor thesis at the Institute for Phytopathology and Applied Zoology, Justus Liebig University Giessen, Giessen, Germany
02/2012	Invited speaker at the Max-Planck-Institute for Biogeochemistry Jena, Jena, Germany
10/2011 - 01/2012	Teaching assistant, Institute for Phytopathology and Applied Zoology, Justus Liebig University Giessen, Giessen, Germany
02/2010 - 11/2011	Waitress at Die Kate, Giessen, Germany
09/2011	Participant in Deutsche Botanikertagung (poster presentation), Freie Universität Berlin, Berlin, Germany
09/2011	Participant in 3rd Sophia Antipolis Workshop on Compatibility Mechanisms in Plant-Microbe Interactions (oral presentation), Sophia Agrobiotech Institute, Sophia Antipolis, France
08/2011	Conference assistant at Transregio 81

Qualification Profile

Deal orientated and thoughtful professional prepares to excel in the field of advanced microscopy research-and-technique and contribute to organize objectives.

Sample Preparation	Permeabilization: Chemical and Mechanical (Freeze Shattering); Fixation; Resin Embedding; Sectioning (Microtomy)
Microscopy	Light Microscopy (LM); Epi-fluorescence Microscopy (EFM); Confocal Laser Scanning Microscopy (CLSM); Two-Photon Microscopy (MPM); Transmission Electron Microscopy (TEM)
Visualizing techniques	Conventional Staining <i>in vivo</i> , <i>in vitro</i> and <i>in planta</i> ; Fluorescence <i>In Situ</i> Hybridisation (FISH); Fluorescence Resonance Energy Transfer (FRET); Immunohistochemical staining (IHC); Immunogold staining (IGS) and Immunofluorescence (IF) Labeling
Protein Biochemistry	Affinity Chromatography; Polyacrylamide Gel Electrophoresis (SDS-PAGE); Protein Extraction; Western Blot
Biochemical Technology	Agarose Gel Electrophoresis; DNA Extraction; Polymerase Chain Reaction (PCR)
Language	German (Mother Tongue); English (Common European Framework of Reference for Languages Certificate)
Electronic Data Processing	Data Analysis: SPSS; Image Processing: Image J, Adobe Fireworks, Adobe Photoshop; MS Office: Word, PowerPoint and Excel

Publications

Kang HG, Hyong WC, von Einem S, Manosalva P, Ehlers K, Liu PP, **Buxa SV**, Moreau M, Mang HG, Kachroo P, Kogel KH, Klessig DF. 2012. CRT1 is a nuclear-translocated MORC endonuclease that participates in multiple levels of plant immunity. *Nature Communication* **3**, 1297.

Musetti R*, **Buxa SV***, de Marco F, Loschi A, Polizzotto R, Kogel KH, van Bel AJE. 2013. Phytoplasma-triggered Ca²⁺ influx is involved in sieve-tube blockage. *Molecular Plant-Microbe Interactions* **26**, 379-386. * equally contributed

van Bel AJE, Furch AC, Will T, **Buxa SV**, Musetti R and Hafke JB. 2014. Spread the news: systemic dissemination and local impact of Ca²⁺ signals along the phloem pathway. *Journal of Experimental Botany*, doi 10.1093/jxb/ert425.